

CITATION REPORT

List of articles citing

A New Constitutive Framework for Arterial Wall Mechanics and a Comparative Study of Material Models

DOI: 10.1023/a:1010835316564
Journal of Elasticity, 2000, 61, 1-48.

Source: <https://exaly.com/paper-pdf/31551958/citation-report.pdf>

Version: 2024-04-24

This report has been generated based on the citations recorded by exaly.com for the above article. For the latest version of this publication list, visit the link given above.

The third column is the impact factor (IF) of the journal, and the fourth column is the number of citations of the article.

#	Paper	IF	Citations
1871	Preface. <i>Journal of Elasticity</i> , 2000 , 61, 9-12	1.5	
1870	Mechanics of the human femoral adventitia including the high-pressure response. 2002 , 282, H2427-40		106
1869	The Convexity Properties of a Class of Constitutive Models for Biological Soft Issues. 2002 , 7, 217-235		37
1868	Assessment of plaque stability by means of high-resolution MRI and finite element analyses of local stresses and strains.		1
1867	Constitutive Modelling of Rubber-Like and Biological Materials with Limiting Chain Extensibility. 2002 , 7, 353-371		61
1866	On Extension and Torsion of a Compressible Elastic Circular Cylinder. 2002 , 7, 373-392		10
1865	A structural model for the viscoelastic behavior of arterial walls: Continuum formulation and finite element analysis. 2002 , 21, 441-463		307
1864	On the mechanics of solids with a growing mass. 2002 , 39, 4627-4664		200
1863	A constrained mixture model for arterial adaptations to a sustained step change in blood flow. 2003 , 2, 109-26		134
1862	On continuous modelling of smooth contact surfaces using NURBS and application to 2D problems. 2003 , 57, 2177-2203		57
1861	Geometrically non-linear and consistently linearized embedded strong discontinuity models for 3D problems with an application to the dissection analysis of soft biological tissues. 2003 , 192, 5059-5098		63
1860	Invariant formulation of hyperelastic transverse isotropy based on polyconvex free energy functions. 2003 , 40, 401-445		283
1859	A boundary element technique for incremental, non-linear elasticity: Part I: Formulation. 2003 , 192, 2461-2479	12	
1858	Determination of constitutive equations for human arteries from clinical data. 2003 , 36, 165-9		99
1857	Review Paper: Continuum biomechanics of soft biological tissues. 2003 , 459, 3-46		370
1856	A theoretical study of the hyperelasticity of electro-gels. 2003 , 459, 2121-2130		19
1855	Dynamic finite element implementation of nonlinear, anisotropic hyperelastic biological membranes. 2003 , 6, 33-44		31

1854	The Influence of Initial Stresses on Blood Vessel Mechanics. 2003 , 03, 215-229	1
1853	Frame-Invariant Polyconvex Strain-Energy Functions for Some Anisotropic Solids. 2003 , 8, 497-506	40
1852	Shear modulus of porcine coronary artery: contributions of media and adventitia. 2003 , 285, H1966-75	77
1851	Blood Flow Simulation in a Grid Environment. 2003 , 195-202	
1850	Computational Biomechanics of Soft Biological Tissue. 2004 ,	14
1849	Role of aortic root motion in the pathogenesis of aortic dissection. 2004 , 109, 763-9	144
1848	Restricting the Hyperelastic Models for Elastomers Based on Some Thermodynamical, Mechanical, and Empirical Criteria. 2004 , 36, 159-175	11
1847	Constitutive theories based on the multiplicative decomposition of deformation gradient: Thermoelasticity, elastoplasticity, and biomechanics. 2004 , 57, 95-108	182
1846	A constitutive formulation of arterial mechanics including vascular smooth muscle tone. 2004 , 287, H1335-43	137
1845	High-Fidelity Micromechanical Modeling of Continuously Reinforced Elastic Multiphase Materials Undergoing Finite Deformations. 2004 , 9, 599-628	19
1844	Automatic analysis of collagen fiber orientation in the outermost layer of human arteries. 2004 , 7, 269-284	25
1843	Computational modeling of healing: an application of the material force method. 2004 , 2, 187-203	12
1842	Towards in vivo aorta material identification and stress estimation. 2004 , 2, 169-86	50
1841	Hemodynamics and wall mechanics in human carotid bifurcation and its consequences for atherogenesis: investigation of inter-individual variation. 2004 , 3, 17-32	119
1840	A mathematical model for the growth of the abdominal aortic aneurysm. 2004 , 3, 98-113	154
1839	A finite element model for performing intravascular ultrasound elastography of human atherosclerotic coronary arteries. 2004 , 30, 803-13	54
1838	A phenomenological model for atherosclerotic plaque growth and rupture. 2004 , 227, 437-43	44
1837	A Simple Model for Anisotropic Damage with Applications to Soft Tissues. 2004 , 4, 236-237	10

1836	Theoretical model and experimental results for the nonlinear elastic behavior of human annulus fibrosus. 2004 , 22, 901-9	123
1835	A strain energy function for arteries accounting for wall composition and structure. 2004 , 37, 989-1000	251
1834	A computational model for collagen fibre remodelling in the arterial wall. 2004 , 226, 53-64	140
1833	Mathematical Modelling and Numerical Simulation of the Cardiovascular System. 2004 , 12, 3-127	70
1832	A rheological network model for the continuum anisotropic and viscoelastic behavior of soft tissue. 2004 , 3, 56-65	77
1831	Effects of a sustained extension on arterial growth and remodeling: a theoretical study. 2005 , 38, 1255-61	66
1830	Mechanical response of fiber-reinforced incompressible non-linearly elastic solids. 2005 , 40, 213-227	186
1829	A one-dimensional model for blood flow in prestressed vessels. 2005 , 24, 23-33	7
1828	A variational approach for materially stable anisotropic hyperelasticity. 2005 , 42, 4352-4371	132
1827	Mechanical modeling of growth considering domain variation. Part I: constitutive framework. 2005 , 42, 4311-4337	13
1826	Physically motivated invariant formulation for transversely isotropic hyperelasticity. 2005 , 42, 6015-6031	28
1825	Aspects of Modeling and Computer Simulation of Soft Tissues: Applications to Arterial Walls. 2005 , 36, 795-801	9
1824	A microstructural hyperelastic model of pulmonary arteries under normo- and hypertensive conditions. 2005 , 33, 1042-52	39
1823	Inverse parameter fitting of biological tissues: a response surface approach. 2005 , 33, 1819-30	22
1822	A new wall stress equation for aneurysm-rupture prediction. 2005 , 33, 209-13	38
1821	Instability analysis in pressurized transversely isotropic Saint-Venant-Birchhoff and neo-Hookean cylindrical thick shells. 2005 , 74, 600-617	6
1820	Modelling of anisotropic growth in biological tissues. A new approach and computational aspects. 2005 , 3, 147-71	107
1819	Nonlinear viscoelastic, thermodynamically consistent, models for biological soft tissue. 2005 , 3, 172-89	52

1818	Aorta in vivo parameter identification using an axial force constraint. 2005 , 3, 191-9		30
1817	A simple model for shear stress mediated lumen reduction in blood vessels. 2005 , 4, 57-61		27
1816	An inelastic multi-mechanism constitutive equation for cerebral arterial tissue. 2005 , 4, 235-48		43
1815	Finite element implementation of a generalized Fung-elastic constitutive model for planar soft tissues. 2005 , 4, 190-9		119
1814	Plane Strain Bending of Cylindrical Sectors of Admissible Compressible Hyperelastic Materials. <i>Journal of Elasticity</i> , 2005 , 81, 129-151	1.5	4
1813	On compatible strain with reference to biomechanics of soft tissues. 2005 , 85, 440-448		2
1812	A general polyconvex strain-energy function for fiber-reinforced materials. 2005 , 5, 245-246		51
1811	Biaxial elastic material properties of porcine coronary media and adventitia. 2005 , 288, H2581-7		63
1810	Differential growth and instability in elastic shells. 2005 , 94, 198103		145
1809	A structural constitutive model for collagenous cardiovascular tissues incorporating the angular fiber distribution. 2005 , 127, 494-503		104
1808	Heat-induced changes in the finite strain viscoelastic behavior of a collagenous tissue. 2005 , 127, 580-6		21
1807	Mechanical characterization of anisotropic planar biological soft tissues using large indentation: a computational feasibility study. 2006 , 128, 428-36		30
1806	Determination of layer-specific mechanical properties of human coronary arteries with nonatherosclerotic intimal thickening and related constitutive modeling. 2005 , 289, H2048-58		619
1805	Influence of corneal biomechanical properties on intraocular pressure measurement: quantitative analysis. 2005 , 31, 146-55		519
1804	Age-related increase in wall stress of the human abdominal aorta: an in vivo study. 2005 , 42, 926-31		40
1803	Three-dimensional mechanical properties of porcine coronary arteries: a validated two-layer model. 2006 , 291, H1200-9		79
1802	On the convexity of transversely isotropic chain network models View all notes . 2006 , 86, 3241-3258		23
1801	Hyperelastic modelling of arterial layers with distributed collagen fibre orientations. 2006 , 3, 15-35		1437

1800	Biomechanics of the cardiovascular system: the aorta as an illustratory example. 2006 , 3, 719-40	76
1799	Mesoscale bounds in finite elasticity and thermoelasticity of random composites. 2006 , 462, 1167-1180	17
1798	Simulation of In-stent Restenosis for the Design of Cardiovascular Stents. 2006 , 255-267	11
1797	Modeling of Eigenstresses and Damage in Arterial Walls. 2006 , 6, 127-128	1
1796	Remarks on cavity formation in fiber-reinforced incompressible non-linearly elastic solids. 2006 , 25, 778-792	23
1795	A polyconvex framework for soft biological tissues. Adjustment to experimental data. 2006 , 43, 6052-6070	222
1794	Simulation of discontinuous damage incorporating residual stresses in circumferentially overstretched atherosclerotic arteries. 2006 , 2, 609-18	98
1793	Dynamic pre-processing software for the hyperviscoelastic modeling of complex anisotropic biological tissue materials. 2006 , 37, 609-623	5
1792	A constitutive model for protein-based materials. 2006 , 27, 5315-25	17
1791	Modeling the propagation of arterial dissection. 2006 , 25, 617-633	87
1790	The influence of the invariant I_8 on the stress-deformation and ellipticity characteristics of doubly fiber-reinforced non-linearly elastic solids. 2006 , 41, 556-563	61
1789	A stochastic-structurally based three dimensional finite-strain damage model for fibrous soft tissue. 2006 , 54, 864-886	80
1788	A composites-based hyperelastic constitutive model for soft tissue with application to the human annulus fibrosus. 2006 , 54, 1952-1971	116
1787	Determination of material models for arterial walls from uniaxial extension tests and histological structure. 2006 , 238, 290-302	231
1786	On constitutive equations for fiber-reinforced nonlinearly viscoelastic solids. 2006 , 33, 764-770	22
1785	Elastic and rupture properties of porcine aortic tissue measured using inflation testing. 2006 , 6, 123-31	40
1784	Role of facet curvature for accurate vertebral facet load analysis. 2006 , 15, 849-56	17
1783	A polyconvex anisotropic strain-energy function for soft collagenous tissues. 2006 , 5, 17-26	50

1782	Modeling initial strain distribution in soft tissues with application to arteries. 2006 , 5, 27-38	21
1781	A model for the human cornea: constitutive formulation and numerical analysis. 2006 , 5, 237-46	149
1780	A constitutive model of the posterior cruciate ligament. 2006 , 28, 99-113	26
1779	Bubble-test method for synthetic and bovine vascular material. 2006 , 39, 1939-42	4
1778	On the numerical treatment of initial strains in biological soft tissues. 2006 , 68, 836-860	37
1777	Influence of initial geometric imperfections on the stability of thick cylindrical shells under internal pressure. 2006 , 23, 577-597	6
1776	A theoretical model of enlarging intracranial fusiform aneurysms. 2006 , 128, 142-9	216
1775	An Anisotropic Hyperelastic Constitutive Model With Fiber-Matrix Shear Interaction for the Human Annulus Fibrosus. 2006 , 73, 815-824	104
1774	Biomechanical modeling of refractive corneal surgery. 2006 , 128, 150-60	112
1773	Microplane constitutive model and computational framework for blood vessel tissue. 2006 , 128, 419-27	28
1772	Directional, regional, and layer variations of mechanical properties of esophageal tissue and its interpretation using a structure-based constitutive model. 2006 , 128, 409-18	42
1771	3D Mechanical properties of the layered esophagus: experiment and constitutive model. 2006 , 128, 899-908	48
1770	Growth in Soft Biological Tissue and Residual Stress Development. 2006 , 47-62	16
1769	Effects of stent design parameters on normal artery wall mechanics. 2006 , 128, 757-65	101
1768	Wireless communicative stent for follow-up of abdominal aortic aneurysm. 2006 ,	6
1767	Effect of elastin degradation on carotid wall mechanics as assessed by a constituent-based biomechanical model. 2007 , 292, H2754-63	118
1766	Surrounding tissues affect the passive mechanics of the vessel wall: theory and experiment. 2007 , 293, H3290-300	63
1765	Theoretical and electrophysiological evidence for axial loading about aortic baroreceptor nerve terminals in rats. 2007 , 293, H3659-72	12

1764	Nonlinear anisotropic stress analysis of anatomically realistic cerebral aneurysms. 2007 , 129, 88-96	34
1763	Application of a microstructural constitutive model of the pulmonary artery to patient-specific studies: validation and effect of orthotropy. 2007 , 129, 193-201	15
1762	Hyperelastic anisotropic microplane constitutive model for annulus fibrosus. 2007 , 129, 632-41	30
1761	Finite element modeling of the left atrium to facilitate the design of an endoscopic atrial retractor. 2007 , 129, 825-37	12
1760	Constitutive model for fiber-reinforced materials with deformable matrices. 2007 , 76, 041903	19
1759	On Constitutive Equations For Anisotropic Nonlinearly Viscoelastic Solids. 2007 , 12, 131-147	19
1758	Regional multiaxial mechanical properties of the porcine anterior lens capsule. 2007 , 129, 97-104	28
1757	Numerical simulation of residual stresses in arterial walls. 2007 , 39, 117-123	20
1756	A method for the approximation of non-uniform fiber misalignment in textile composites using picture frame test. 2007 , 38, 1493-1501	30
1755	Computational stress-deformation analysis of arterial walls including high-pressure response. 2007 , 116, 78-85	87
1754	Biochemical and Biomechanical Aspects of Blood Flow. 2007 , 33-100	
1753	Three-part passive constitutive laws for the aorta in simple elongation. 2007 , 31, 397-409	6
1752	Multiscale, structure-based modeling for the elastic mechanical behavior of arterial walls. 2007 , 129, 611-8	87
1751	Flow-induced shear strain in intima of porcine coronary arteries. 2007 , 103, 587-93	9
1750	Computational method of inverse elastostatics for anisotropic hyperelastic solids. 2007 , 69, 1239-1261	54
1749	An uncoupled directional damage model for fibred biological soft tissues. Formulation and computational aspects. 2007 , 69, 2036-2057	107
1748	Transversely isotropic membrane shells with application to mitral valve mechanics. Constitutive modelling and finite element implementation. 2007 , 71, 987-1008	89
1747	A computational framework for network modeling of fibrous biological tissue deformation and rupture. 2007 , 196, 2972-2980	17

1746	Theory of small on large: Potential utility in computations of fluid-solid interactions in arteries. 2007 , 196, 3070-3078	189
1745	An anisotropic visco-hyperelastic model for ligaments at finite strains. Formulation and computational aspects. 2007 , 44, 760-778	79
1744	Mechanical response of neo-Hookean fiber reinforced incompressible nonlinearly elastic solids. 2007 , 44, 1949-1969	56
1743	Swelling of an internally pressurized nonlinearly elastic tube with fiber reinforcing. 2007 , 44, 4009-4029	46
1742	Structural damage models for fibrous biological soft tissues. 2007 , 44, 5894-5911	59
1741	Modeling the anisotropic finite-deformation viscoelastic behavior of soft fiber-reinforced composites. 2007 , 44, 8366-8389	61
1740	The effect of fiber recruitment on the swelling of a pressurized anisotropic non-linearly elastic tube. 2007 , 42, 258-270	16
1739	A constitutive model for fibrous tissues considering collagen fiber crimp. 2007 , 42, 391-402	60
1738	On thermodynamically consistent constitutive equations for fiber-reinforced nonlinearly viscoelastic solids with application to biomechanics. 2007 , 34, 561-571	20
1737	Radial metrology application to whole-body measurement on hyperelastic tubular samples. 2007 , 45, 1059-1066	4
1736	A model for saccular cerebral aneurysm growth by collagen fibre remodelling. 2007 , 247, 775-87	87
1735	Stress-modulated collagen fiber remodeling in a human carotid bifurcation. 2007 , 248, 460-70	52
1734	Comparison of mechanical behavior among the extrapulmonary arteries from rats. 2007 , 40, 812-9	17
1733	A volumetric model for growth of arterial walls with arbitrary geometry and loads. 2007 , 40, 961-71	38
1732	Numerical analysis of pulsatile blood flow and vessel wall mechanics in different degrees of stenoses. 2007 , 40, 3715-24	105
1731	Large-scale simulation of arterial walls: mechanical modeling. 2007 , 7, 4020017-4020018	
1730	Ageing of the conduit arteries. 2007 , 211, 157-72	449
1729	Structural strain energy function applied to the ageing of the human aorta. 2007 , 40, 3061-9	58

1728	On the Active Response of Soft Living Tissues. <i>Journal of Elasticity</i> , 2007 , 88, 27-39	1.5	93
1727	A polyconvex hyperelastic model for fiber-reinforced materials in application to soft tissues. 2007 , 42, 8853-8863		82
1726	Fluid-structure interaction within a layered aortic arch model. 2006 , 32, 435-54		37
1725	Transient, three-dimensional, multiscale simulations of the human aortic valve. 2007 , 7, 140-55		111
1724	Stress-driven collagen fiber remodeling in arterial walls. 2007 , 6, 163-75		134
1723	Introducing mesoscopic information into constitutive equations for arterial walls. 2007 , 6, 333-44		51
1722	Mechanical properties and compositions of tissue engineered and native arteries. 2007 , 35, 348-55		112
1721	Layer-specific 3D residual deformations of human aortas with non-atherosclerotic intimal thickening. 2007 , 35, 530-45		160
1720	Modeling plaque fissuring and dissection during balloon angioplasty intervention. 2007 , 35, 711-23		66
1719	Biochemomechanics of cerebral vasospasm and its resolution: II. Constitutive relations and model simulations. 2007 , 35, 1498-509		70
1718	An ultrastructural analysis of collagen in tissue engineered arteries. 2007 , 35, 1749-55		47
1717	Assessing the use of the "opening angle method" to enforce residual stresses in patient-specific arteries. 2007 , 35, 1821-37		67
1716	A numerical model to study the interaction of vascular stents with human atherosclerotic lesions. 2007 , 35, 1857-69		59
1715	Finite Element Modeling of Balloon Angioplasty by Considering Overstretch of Remnant Non-diseased Tissues in Lesions. 2007 , 40, 47-60		50
1714	Computational Modelling of Diarthrodial Joints. Physiological, Pathological and Pos-Surgery Simulations. 2007 , 14, 47-91		39
1713	A procedure to simulate coronary artery bypass graft surgery. 2007 , 45, 819-27		33
1712	The rectilinear shear of fiber-reinforced incompressible non-linearly elastic solids. 2007 , 42, 342-354		20
1711	Modeling the mechanics of tissue-engineered human heart valve leaflets. 2007 , 40, 325-34		73

1710	Stress-strain behavior of the passive basilar artery in normotension and hypertension. 2007 , 40, 2559-63	41
1709	The mathematical formulation of a generalized Hooke's law for blood vessels. 2007 , 28, 3569-78	14
1708	Prediction of arterial failure based on a microstructural bi-layer fiber-matrix model with softening. 2008 , 41, 447-53	66
1707	A variational constitutive model for soft biological tissues. 2008 , 41, 1458-66	57
1706	On modelling nonlinear viscoelastic effects in ligaments. 2008 , 41, 2659-66	58
1705	Characterization of arterial wall mechanical behavior and stresses from human clinical data. 2008 , 41, 2618-27	91
1704	Stress related collagen ultrastructure in human aortic valves--implications for tissue engineering. 2008 , 41, 2612-7	39
1703	Experimental study and constitutive modelling of the passive mechanical properties of the ovine infrarenal vena cava tissue. 2008 , 41, 3038-45	51
1702	Convex Fung-type potentials for biological tissues. 2008 , 43, 279-288	24
1701	Passive mechanical properties and constitutive modeling of blood vessels in relation to microstructure. 2008 , 46, 1187-99	23
1700	Mechanical Models of Artery Walls. 2008 , 15, 1-36	38
1699	Remodelling of the angular collagen fiber distribution in cardiovascular tissues. 2008 , 7, 93-103	96
1698	Growth and remodeling in a thick-walled artery model: effects of spatial variations in wall constituents. 2008 , 7, 245-62	120
1697	A microstructurally motivated model of the mechanical behavior of tissue engineered blood vessels. 2008 , 36, 1782-92	20
1696	Biaxial response of passive human cerebral arteries. 2008 , 36, 2028-41	33
1695	Fluid-structure interaction modeling of a patient-specific cerebral aneurysm: influence of structural modeling. 2008 , 43, 151-159	127
1694	Fluid flow of incompressible viscous fluid through a non-linear elastic tube. 2008 , 78, 895-907	3
1693	A microstructurally motivated anisotropic viscoelastic model for soft tissues. 2008 , 8, 10171-10172	1

1692	Quantifying the contributions of structure to the annulus fibrosus mechanical function using a nonlinear, anisotropic, hyperelastic model. 2008 , 26, 1675; author reply 1675-6	1
1691	On finite-strain damage of viscoelastic-fibred materials. Application to soft biological tissues. 2008 , 74, 1198-1218	45
1690	Smooth contact strategies with emphasis on the modeling of balloon angioplasty with stenting. 2008 , 75, 826-855	12
1689	Strain field measurements on mouse carotid arteries using microscopic three-dimensional digital image correlation. 2008 , 84, 178-90	97
1688	Simulation of Deformation, Damage and Residual Stresses in Arterial Walls. 2008 , 10, 315-321	4
1687	Mechanical characterization of anisotropic planar biological soft tissues using finite indentation: experimental feasibility. 2008 , 41, 422-9	55
1686	Finite element simulation of arcuates for astigmatism correction. 2008 , 41, 797-805	55
1685	Modelling adaptative volumetric finite growth in patient-specific residually stressed arteries. 2008 , 41, 1773-81	26
1684	A new constitutive model for multi-layered collagenous tissues. 2008 , 41, 2766-71	55
1683	Towards an analytical model of soft biological tissues. 2008 , 41, 3309-13	76
1682	An approach to the mechanical constitutive modelling of arterial tissue based on homogenization and optimization. 2008 , 41, 2673-80	37
1681	A multiscale computational comparison of the bicuspid and tricuspid aortic valves in relation to calcific aortic stenosis. 2008 , 41, 3482-7	99
1680	Quantification of the mechanical behavior of carotid arteries from wild-type, dystrophin-deficient, and sarcoglycan-delta knockout mice. 2008 , 41, 3213-8	57
1679	Wrinkling of anisotropic soft membranes. 2008 , 35, 246-255	1
1678	A methodology to study the morphologic changes in lesions during in vitro angioplasty using MRI and image processing. 2008 , 12, 163-73	4
1677	Finite element implementation of a stochastic three dimensional finite-strain damage model for fibrous soft tissue. 2008 , 197, 946-958	31
1676	Application of the natural element method to finite deformation inelastic problems in isotropic and fiber-reinforced biological soft tissues. 2008 , 197, 1983-1996	14
1675	On the permeability of fibre-reinforced porous materials. 2008 , 45, 2160-2172	49

1674	Residual stresses in soft tissue as a consequence of growth and remodeling: application to an arterial geometry. 2008 , 27, 959-974	40
1673	An energetic approach to the analysis of anisotropic hyperelastic materials. 2008 , 46, 164-181	25
1672	Numerical modelling of fracture in human arteries. 2008 , 11, 553-67	55
1671	Real-time deformable models of non-linear tissues by model reduction techniques. 2008 , 91, 223-31	80
1670	Smooth muscle contraction: mechanochemical formulation for homogeneous finite strains. 2008 , 96, 465-81	75
1669	Tissue tension and axial growth of cylindrical structures in plants and elastic tissues. 2008 , 84, 58004	49
1668	Normal basilar artery structure and biaxial mechanical behaviour. 2008 , 11, 539-51	67
1667	Muscle performance in a soft-bodied terrestrial crawler: constitutive modelling of strain-rate dependency. 2008 , 5, 349-62	38
1666	Modelling and convergence in arterial wall simulations using a parallel FETI solution strategy. 2008 , 11, 569-83	39
1665	Functional tissue-engineered valves from cell-remodeled fibrin with commissural alignment of cell-produced collagen. 2008 , 14, 83-95	100
1664	Asymmetric mechanical properties of porcine aortic sinuses. 2008 , 85, 1631-8	33
1663	Assessment of true intraocular pressure: the gap between theory and practical data. 2008 , 53, 203-18	139
1662	An anisotropic model for tissue growth and remodeling during early development of cerebral aneurysms. 2008 , 43, 565-577	13
1661	Non-linear viscoelastic behavior of abdominal aortic aneurysm thrombus. 2008 , 7, 127-37	46
1660	Soft tissue modelling for applications in virtual surgery and surgical robotics. 2008 , 11, 351-66	76
1659	Mechanical stresses in abdominal aortic aneurysms: influence of diameter, asymmetry, and material anisotropy. 2008 , 130, 021023	116
1658	A structural model of the venous wall considering elastin anisotropy. 2008 , 130, 031017	34
1657	Modeling of saccular aneurysm growth in a human middle cerebral artery. 2008 , 130, 051012	35

1656	Numerical approximation of tangent moduli for finite element implementations of nonlinear hyperelastic material models. 2008 , 130, 061003	66
1655	Three-dimensional modeling and computational analysis of the human cornea considering distributed collagen fibril orientations. 2008 , 130, 061006	151
1654	A nonlinear anisotropic viscoelastic model for the tensile behavior of the corneal stroma. 2008 , 130, 041020	69
1653	The validation of a generalized Hooke's law for coronary arteries. 2008 , 294, H66-73	15
1652	Estimation of the distributions of anisotropic, elastic properties and wall stresses of saccular cerebral aneurysms by inverse analysis. 2008 , 464, 807-825	36
1651	Wall stress and flow dynamics in abdominal aortic aneurysms: finite element analysis vs. fluid-structure interaction. 2008 , 11, 301-22	115
1650	On planar biaxial tests for anisotropic nonlinearly elastic solids. A continuum mechanical framework. 2009 , 14, 474-489	129
1649	Differential growth and residual stress in cylindrical elastic structures. 2009 , 367, 3607-30	37
1648	MECHANISM OF LEFT VENTRICULAR PRESSURE INCREASE DURING ISOVOLUMIC CONTRACTION, AND DETERMINATION OF ITS EQUIVALENT MYOCARDIAL FIBERS ORIENTATION. 2009 , 09, 177-198	7
1647	Stresses in peripheral arteries following stent placement: a finite element analysis. 2009 , 12, 25-33	52
1646	Anisotropy and Nonlinear Elasticity in Arterial Wall Mechanics. 2009 , 179-258	22
1645	Inverse finite element analysis of indentation tests to determine hyperelastic parameters of soft-tissue layers. 2009 , 44, 347-362	10
1644	Finite element model of the patched human carotid. 2009 , 43, 533-41	10
1643	Invariant-based anisotropic constitutive models of the healthy and aneurysmal abdominal aortic wall. 2009 , 131, 021009	25
1642	A phenomenological approach toward patient-specific computational modeling of articular cartilage including collagen fiber tracking. 2009 , 131, 091006	38
1641	Influence of medial collagen organization and axial in situ stretch on saccular cerebral aneurysm growth. 2009 , 131, 101010	18
1640	3D MRI-based anisotropic FSI models with cyclic bending for human coronary atherosclerotic plaque mechanical analysis. 2009 , 131, 061010	64
1639	Coupling the hemodynamic environment to the evolution of cerebral aneurysms: computational framework and numerical examples. 2009 , 131, 101003	59

1638	A structural multi-mechanism damage model for cerebral arterial tissue. 2009 , 131, 101013	33
1637	A methodology to analyze changes in lipid core and calcification onto fibrous cap vulnerability: the human atherosclerotic carotid bifurcation as an illustratory example. 2009 , 131, 121002	44
1636	A new observation on the stress distribution in the coronary artery wall. 2009 , 131, 111011	6
1635	A novel cylindrical biaxial computer-controlled bioreactor and biomechanical testing device for vascular tissue engineering. 2009 , 15, 3331-40	30
1634	Myocardial material parameter estimation: a comparison of invariant based orthotropic constitutive equations. 2009 , 12, 283-95	13
1633	The Effect of Evolving Damage on the Finite Strain Response of Inelastic and Viscoelastic Composites. 2009 , 2, 1858-1894	3
1632	Modeling the Mechanical Behavior of Lung Tissue at the Microlevel. 2009 , 135, 434-438	28
1631	Risk evaluation and interventional planning for cerebral aneurysms: computational models for growth, coiling and thrombosis. 2009 , 23, 595-607	5
1630	Quantifying nonlinear anisotropic elastic material properties of biological tissue by use of membrane inflation. 2009 , 12, 353-69	20
1629	VASCULAR MECHANICS, MECHANOBIOLOGY, AND REMODELING. 2009 , 9, 243-257	30
1628	Modelling evolution of saccular cerebral aneurysms. 2009 , 44, 375-389	18
1627	A finite dissipative theory of temporary interfibrillar bridges in the extracellular matrix of ligaments and tendons. 2009 , 6, 909-24	43
1626	Hyperelastic Model of Anisotropic Fiber Reinforcements within Intestinal Walls for Applications in Medical Robotics. 2009 , 28, 1279-1288	64
1625	In vivo IVUS-based 3-D fluid-structure interaction models with cyclic bending and anisotropic vessel properties for human atherosclerotic coronary plaque mechanical analysis. 2009 , 56, 2420-8	76
1624	Fluid-structure interaction analysis of a patient-specific right coronary artery with physiological velocity and pressure waveforms. 2009 , 25, 565-580	88
1623	Computational Continuum Biomechanics with Application to Swelling Media and Growth Phenomena. 2009 , 32, 135-156	12
1622	A Computational Framework for Patient-Specific Analysis of Articular Cartilage Incorporating Structural Information from DT-MRI. 2009 , 32, 157-177	
1621	A Universal Model for the Elastic, Inelastic and Active Behaviour of Soft Biological Tissues. 2009 , 32, 221-236	12

1620	On the use of non-linear transformations for the evaluation of anisotropic rotationally symmetric directional integrals. Application to the stress analysis in fibred soft tissues. 2009 , 79, 474-504	25
1619	Numerical integration on the sphere and its effect on the material symmetry of constitutive equations—A comparative study. 2009 , 81, n/a-n/a	75
1618	Stress field in actin gel growing on spherical substrate. 2009 , 8, 9-24	9
1617	Evolving mechanical properties of a model of abdominal aortic aneurysm. 2009 , 8, 25-42	95
1616	Determination of human arterial wall parameters from clinical data. 2009 , 8, 141-8	43
1615	A structural constitutive model for the human lens capsule. 2009 , 8, 217-31	29
1614	The modelling of fibre reorientation in soft tissue. 2009 , 8, 359-70	19
1613	Origin of axial prestretch and residual stress in arteries. 2009 , 8, 431-46	134
1612	Nonlinear solid finite element analysis of mitral valves with heterogeneous leaflet layers. 2009 , 43, 353-368	48
1611	Experimental studies and numerical analysis of the inflation and interaction of vascular balloon catheter-stent systems. 2009 , 37, 315-30	47
1610	Mechanics of carotid arteries in a mouse model of Marfan Syndrome. 2009 , 37, 1093-104	68
1609	An experimental and theoretical study on the anisotropy of elastin network. 2009 , 37, 1572-83	86
1608	A simulation of vessel-clamp interaction: transient closure dynamics. 2009 , 37, 1772-80	12
1607	The effect of material model formulation in the stress analysis of abdominal aortic aneurysms. 2009 , 37, 2218-21	49
1606	On modelling of anisotropic viscoelasticity for soft tissue simulation: numerical solution and GPU execution. 2009 , 13, 234-44	89
1605	On parameter estimation for biaxial mechanical behavior of arteries. 2009 , 42, 524-30	51
1604	On modelling damage process in vaginal tissue. 2009 , 42, 642-51	64
1603	The role of the carotid sinus in the reduction of arterial wall stresses due to head movements—potential implications for cervical artery dissection. 2009 , 42, 755-61	7

1602	A semi-analytical solution for the confined compression of hydrated soft tissue. 2009 , 44, 197-205	7
1601	Parallel Iterative Substructuring in Structural Mechanics. 2009 , 16, 425-463	20
1600	Modeling effects of axial extension on arterial growth and remodeling. 2009 , 47, 979-87	22
1599	Three-dimensional stress and strain distribution in a two-layer model of a coronary artery. 2009 , 23, 49-55	3
1598	Finite element simulations of laser refractive corneal surgery. 2009 , 25, 15-24	53
1597	Modelling Mechanical Properties in Native and Biomimetically Formed Vascular Grafts. 2009 , 6, 371-377	3
1596	Simulation of Damage Hysteresis in Soft Biological Tissues. 2009 , 9, 155-156	4
1595	An anisotropic viscoelastic model for collagenous soft tissues at large strains [Computational aspects. 2009 , 9, 161-162	
1594	Propagation and interaction of non-linear elastic plane waves in soft solids. 2009 , 44, 494-498	6
1593	Modeling of anisotropic softening phenomena: Application to soft biological tissues. 2009 , 25, 901-919	76
1592	Inhomogeneous shear of orthotropic incompressible non-linearly elastic solids: Singular solutions and biomechanical interpretation. 2009 , 47, 1170-1181	9
1591	Inflation of a circular elastomeric membrane into a horizontally semi-infinite liquid reservoir of finite vertical depth: Estimation of material parameters from volume-pressure data. 2009 , 47, 718-734	2
1590	The elasticity of arterial tissue affected by Marfan's syndrome. 2009 , 36, 659-668	35
1589	An anisotropic pseudo-elastic approach for modelling Mullins effect in fibrous biological materials. 2009 , 36, 784-790	45
1588	Mechanical properties of arteries cryopreserved at -80 degrees C and -150 degrees C. 2009 , 31, 825-32	20
1587	Mechanical behavior of human aortas: Experiments, material constants and 3-D finite element modeling including residual stress. 2009 , 42, 996-1004	50
1586	Modelling the mechanical response of elastin for arterial tissue. 2009 , 42, 1320-5	63
1585	An experimental study on the ultimate strength of the adventitia and media of human atherosclerotic carotid arteries in circumferential and axial directions. 2009 , 42, 2535-9	79

1584	Biomechanical and histological characteristics of passive esophagus: experimental investigation and comparative constitutive modeling. 2009 , 42, 2654-63	42
1583	Constitutive modeling of crimped collagen fibrils in soft tissues. 2009 , 2, 522-33	120
1582	Anisotropic micro-sphere-based finite elasticity applied to blood vessel modelling. 2009 , 57, 178-203	94
1581	Mechanics of composites with two families of finitely extensible fibers undergoing large deformations. 2009 , 57, 1165-1181	29
1580	Soft-cuticle biomechanics: a constitutive model of anisotropy for caterpillar integument. 2009 , 256, 447-57	37
1579	Elastic properties of anisotropic vascular membranes examined by inverse analysis. 2009 , 198, 3622-3632	28
1578	A Computational Framework for Fluid-Solid-Growth Modeling in Cardiovascular Simulations. 2009 , 198, 3583-3602	156
1577	Open Problems in Computational Vascular Biomechanics: Hemodynamics and Arterial Wall Mechanics. 2009 , 198, 3514-3523	105
1576	Modélisation de tissus biologiques en hyperélasticité anisotrope. Étude théorique et approche éléments finis. 2009 , 337, 101-106	10
1575	On the Mullins effect and hysteresis of fibered biological materials: A comparison between continuous and discontinuous damage models. 2009 , 46, 1727-1735	61
1574	A structural multi-mechanism constitutive equation for cerebral arterial tissue. 2009 , 46, 2920-2928	35
1573	Computational modelling for cerebral aneurysms: risk evaluation and interventional planning. 2009 , 82 Spec No 1, S62-71	16
1572	Constitutive modelling of passive myocardium: a structurally based framework for material characterization. 2009 , 367, 3445-75	448
1571	Lower- and higher-order aberrations predicted by an optomechanical model of arcuate keratotomy for astigmatism. 2009 , 35, 158-65	12
1570	Microstructurally motivated constitutive modeling of mouse arteries cultured under altered axial stretch. 2009 , 131, 101015	25
1569	Abdominal aortic aneurysm risk of rupture: patient-specific FSI simulations using anisotropic model. 2009 , 131, 031001	93
1568	Parameter sensitivity study of a constrained mixture model of arterial growth and remodeling. 2009 , 131, 101006	40
1567	Bioengineering challenges for heart valve tissue engineering. 2009 , 11, 289-313	208

1566	Complementary vasoactivity and matrix remodelling in arterial adaptations to altered flow and pressure. 2009 , 6, 293-306	162
1565	Fluid structure interaction for patient specific risk assessment in ruptured abdominal aortic aneurysms. 2009 ,	
1564	Evaluation of fundamental hypotheses underlying constrained mixture models of arterial growth and remodelling. 2009 , 367, 3585-606	77
1563	A fibre-reinforced fluid model of anisotropic plant cell growth. 2010 , 655, 472-503	53
1562	A unified multiscale mechanical model for soft collagenous tissues with regular fiber arrangement. 2010 , 43, 355-63	81
1561	Propagation of harmonic waves in prestressed fiber viscoelastic thick tubes filled with a viscous dusty fluid. 2010 , 34, 2597-2614	5
1560	On identification of the arterial model parameters from experiments applicable <i>in vivo</i> 2010 , 80, 1232-1245	5
1559	Remodelling of living bone induced by dynamic loading and drug delivery—numerical modelling and clinical treatment. 2010 , 80, 1278-1288	5
1558	On the use of the Bingham statistical distribution in microsphere-based constitutive models for arterial tissue. 2010 , 37, 700-706	42
1557	Experimental characterization and constitutive modeling of the mechanical behavior of the human trachea. 2010 , 32, 76-82	65
1556	On the mechanical modeling of anisotropic biological soft tissue and iterative parallel solution strategies. 2010 , 80, 479-488	15
1555	Remodeling and growth of living tissue: a multiphase theory. 2010 , 80, 453-465	33
1554	Evaluating patient-specific abdominal aortic aneurysm wall stress based on flow-induced loading. 2010 , 9, 127-39	24
1553	An efficient two-stage approach for image-based FSI analysis of atherosclerotic arteries. 2010 , 9, 213-23	16
1552	On the multiscale modeling of heart valve biomechanics in health and disease. 2010 , 9, 373-87	59
1551	Characterizing the mechanical contribution of fiber angular distribution in connective tissue: comparison of two modeling approaches. 2010 , 9, 651-8	73
1550	A model for arterial adaptation combining microstructural collagen remodeling and 3D tissue growth. 2010 , 9, 671-87	30
1549	Patient-based abdominal aortic aneurysm rupture risk prediction with fluid structure interaction modeling. 2010 , 38, 3323-37	59

1548	Biomechanical and microstructural properties of common carotid arteries from fibulin-5 null mice. 2010 , 38, 3605-17	63
1547	DT-MRI based computation of collagen fiber deformation in human articular cartilage: a feasibility study. 2010 , 38, 2447-63	49
1546	Mechanics of formation and rupture of human aneurysm. 2010 , 31, 593-604	3
1545	A Computational Study of Structural Designs for a Small-Diameter Composite Vascular Graft Promoting Tissue Regeneration. 2010 , 1, 269-281	11
1544	A passive strain-energy function for elastic and muscular arteries: correlation of material parameters with histological data. 2010 , 48, 507-18	29
1543	Finite element approach applied to human digital model for biomechanical modeling. 2010 , 4, 75-82	2
1542	A numerical study of arterial media dissection processes. 2010 , 166, 21-33	33
1541	Mechanical characterization of atherosclerotic arteries using finite-element modeling: feasibility study on mock arteries. 2010 , 57, 1520-8	6
1540	Applying DTI white matter orientations to finite element head models to examine diffuse TBI under high rotational accelerations. 2010 , 103, 304-9	41
1539	Image-Based Patient-Specific Ventricle Models with Fluid-Structure Interaction for Cardiac Function Assessment and Surgical Design Optimization. 2010 , 30, 51-62	45
1538	Numerical framework for patient-specific computational modelling of vascular tissue. 2010 , 26, 35-51	36
1537	Towards a comprehensive computational model for the respiratory system. 2010 , 26, n/a-n/a	14
1536	Passive nonlinear elastic behaviour of skeletal muscle: experimental results and model formulation. 2010 , 43, 318-25	75
1535	Modeling collagen remodeling. 2010 , 43, 166-75	66
1534	A constitutive formulation of vascular tissue mechanics including viscoelasticity and softening behaviour. 2010 , 43, 984-9	55
1533	Biaxial mechanical testing of human sclera. 2010 , 43, 1696-701	89
1532	Structural analysis of the natural aortic valve in dynamics: from unpressurized to physiologically loaded. 2010 , 43, 1916-22	52
1531	Mechanical anisotropy of inflated elastic tissue from the pig aorta. 2010 , 43, 2070-8	49

1530	A transversely isotropic constitutive model of excised guinea pig spinal cord white matter. 2010 , 43, 2839-43	19
1529	Anisotropic and hyperelastic identification of in vitro human arteries from full-field optical measurements. 2010 , 43, 2978-85	104
1528	A biomechanical analysis of venous tissue in its normal and post-phlebotic conditions. 2010 , 43, 2941-7	21
1527	Scalable parallel methods for monolithic coupling in fluid-structure interaction with application to blood flow modeling. 2010 , 229, 642-659	81
1526	Bifurcation of thick-walled cylindrical shells and the mechanical response of arterial tissue affected by Marfan's syndrome. 2010 , 37, 1-6	42
1525	A new variational estimate for the effective response of hyperelastic composites. 2010 , 58, 466-483	25
1524	Methods to compute 3D residual stress distributions in hyperelastic tubes with application to arterial walls. 2010 , 48, 1066-1082	13
1523	Modeling in cardiovascular biomechanics. 2010 , 48, 1563-1575	3
1522	A 3-D Framework for Arterial Growth and Remodeling in Response to Altered Hemodynamics. 2010 , 48, 1357-1372	32
1521	Stability of localized bulging in inflated membrane tubes under volume control. 2010 , 48, 1242-1252	38
1520	Dependence of the frequency spectrum of small amplitude vibrations superimposed on finite deformations of a nonlinear, cylindrical elastic body on residual stress. 2010 , 48, 1289-1312	6
1519	On deforming a sector of a circular cylindrical tube into an intact tube: Existence, uniqueness, and stability. 2010 , 48, 1212-1224	22
1518	A closed form solution for the uniaxial tension test of biological soft tissues. 2010 , 45, 535-541	8
1517	Finite dynamic deformations of a hyperelastic, anisotropic, incompressible and prestressed tube. Applications to in vivo arteries. 2010 , 29, 523-529	11
1516	In vivo characterization of the aortic wall stress-strain relationship. 2010 , 50, 654-65	36
1515	On the biomechanical function of scaffolds for engineering load-bearing soft tissues. 2010 , 6, 2365-81	105
1514	A 3D non-Newtonian fluid-structure interaction model for blood flow in arteries. 2010 , 234, 2783-2791	61
1513	Torsional deformations in incompressible fibre-reinforced cylindrical pipes. 2010 , 29, 266-273	4

1512	On non-physical response in models for fiber-reinforced hyperelastic materials. 2010 , 47, 2056-2061	58
1511	Modeling of blood flow in arterial trees. 2010 , 2, 612-623	18
1510	Sensitivity Analysis of Plaque Components within Arterial Wall Simulations. 2010 , 10, 73-74	2
1509	The Effect of Intraocular Pressure on the Outcome of Myopic Photorefractive Keratectomy: A Numerical Approach. 2010 , 1, 461-476	7
1508	Systemic Circulation. 2010 , 91-116	
1507	A partitioned Newton method for the interaction of a fluid and a 3D shell structure. 2010 , 19, 479-512	1
1506	Modelling the layer-specific three-dimensional residual stresses in arteries, with an application to the human aorta. 2010 , 7, 787-99	136
1505	Nonlinear elasticity of biological tissues with statistical fibre orientation. 2010 , 7, 955-66	97
1504	Implémentation éphentes finis du modéle hyperélastique anisotrope HGO. 2010 , 19, 441-464	2
1503	Structural inhomogeneity and fiber orientation in the inner arterial media. 2010 , 298, H1537-45	85
1502	Third- and fourth-order elasticities of biological soft tissues. 2010 , 127, 2103-9	45
1501	Hemodynamics and Fluid-Structure-Interaction in a Virtual Heart. 2010 , 52, 250-257	
1500	Deformation measurements and material property estimation of mouse carotid artery using a microstructure-based constitutive model. 2010 , 132, 121010	23
1499	Usefulness and limitations of computational models in aortic disease risk stratification. 2010 , 52, 1572-9	21
1498	Prediction of nonlinear elastic behaviour of vaginal tissue: experimental results and model formulation. 2010 , 13, 327-37	29
1497	A Hyperelastic Approach for Composite Reinforcement Large Deformation Analysis. 2010 , 44, 5-26	79
1496	Finite element modelling of cell wall properties for onion epidermis using a fibre-reinforced hyperelastic model. 2010 , 172, 300-4	10
1495	Anisotropic and tension-compression asymmetric model for composites consolidation. 2010 , 41, 284-294	3

1494	Computational Modeling of Aortic Heart Valves. 2010 , 221-252	6
1493	Volumetric-Distortional Decomposition of Deformation and Elasticity Tensor. 2010 , 15, 672-690	29
1492	A Viscoelastic Anisotropic Model for Soft Collageneous Tissues Based on Distributed Fiber Matrix Units. 2010 , 55-65	3
1491	Constitutive modelling of arteries. 2010 , 466, 1551-1597	331
1490	Mechanical bidomain model of cardiac tissue. 2010 , 82, 041904	11
1489	The influence of fiber orientation on the equilibrium properties of neutral and charged biphasic tissues. 2010 , 132, 114506	17
1488	Variational Foundations of Large Strain Multiscale Solid Constitutive Models: Kinematical Formulation. 2010 , 341-378	14
1487	Applications of anisotropic polyconvex energies: thin shells and biomechanics of arterial walls. 2010 , 131-175	3
1486	MECHANICAL BEHAVIOUR OF TRANSVERSELY ISOTROPIC POROUS NEO-HOOKEAN SOLIDS. 2010 , 02, 11-39	12
1485	Tissue-engineered heart valves develop native-like collagen fiber architecture. 2010 , 16, 1527-37	33
1484	A constitutive model for the mechanical characterization of the plantar fascia. 2010 , 51, 337-46	23
1483	Fluid Structure Interaction for patient specific risk assessment in abdominal aortic aneurysms. 2010	
1482	Blood flow pattern in a coronary bypass with moderate stenosis. 2011 ,	0
1481	Material parameter identification of arterial wall layers from homogenised stress-strain data. 2011 , 14, 33-41	2
1480	Multiscale-patient-specific artery and atherogenesis models. 2011 , 58, 3464-8	26
1479	Indentation versus tensile measurements of Young's modulus for soft biological tissues. 2011 , 17, 155-64	422
1478	The layered structure of coronary adventitia under mechanical load. 2011 , 101, 2555-62	62
1477	Biomechanical Aspects of Abdominal Aortic Aneurysm (AAA) and its Risk of Rupture: Fluid Structure Interaction (FSI) Studies. 2011 , 181-220	6

1476	Modelling Cerebral Aneurysm Evolution. 2011 , 373-399	4
1475	Patient-Specific Modeling of the Cornea. 2011 , 461-483	2
1474	An anisotropic microsphere-based approach for fiber orientation adaptation in soft tissue. 2011 , 58, 3500-3	4
1473	Blood Flow Simulation in Atherosclerotic Vascular Network Using Fiber-Spring Representation of Diseased Wall. 2011 , 6, 333-349	8
1472	Anisotropic AAA: computational comparison between four and two fiber family material models. 2011 , 44, 2418-26	14
1471	A constitutive model for vascular tissue that integrates fibril, fiber and continuum levels with application to the isotropic and passive properties of the infrarenal aorta. 2011 , 44, 2544-50	63
1470	Evolving biaxial mechanical properties of mouse carotid arteries in hypertension. 2011 , 44, 2532-7	25
1469	A Variational Approach for Estimating the Compliance of the Cardiovascular Tissue: An Inverse Fluid-Structure Interaction Problem. 2011 , 33, 1181-1211	42
1468	A finite element model of stress-mediated vascular adaptation: application to abdominal aortic aneurysms. 2011 , 14, 803-17	48
1467	Nonlinear Elastic Scaffold Design, Modeling and Fabrication for Soft Tissue Engineering. 2011 , 35-53	3
1466	Pulmonary vascular stiffness: measurement, modeling, and implications in normal and hypertensive pulmonary circulations. 2011 , 1, 1413-35	31
1465	In vivo estimation of the contribution of elastin and collagen to the mechanical properties in the human abdominal aorta: effect of age and sex. 2011 , 110, 176-87	60
1464	A Decision Support System for Endoprosthetic Patient-Specific Surgery of the Human Trachea. 2011 , 281-334	
1463	Mesosopic approaches for understanding the mechanical behaviour of reinforcements in composites. 2011 , 486-528	
1462	Modeling failure of soft anisotropic materials with application to arteries. 2011 , 4, 1582-94	52
1461	Stiffening by fiber reinforcement in soft materials: a hyperelastic theory at large strains and its application. 2011 , 4, 1359-68	39
1460	Biaxial mechanical modeling of the small intestine. 2011 , 4, 1727-40	61
1459	Regional and fiber orientation dependent shear properties and anisotropy of bovine meniscus. 2011 , 4, 2024-30	31

1458	A mesostructurally-based anisotropic continuum model for biological soft tissues--decoupled invariant formulation. 2011 , 4, 1637-57	34
1457	A linearized and incompressible constitutive model for arteries. 2011 , 286, 85-91	13
1456	Theoretical models for coronary vascular biomechanics: progress & challenges. 2011 , 104, 49-76	51
1455	The numerical implementation of invariant-based viscoelastic formulations at finite strains. An anisotropic model for the passive myocardium. 2011 , 200, 3637-3645	24
1454	Hyperelastic modelling for mesoscopic analyses of composite reinforcements. 2011 , 71, 1623-1631	98
1453	Effects of age on the elastic properties of the intraluminal thrombus and the thrombus-covered wall in abdominal aortic aneurysms: biaxial extension behaviour and material modelling. 2011 , 42, 207-19	101
1452	Mechanical behaviour of synthetic surgical meshes: finite element simulation of the herniated abdominal wall. 2011 , 7, 3905-13	72
1451	A constitutive framework for modelling thin incompressible viscoelastic materials under plane stress in the finite strain regime. 2011 , 15, 389-406	5
1450	Solving hyperelastic material problems by asymptotic numerical method. 2011 , 47, 77-92	19
1449	A rate dependent directional damage model for fibred materials: application to soft biological tissues. 2011 , 48, 407-420	22
1448	Modeling active muscle contraction in mitral valve leaflets during systole: a first approach. 2011 , 10, 11-26	37
1447	Modelling evolution and the evolving mechanical environment of saccular cerebral aneurysms. 2011 , 10, 109-32	46
1446	A generic constitutive model for the passive porcine coronary artery. 2011 , 10, 249-58	23
1445	Role of elastin anisotropy in structural strain energy functions of arterial tissue. 2011 , 10, 599-611	37
1444	A constrained mixture model for developing mouse aorta. 2011 , 10, 671-87	24
1443	Prediction of fibre architecture and adaptation in diseased carotid bifurcations. 2011 , 10, 831-43	19
1442	Carotid artery mechanical properties and stresses quantified using in vivo data from normotensive and hypertensive humans. 2011 , 10, 867-82	28
1441	Linear and nonlinear viscoelastic modeling of aorta and carotid pressure-area dynamics under in vivo and ex vivo conditions. 2011 , 39, 1438-56	64

1440	Dissection properties and mechanical strength of tissue components in human carotid bifurcations. 2011 , 39, 1703-19	40
1439	A multi-layered computational model of coupled elastin degradation, vasoactive dysfunction, and collagenous stiffening in aortic aging. 2011 , 39, 2027-45	49
1438	On the adequacy of the existing restrictions on the constitutive relations to ensure reasonable elastic response of compressible bodies. 2011 , 38, 123-125	1
1437	Experimental study and constitutive modelling of the passive mechanical properties of the porcine carotid artery and its relation to histological analysis: Implications in animal cardiovascular device trials. 2011 , 33, 665-76	43
1436	An irreversible constitutive model for fibrous soft biological tissue: a 3-D microfiber approach with demonstrative application to abdominal aortic aneurysms. 2011 , 7, 2457-66	77
1435	A corrosion model for bioabsorbable metallic stents. 2011 , 7, 3523-33	117
1434	Analyzing the harmonic wave propagation in the layered thick tubes. 2011 , 35, 4091-4102	2
1433	FE simulation of human trachea swallowing movement before and after the implantation of an endoprosthesis. 2011 , 35, 4902-4912	12
1432	A Computer-Controlled Apparatus for the Characterization of Mechanical and Viscoelastic Properties of Tissue-Engineered Vascular Constructs. 2011 , 2, 24-34	7
1431	A Numerical Tool for the Coupled Mechanical Assessment of Anastomoses of PTFE Arterio-venous Access Grafts. 2011 , 2, 160-172	4
1430	Differential histomechanical response of carotid artery in relation to species and region: mathematical description accounting for elastin and collagen anisotropy. 2011 , 49, 867-79	27
1429	Quasi-linear viscoelastic modeling of arterial wall for surgical simulation. 2011 , 6, 829-38	15
1428	On the Incorporation of Residual Stresses in Arterial Walls. 2011 , 11, 83-84	
1427	A Coupled Model for the Left Ventricle Including Regional Differences in Structure. 2011 , 11, 85-86	1
1426	p-FEMs for hyperelastic anisotropic nearly incompressible materials under finite deformations with applications to arteries simulation. 2011 , 88, 1152-1174	15
1425	Influencing factors in image-based fluid-structure interaction computation of cerebral aneurysms. 2011 , 65, 324-340	49
1424	Computational modeling of passive myocardium. 2011 , 27, 1-12	98
1423	A model for the anisotropic response of fibrous soft tissues using six discrete fibre bundles. 2011 , 27, 1793-1811	25

1422	Bacterial cellulose as a potential vascular graft: Mechanical characterization and constitutive model development. 2011 , 97, 105-13	50
1421	A new parameter identification method of soft biological tissue combining genetic algorithm with analytical optimization. 2011 , 200, 208-215	17
1420	Fluid-structure interaction simulation of aortic blood flow. 2011 , 43, 46-57	123
1419	Multi-Physics MRI-Based Two-Layer Fluid-Structure Interaction Anisotropic Models of Human Right and Left Ventricles with Different Patch Materials: Cardiac Function Assessment and Mechanical Stress Analysis. 2011 , 89, 1059-1068	31
1418	Numerical modeling of a human stented trachea under different stent designs. 2011 , 38, 855-862	22
1417	Application of finite element analysis to the design of tissue leaflets for a percutaneous aortic valve. 2011 , 4, 85-98	42
1416	Perspectives on biological growth and remodeling. 2011 , 59, 863-883	307
1415	Surface wrinkling of mucosa induced by volumetric growth: Theory, simulation and experiment. 2011 , 59, 758-774	161
1414	A Micromechanics Finite-Strain Constitutive Model of Fibrous Tissue. 2011 , 59, 1823-1837	44
1413	Prediction of the softening and damage effects with permanent set in fibrous biological materials. 2011 , 59, 1808-1822	41
1412	A mechanochemical 3D continuum model for smooth muscle contraction under finite strains. 2011 , 268, 120-30	63
1411	A new derivation of the bifurcation conditions of inflated cylindrical membranes of elastic material under axial loading. Application to aneurysm formation. 2011 , 38, 203-210	47
1410	Numerical simulation of the failure of ventricular tissue due to deep penetration: the impact of constitutive properties. 2011 , 44, 45-51	26
1409	Growth and surface folding of esophageal mucosa: a biomechanical model. 2011 , 44, 182-8	56
1408	On a phenomenological model for active smooth muscle contraction. 2011 , 44, 2090-5	31
1407	Multi Element Diverging Beam from a Linear Array Transducer for Transverse Cross Sectional Imaging of Carotid Artery: Simulations and Phantom Vessel Validation. 2011 , 50, 07HF05	9
1406	On constitutive descriptors of the biaxial mechanical behaviour of human abdominal aorta and aneurysms. 2011 , 8, 435-50	125
1405	Biaxial biomechanical properties of self-assembly tissue-engineered blood vessels. 2011 , 8, 244-56	11

1404	Analysis of Mechanical Properties of Pipes with Helical Reinforcement under Axial Tension. 2011 , 189-193, 1822-1826	1
1403	Theory and finite element implementation of orthotropic and transversely isotropic incompressible hyperelastic membrane. 2011 , 7, 424-439	10
1402	COMPRESSION INSTABILITIES OF TISSUES WITH LOCALIZED STRAIN SOFTENING. 2011 , 03, 69-83	5
1401	Differential passive and active biaxial mechanical behaviors of muscular and elastic arteries: basilar versus common carotid. 2011 , 133, 051009	50
1400	FSI Analysis of a healthy and a stenotic human trachea under impedance-based boundary conditions. 2011 , 133, 021001	31
1399	A nonlinear biphasic fiber-reinforced porohyperviscoelastic model of articular cartilage incorporating fiber reorientation and dispersion. 2011 , 133, 081004	16
1398	The Mechanics of Native and Engineered Cardiac Soft Tissues. 2011 , 113-132	0
1397	Hermitian splines for modeling biological soft tissue systems that exhibit nonlinear force-elongation curves. 2011 , 133, 094505	
1396	Characterisation of failure in human aortic tissue using digital image correlation. 2011 , 14, 73-74	4
1395	Experimental and modeling study of collagen scaffolds with the effects of crosslinking and fiber alignment. 2011 , 2011, 172389	50
1394	FSI analysis of a human trachea before and after prosthesis implantation. 2011 , 133, 071003	27
1393	A microstructurally driven model for pulmonary artery tissue. 2011 , 133, 051002	29
1392	Linked opening angle and histological and mechanical aspects of the proximal pulmonary arteries of healthy and pulmonary hypertensive rats and calves. 2011 , 301, H1810-8	12
1391	Experimentally validated microstructural 3D constitutive model of coronary arterial media. 2011 , 133, 031007	40
1390	Wall stress of the cervical carotid artery in patients with carotid dissection: a case-control study. 2011 , 300, H1451-8	20
1389	Remodeling of the collagen fiber architecture due to compaction in small vessels under tissue engineered conditions. 2011 , 133, 071002	8
1388	Constitutive modeling of coronary arterial media--comparison of three model classes. 2011 , 133, 061008	31
1387	Comparative analysis of the biaxial mechanical behavior of carotid wall tissue and biological and synthetic materials used for carotid patch angioplasty. 2011 , 133, 111008	24

1386	Mechanical identification of hyperelastic anisotropic properties of mouse carotid arteries. 2011 , 11-17	
1385	Calculation of human femoral vein wall parameters in vivo from clinical data for specific patient. 2012 , 134, 124501	1
1384	Elastic characterization of transversely isotropic soft materials by dynamic shear and asymmetric indentation. 2012 , 134, 061004	36
1383	Viscoelastic material properties of the myocardium and cardiac jelly in the looping chick heart. 2012 , 134, 024502	17
1382	A mechanical characterization of the porcine atria at the healthy stage and after ventricular tachypacing. 2012 , 134, 021008	10
1381	In vivo and in vitro measurements of pulmonary arterial stiffness: A brief review. 2012 , 2, 505-17	28
1380	THE EFFECT OF ASYMMETRY AND AXIAL PRESTRAINING ON THE AMPLITUDE OF MECHANICAL STRESSES IN ABDOMINAL AORTIC ANEURYSM. 2012 , 12, 1250089	4
1379	AN OSMOTICALLY INFLATABLE SEAL TO TREAT ENDOLEAKS OF TYPE 1, FOLLOWING ENDOVASCULAR ANEURYSM REPAIR. 2012 , 12, 1250070	2
1378	Using in vivo Cine and 3D multi-contrast MRI to determine human atherosclerotic carotid artery material properties and circumferential shrinkage rate and their impact on stress/strain predictions. 2012 , 134, 011008	22
1377	NUMERICAL ANALYSIS OF THE WALL STRESS IN ABDOMINAL AORTIC ANEURYSM: INFLUENCE OF THE MATERIAL MODEL NEAR-INCOMPRESSIBILITY. 2012 , 12, 1250005	11
1376	GRID CONTINUUM DESCRIPTION: A NOVEL APPROACH IN TWO-SCALE HYPERELASTICITY. 2012 , 04, 1250004	
1375	Detection of Boundaries of Carotid Arterial Wall by Analyzing Ultrasonic RF Signals. 2012 , 51, 07GF07	9
1374	Determination of the layer-specific distributed collagen fibre orientations in human thoracic and abdominal aortas and common iliac arteries. 2012 , 9, 1275-86	218
1373	Large strain analysis of a soft polymer electromechanical sensor coupled to an arterial segment. 2012 , 23, 575-586	5
1372	A literature review of the numerical analysis of abdominal aortic aneurysms treated with endovascular stent grafts. 2012 , 2012, 820389	16
1371	Parallel simulation of patient-specific atherosclerotic arteries for the enhancement of intravascular ultrasound diagnostics. 2012 , 29, 888-906	25
1370	Impact of Microgravity and Partial Gravity on Cardiac Shape. 2012 ,	
1369	Histo-Mechanical Modeling of the Wall of Abdominal Aorta Aneurysms. 2012 , 45, 1035-1040	1

1368	The Effects of Brachial Arterial Stiffening on The Accuracy of Oscillometric Blood Pressure Measurement: A Computational Model Study. 2012 , 7, 15-30	4
1367	Effects of imperfections on localized bulging in inflated membrane tubes. 2012 , 370, 1896-911	36
1366	Characterization of human skin through skin expansion. 2012 , 7, 641-655	7
1365	A murine experimental model for the mechanical behaviour of viable right-ventricular myocardium. 2012 , 590, 4571-84	25
1364	A three-dimensional chemo-mechanical continuum model for smooth muscle contraction. 2012 , 13, 215-29	26
1363	A covariant constitutive theory for anisotropic hyperelastic solids with initial strains. 2012 , 17, 104-119	4
1362	A Biphasic Approach for the Simulation of Growth Processes in Soft Biological Tissues Incorporating Damage-Induced Stress Softening. 2012 , 12, 91-92	
1361	Computational hemodynamic optimization predicts dominant aortic arch selection is driven by embryonic outflow tract orientation in the chick embryo. 2012 , 11, 1057-73	19
1360	Extracellular matrix and the mechanics of large artery development. 2012 , 11, 1169-86	28
1359	Stability of aneurysm solutions in a fluid-filled elastic membrane tube. 2012 , 28, 1209-1218	31
1358	Patient-specific multiscale modeling of blood flow for coronary artery bypass graft surgery. 2012 , 40, 2228-42	128
1357	Mechanics of a fiber network within a non-fibrillar matrix: model and comparison with collagen-agarose co-gels. 2012 , 40, 2111-21	50
1356	A nonlinear constitutive model for stress relaxation in ligaments and tendons. 2012 , 40, 2541-50	31
1355	A mixed Von Mises distribution for modeling soft biological tissues with two distributed fiber properties. 2012 , 49, 2914-2923	16
1354	A method for the quantification of the pressure dependent 3D collagen configuration in the arterial adventitia. 2012 , 180, 335-42	42
1353	A texture matching method considering geometric transformations in noninvasive ultrasonic measurement of arterial elasticity. 2012 , 38, 524-33	9
1352	Mechanical identification of layer-specific properties of mouse carotid arteries using 3D-DIC and a hyperelastic anisotropic constitutive model. 2012 , 15, 37-48	33
1351	Mechanical characterisation of the human thoracic descending aorta: experiments and modelling. 2012 , 15, 185-93	38

1350	Regional mechanics determine collagen fiber structure in healing myocardial infarcts. 2012 , 52, 1083-90	80
1349	Spatial orientation of collagen fibers in the abdominal aortic aneurysm's wall and its relation to wall mechanics. 2012 , 8, 3091-103	107
1348	An anisotropic inelastic constitutive model to describe stress softening and permanent deformation in arterial tissue. 2012 , 12, 9-19	52
1347	Arterial clamping: finite element simulation and in vivo validation. 2012 , 12, 107-18	34
1346	Layer-specific damage experiments and modeling of human thoracic and abdominal aortas with non-atherosclerotic intimal thickening. 2012 , 12, 93-106	141
1345	Computational fluid-dynamics optimization of a human tracheal endoprosthesis. 2012 , 39, 575-581	6
1344	A theoretical and non-destructive experimental approach for direct inclusion of measured collagen orientation and recruitment into mechanical models of the artery wall. 2012 , 45, 762-71	121
1343	Mechanics, mechanobiology, and modeling of human abdominal aorta and aneurysms. 2012 , 45, 805-14	218
1342	A subject-specific anisotropic visco-hyperelastic finite element model of female pelvic floor stress and strain during the second stage of labor. 2012 , 45, 455-60	70
1341	Method for characterizing viscoelasticity of human gluteal tissue. 2012 , 45, 1252-8	19
1340	Patient-specific modeling of biomechanical interaction in transcatheter aortic valve deployment. 2012 , 45, 1965-71	67
1339	Contribution of elastin and collagen to the inflation response of the pig thoracic aorta: assessing elastin's role in mechanical homeostasis. 2012 , 45, 2133-41	23
1338	Effects of pressure on arterial failure. 2012 , 45, 2577-88	21
1337	Compressive properties of passive skeletal muscle-the impact of precise sample geometry on parameter identification in inverse finite element analysis. 2012 , 45, 2673-9	47
1336	Bringing Vascular Biomechanics into Clinical Practice. Simulation-Based Decisions for Elective Abdominal Aortic Aneurysms Repair. 2012 , 1-37	4
1335	Collagen. 2012 , 35-55	22
1334	Transversely isotropic cyclic stress-softening model for the Mullins effect. 2012 , 468, 4041-4057	3
1333	Applications of variational data assimilation in computational hemodynamics. 2012 , 363-394	14

1332	Structurally motivated damage models for arterial walls. Theory and application. 2012 , 143-185	4
1331	Modeling Growth in Biological Materials. 2012 , 54, 52-118	84
1330	Multi-Scale Modelling of Vascular Disease: Abdominal Aortic Aneurysm Evolution. 2012 , 309-339	2
1329	Coupling effects of void shape and void size on the growth of an elliptic void in a fiber-reinforced hyper-elastic thin plate. 2012 , 25, 312-320	3
1328	A comparative analysis of the collagen architecture in the carotid artery: second harmonic generation versus diffusion tensor imaging. 2012 , 426, 54-8	36
1327	Constitutive modeling of mouse carotid arteries using experimentally measured microstructural parameters. 2012 , 102, 2916-25	49
1326	p-FEMs in biomechanics: Bones and arteries. 2012 , 249-252, 169-184	14
1325	Construction and characterization of an electrospun tubular scaffold for small-diameter tissue-engineered vascular grafts: a scaffold membrane approach. 2012 , 13, 140-55	58
1324	Multilayer material properties of aorta determined from nanoindentation tests. 2012 , 15, 199-207	24
1323	Evaluation of migration forces of a retrievable filter: experimental setup and finite element study. 2012 , 34, 1167-76	6
1322	A numerical parametric study of the mechanical action of pulsatile blood flow onto axisymmetric stenosed arteries. 2012 , 34, 1483-95	17
1321	Comparison and critical analysis of invariant-based models with respect to their ability in fitting human aortic valve data. 2012 , 4, 1-14	18
1320	Problems and Fundamental Models for Inverse Methods in Composite Materials. 2012 , 7	
1319	Effects of dispersion of fiber orientation on the mechanical property of the arterial wall. 2012 , 301, 153-60	7
1318	Quantitative assessment of collagen fibre orientations from two-dimensional images of soft biological tissues. 2012 , 9, 3081-93	72
1317	Finite element modeling of cerebral angioplasty using a structural multi-mechanism anisotropic damage model. 2012 , 92, 457-474	13
1316	Relaxed incremental variational formulation for damage at large strains with application to fiber-reinforced materials and materials with truss-like microstructures. 2012 , 92, 551-570	23
1315	Numerical modelling of the fibre-matrix interaction in biaxial loading for hyperelastic soft tissue models. 2012 , 28, 401-11	3

1314	A three-layer model for buckling of a human aortic segment under specific flow-pressure conditions. 2012 , 28, 495-512	17
1313	Fluid-structure interaction simulations of the Fontan procedure using variable wall properties. 2012 , 28, 513-27	60
1312	Dynamical cavitation and oscillation of an anisotropic incompressible hyper-elastic sphere. 2012 , 55, 822-827	1
1311	Multiphasic Intervertebral Disc Mechanics: Theory and Application. 2012 , 19, 261-339	14
1310	Remodelling of collagen fibre transition stretch and angular distribution in soft biological tissues and cell-seeded hydrogels. 2012 , 11, 325-39	28
1309	The fiber orientation in the coronary arterial wall at physiological loading evaluated with a two-fiber constitutive model. 2012 , 11, 533-42	13
1308	Anisotropic microsphere-based approach to damage in soft fibered tissue. 2012 , 11, 595-608	34
1307	Extra-fibrillar matrix mechanics of annulus fibrosus in tension and compression. 2012 , 11, 781-90	32
1306	Elucidating atherosclerotic vulnerable plaque rupture by modeling cross substitution of ApoE-/- mouse and human plaque components stiffnesses. 2012 , 11, 801-13	14
1305	Experimental characterization of rupture in human aortic aneurysms using a full-field measurement technique. 2012 , 11, 841-53	55
1304	Characterization of changes to the mechanical properties of arteries due to cold storage using nanoindentation tests. 2012 , 40, 1434-42	22
1303	Impact of residual stretch and remodeling on collagen engagement in healthy and pulmonary hypertensive calf pulmonary arteries at physiological pressures. 2012 , 40, 1419-33	19
1302	Generalisation of elastic models for a layer with elastically restrained boundaries. 2012 , 57, 79-89	
1301	Analyzing of the effect of the dusty fluid, anisotropy and layered of the wall on the wave propagation. 2012 , 36, 2486-2497	1
1300	Constitutive framework for the modeling of damage in collagenous soft tissues with application to arterial walls. 2012 , 213-216, 139-151	100
1299	Artery active mechanical response: High order finite element implementation and investigation. 2012 , 237-240, 51-66	14
1298	Initiation of aneurysms as a mechanical bifurcation phenomenon. 2012 , 47, 179-184	29
1297	Generalisations of the strain-energy function of linear elasticity to model biological soft tissue. 2012 , 47, 268-272	8

1296	Cubically non-linear effects of plane waves in isotropic soft solid materials. 2012 , 47, 362-366	4
1295	A constitutive model for active-passive transition of muscle fibers. 2012 , 47, 377-387	27
1294	Folding of fiber composites with a hyperelastic matrix. 2012 , 49, 395-407	35
1293	Constitutive modeling of fiber composites with a soft hyperelastic matrix. 2012 , 49, 635-647	36
1292	Experiments and mechanochemical modeling of smooth muscle contraction: significance of filament overlap. 2012 , 297, 176-86	52
1291	Long time evolution of atherosclerotic plaques. 2012 , 297, 1-10	41
1290	Uniform transmural strain in pre-stressed arteries occurs at physiological pressure. 2012 , 303, 93-7	21
1289	A Multilayered Wall Model of Arterial Growth and Remodeling. 2012 , 44, 110-119	32
1288	Fiber distributed hyperelastic modeling of biological tissues. 2012 , 44, 151-162	74
1287	Elastic properties of cancellous bone in terms of elastic properties of its mineral and protein phases with application to their osteoporotic degradation. 2012 , 44, 139-150	7
1286	Elasticity and permeability of porous fibre-reinforced materials under large deformations. 2012 , 44, 58-71	71
1285	Arterial stiffness identification of the human carotid artery using the stress-strain relationship in vivo. 2012 , 52, 402-11	121
1284	Fibre-matrix interaction in the human annulus fibrosus. 2012 , 5, 193-205	19
1283	3D constitutive modeling of the biaxial mechanical response of intact and layer-dissected human carotid arteries. 2012 , 5, 116-28	75
1282	Mechanical characterization of a customized decellularized scaffold for vascular tissue engineering. 2012 , 8, 58-70	70
1281	Apparent behaviour of charged and neutral materials with ellipsoidal fibre distributions and cross-validation of finite element implementations. 2012 , 9, 122-9	6
1280	Influence of geometrical parameters on radial force during self-expanding stent deployment. Application for a variable radial stiffness stent. 2012 , 10, 166-75	59
1279	Towards a biomimetism of abdominal healthy and aneurysmal arterial tissues. 2012 , 10, 151-65	10

1278	A continuum description of the damage process in the arterial wall of abdominal aortic aneurysms. 2012 , 28, 87-99	20
1277	Computational model of soft tissues in the human upper airway. 2012 , 28, 111-32	16
1276	Augmented Lagrange methods for quasi-incompressible materials--applications to soft biological tissue. 2013 , 29, 332-50	12
1275	Numerical Comparison and Calibration of Geometrical Multiscale Models for the Simulation of Arterial Flows. 2013 , 4, 440-463	8
1274	Numerical transient state analysis of partly obstructed haemodynamics using FSI approach. 2013 , 3,	
1273	On the deformation behavior of human amnion. 2013 , 46, 1777-83	38
1272	Reality based modeling and simulation of gallbladder shape deformation using variational methods. 2013 , 8, 857-65	7
1271	WITHDRAWN: General constitutive solutions for isotropic hyperelastic materials. 2013 ,	
1270	Age-related changes in longitudinal prestress in human abdominal aorta. 2013 , 83, 875-888	24
1269	On anisotropic elasticity and questions concerning its Finite Element implementation. 2013 , 52, 1185-1197	40
1268	At least three invariants are necessary to model the mechanical response of incompressible, transversely isotropic materials. 2013 , 52, 959-969	47
1267	Power type strain energy function model and prediction of the anisotropic mechanical properties of skin using uniaxial extension data. 2013 , 51, 1147-56	4
1266	Intracranial Aneurysms: Modeling Inception and Enlargement. 2013 , 161-173	
1265	Velocity profiles in the human ductus venosus: a numerical fluid structure interaction study. 2013 , 12, 1019-35	8
1264	Determination of hyperelastic properties for umbilical artery in preeclampsia from uniaxial extension tests. 2013 , 169, 207-12	7
1263	Effects of carotid artery stenting on arterial geometry. 2013 , 217, 251-62	19
1262	Impact of weightlessness on cardiac shape and left ventricular stress/strain distributions. 2013 , 135, 121008	2
1261	A Fiber Distributed Model of Biological Tissues. 2013 , 6, 79-86	6

1260	Age-Dependent Arterial Mechanics via a Multiscale Elastic Approach. 2013 , 14, 141-151	25
1259	Experimental investigation and constitutive modeling of the 3D histomechanical properties of vein tissue. 2013 , 12, 431-51	30
1258	Mechanical, biological and structural characterization of in vitro ruptured human carotid plaque tissue. 2013 , 9, 9027-35	50
1257	Regional variations in the nonlinearity and anisotropy of bovine aortic elastin. 2013 , 12, 1181-94	19
1256	The role of 3-D collagen organization in stromal elasticity: a model based on X-ray diffraction data and second harmonic-generated images. 2013 , 12, 1101-13	52
1255	Mechanics of the mitral valve: a critical review, an in vivo parameter identification, and the effect of prestrain. 2013 , 12, 1053-71	59
1254	On the mechanical behaviour of carotid artery plaques: the influence of curve-fitting experimental data on numerical model results. 2013 , 12, 975-85	27
1253	A continuum model for skeletal muscle contraction at homogeneous finite deformations. 2013 , 12, 965-73	14
1252	Twist buckling behavior of arteries. 2013 , 12, 915-27	24
1251	Development of fibroblast-seeded collagen gels under planar biaxial mechanical constraints: a biomechanical study. 2013 , 12, 849-68	8
1250	The quasi-static failure properties of the abdominal aortic aneurysm wall estimated by a mixed experimental-numerical approach. 2013 , 41, 1554-66	32
1249	Biomechanical phenotyping of central arteries in health and disease: advantages of and methods for murine models. 2013 , 41, 1311-30	99
1248	A fiber-based constitutive model predicts changes in amount and organization of matrix proteins with development and disease in the mouse aorta. 2013 , 12, 497-510	32
1247	Finite Element simulation of buckling-induced vein tortuosity and influence of the wall constitutive properties. 2013 , 26, 119-26	15
1246	Fluid-structure interaction model of aortic valve with porcine-specific collagen fiber alignment in the cusps. 2013 , 135, 101001-6	33
1245	On the physical consistency between three-dimensional and one-dimensional models in haemodynamics. 2013 , 244, 97-112	32
1244	Growth and residual stresses of arterial walls. 2013 , 337, 80-8	10
1243	Modeling Momentum and Mass Transport in Cellular Biological Media: From the Molecular to the Tissue Scale. 2013 , 1-40	2

1242	Mechanobiology of the Arterial Wall. 2013 , 275-347	15
1241	Determination of material parameters of the two-dimensional Holzapfel-Weizsäcker type model based on uniaxial extension data of arterial walls. 2013 , 16, 358-67	7
1240	Modeling of abdominal aortic aneurism rupture by using experimental bubble inflation test. 2013 ,	2
1239	A finite element-based constrained mixture implementation for arterial growth, remodeling, and adaptation: theory and numerical verification. 2013 , 29, 822-49	67
1238	Biaxial and failure properties of passive rat middle cerebral arteries. 2013 , 46, 91-6	16
1237	Using contracting band to improve right ventricle ejection fraction for patients with repaired tetralogy of Fallot: a modeling study using patient-specific CMR-based 2-layer anisotropic models of human right and left ventricles. 2013 , 145, 285-93, 293.e1-2	10
1236	Deficiencies in numerical models of anisotropic nonlinearly elastic materials. 2013 , 12, 781-91	32
1235	References. 2013 , 943-972	
1234	A phenomenological constitutive model for the nonlinear viscoelastic responses of biodegradable polymers. 2013 , 224, 287-305	20
1233	A three-constituent damage model for arterial clamping in computer-assisted surgery. 2013 , 12, 123-36	34
1232	Analytical and numerical analyses of the micromechanics of soft fibrous connective tissues. 2013 , 12, 151-66	9
1231	Finite element modeling of mitral valve dynamic deformation using patient-specific multi-slices computed tomography scans. 2013 , 41, 142-53	78
1230	Hemodynamically motivated choice of patch angioplasty for the performance of carotid endarterectomy. 2013 , 41, 263-78	12
1229	Understanding the passive mechanical behavior of the human abdominal wall. 2013 , 41, 433-44	40
1228	Analysis of the uniaxial and multiaxial mechanical response of a tissue-engineered vascular graft. 2013 , 19, 583-92	9
1227	A quasi-static model of wheel-tissue interaction for surgical robotics. 2013 , 35, 1368-76	4
1226	Patient-specific aortic endografting simulation: from diagnosis to prediction. 2013 , 43, 386-94	46
1225	A novel experimental approach for three-dimensional geometry assessment of calcified human stenotic arteries in vitro. 2013 , 39, 1875-86	7

1224	Asymptotic long wave models for a pre-stressed elastic layer with elastically restrained boundaries. 2013 , 50, 1944-1953	1
1223	Full-field bulge test for planar anisotropic tissues: part II--a thin shell method for determining material parameters and comparison of two distributed fiber modeling approaches. 2013 , 9, 5926-42	62
1222	Anisotropic behaviour of human gallbladder walls. 2013 , 20, 363-75	14
1221	In-situ characterization of the uncrimping process of arterial collagen fibers using two-photon confocal microscopy and digital image correlation. 2013 , 46, 2726-9	18
1220	Hierarchical micro-adaptation of biological structures by mechanical stimuli. 2013 , 50, 2353-2370	6
1219	Biaxial deformation of collagen and elastin fibers in coronary adventitia. 2013 , 115, 1683-93	45
1218	Multiaxial mechanical response and constitutive modeling of esophageal tissues: Impact on esophageal tissue engineering. 2013 , 9, 9379-91	48
1217	A Multiphysics Modeling Approach to Develop Right Ventricle Pulmonary Valve Replacement Surgical Procedures with a Contracting Band to Improve Ventricle Ejection Fraction. 2013 , 122, 78-87	10
1216	A new invariant-based method for building biomechanical behavior laws [Application to an anisotropic hyperelastic material with two fiber families. 2013 , 50, 2251-2258	5
1215	The role of elastin and collagen in the softening behavior of the human thoracic aortic media. 2013 , 46, 1859-65	56
1214	Hyperelastic remodeling in the intrauterine growth restricted (IUGR) carotid artery in the near-term fetus. 2013 , 46, 956-63	13
1213	Anisotropic Mullins stress softening of a deformed silicone holey plate. 2013 , 49, 36-43	15
1212	Time accurate partitioned algorithms for the solution of fluid-structure interaction problems in haemodynamics. 2013 , 86, 470-482	34
1211	Non-linear micromechanics of soft tissues. 2013 , 58, 79-85	26
1210	Ballistic helmets [Their design, materials, and performance against traumatic brain injury. 2013 , 101, 313-331	101
1209	Medical Applications of Poly(vinyl alcohol) Cryogels. 2013 , 147-159	3
1208	Modelling framework for mass-growth. 2013 , 50, 50-57	9
1207	Multiscale Elastic Models of Collagen Bio-structures: From Cross-Linked Molecules to Soft Tissues. 2013 , 73-102	11

1206 Cardiovascular Tissue Damage: An Experimental and Computational Framework. **2013**, 129-148

1205 A new strain energy function to characterize apple and potato tissues. **2013**, 118, 178-187 11

1204 Characterization of biaxial mechanical behavior of porcine aorta under gradual elastin degradation. **2013**, 41, 1528-38 49

1203 Computational modelling of bulging of inflated cylindrical shells applicable to aneurysm formation and propagation in arterial wall tissue. **2013**, 73, 20-29 31

1202 Review of Methods for Determining Residual Stresses in Biological Materials. **2013**, 173-182 2

1201 The influence of residual stress on finite deformation elastic response. **2013**, 56, 43-49 55

1200 Influence of random uncertainties of anisotropic fibrous model parameters on arterial pressure estimation. **2013**, 34, 529-540 4

1199 Rotation, inversion and perversion in anisotropic elastic cylindrical tubes and membranes. **2013**, 469, 20130011 35

1198 BREAKING ANALYSIS OF ARTIFICIAL ELASTIC TUBES AND HUMAN ARTERY. **2013**, 05, 1350024 5

1197 Increased arterial stiffness and extracellular matrix reorganization in intrauterine growth-restricted fetal sheep. **2013**, 73, 147-54 51

1196 A coupled fiber-matrix model demonstrates highly inhomogeneous microstructural interactions in soft tissues under tensile load. **2013**, 135, 011008 31

1195 Eulerian Framework for Inelasticity Based on the Jaumann Rate and a Hyperelastic Constitutive RelationPart I: Rate-Form Hyperelasticity. **2013**, 80, 4

1194 Determination and modeling of the inelasticity over the length of the porcine carotid artery. **2013**, 135, 31004 11

1193 Are geometrical and structural variations along the length of the aorta governed by a principle of "optimal mechanical operation"? **2013**, 135, 81006 17

1192 A preliminary analysis of the data from an in vitro inflation-extension test can validate the assumption of arterial tissue elasticity. **2013**, 135, 84502 5

1191 The influence of thyroarytenoid and cricothyroid muscle activation on vocal fold stiffness and eigenfrequencies. **2013**, 133, 2972-83 27

1190 Static Stress Distribution in Microvessel Wall with a Layered Model. **2013**, 772, 258-263

1189 The anisotropic hyperelastic biomechanical response of the vocal ligament and implications for frequency regulation: a case study. **2013**, 133, 1625-36 13

1188	Review: the role of biomechanical modeling in the rupture risk assessment for abdominal aortic aneurysms. 2013 , 135, 021010	24
1187	Mechanical response of the herniated human abdomen to the placement of different prostheses. 2013 , 135, 51004	24
1186	An automated approach for three-dimensional quantification of fibrillar structures in optically cleared soft biological tissues. 2013 , 10, 20120760	66
1185	Elastin and collagen fibre microstructure of the human aorta in ageing and disease: a review. 2013 , 10, 20121004	255
1184	Effects of elastase and collagenase on the nonlinearity and anisotropy of porcine aorta. 2013 , 34, 1657-73	20
1183	Detection of Arterial Wall Boundaries Using an Echo Model Composed of Multiple Ultrasonic Pulses. 2013 , 52, 07HF03	8
1182	A mathematical evaluation of hemodynamic parameters after carotid eversion and conventional patch angioplasty. 2013 , 305, H716-24	12
1181	Experimental parameter estimation method for nonlinear viscoelastic composite material models: an application on arterial tissue. 2013 , 16, 1249-61	1
1180	Towards patient-specific modeling of coronary hemodynamics in healthy and diseased state. 2013 , 2013, 393792	14
1179	Biomechanics of porcine renal arteries and role of axial stretch. 2013 , 135, 81007	20
1178	Real-time simulation of biological soft tissues: a PGD approach. 2013 , 29, 586-600	54
1177	Patient-specific finite element analysis of carotid artery stenting: a focus on vessel modeling. 2013 , 29, 645-64	32
1176	Mechanical properties of the extra-fibrillar matrix of human annulus fibrosus are location and age dependent. 2013 , 31, 1725-32	24
1175	A novel approach to modelling and simulating the contact behaviour between a human hand model and a deformable object. 2013 , 16, 130-40	19
1174	Structurally Motivated Models of the Arterial Wall Tissue. 2013 , 05, 1330002	0
1173	On acoustoelasticity and the elastic constants of soft biological tissues. 2013 , 8, 359-367	8
1172	Wave velocity formulas to evaluate elastic constants of soft biological tissues. 2013 , 8, 51-64	8
1171	Improving the efficiency of abdominal aortic aneurysm wall stress computations. 2014 , 9, e101353	19

1170	Material models and properties in the finite element analysis of knee ligaments: a literature review. 2014 , 2, 54	33
1169	On the Rule of Mixtures for Predicting Stress-Softening and Residual Strain Effects in Biological Tissues and Biocompatible Materials. 2014 , 7, 441-456	13
1168	On three- and two-dimensional fiber distributed models of biological tissues. 2014 , 37, 170-179	31
1167	Finite element based nonlinear normalization of human lumbar intervertebral disc stiffness to account for its morphology. 2014 , 136, 061003	9
1166	A computational method for predicting inferior vena cava filter performance on a patient-specific basis. 2014 , 136,	20
1165	Nonlinear compliance modulates dynamic bronchoconstriction in a multiscale airway model. 2014 , 107, 3030-3042	27
1164	Instability of viscous flow over a deformable two-layered gel: experiments and theory. 2014 , 90, 043004	10
1163	Development of a computational biomechanical model of the human upper-airway soft-tissues toward simulating obstructive sleep apnea. 2014 , 27, 182-200	8
1162	Simulation of transcatheter aortic valve implantation: a patient-specific finite element approach. 2014 , 17, 1347-57	62
1161	Classical and all-floating FETI methods for the simulation of arterial tissues. 2014 , 99, 290-312	14
1160	Artery buckling stimulates cell proliferation and NF- κ B signaling. 2014 , 307, H542-51	10
1159	Modelling the influence of endothelial heterogeneity on the progression of arterial disease: application to abdominal aortic aneurysm evolution. 2014 , 30, 563-86	11
1158	Long-range force transmission in fibrous matrices enabled by tension-driven alignment of fibers. 2014 , 107, 2592-603	190
1157	Embedding of human vertebral bodies leads to higher ultimate load and altered damage localisation under axial compression. 2014 , 17, 1311-22	14
1156	A STRUCTURE-MOTIVATED MODEL OF THE PASSIVE MECHANICAL RESPONSE OF THE PRIMARY PORCINE RENAL ARTERY. 2014 , 14, 1450033	13
1155	Hypo-Elastic vs Hyper-Elastic Constitutive Equation for Textile Materials at Meso-Scale. 2014 , 611-612, 243-249	1
1154	Evolution of anisotropy in soft tissue. 2014 , 470, 20130548	22
1153	A constitutive model for cytoskeletal contractility of smooth muscle cells. 2014 , 470, 20130771	4

1152	Modelling volumetric growth in a thick walled fibre reinforced artery. 2014 , 73, 134-150	26
1151	A 2D Mathematical Model of Blood Flow and its Interactions in an Atherosclerotic Artery. 2014 , 9, 46-68	5
1150	Constitutive Effects of Hydrolytic Degradation in Electro-Spun Polyester-Urethane Scaffolds for Soft Tissue Regeneration. 2014 , 49-67	
1149	Flow-induced wall mechanics of patient-specific aneurysmal cerebral arteries: Nonlinear isotropic versus anisotropic wall stress. 2014 , 228, 37-48	4
1148	Modeling of Multilayered Sheets for Thermoforming Applications. 2014 , 941-944, 2378-2382	
1147	Human coronary plaque wall thickness correlated positively with flow shear stress and negatively with plaque wall stress: an IVUS-based fluid-structure interaction multi-patient study. 2014 , 13, 32	18
1146	Effect of tissue properties, shape and orientation of microcalcifications on vulnerable cap stability using different hyperelastic constitutive models. 2014 , 47, 870-7	47
1145	Effects of mechanical properties and atherosclerotic artery size on biomechanical plaque disruption - mouse vs. human. 2014 , 47, 765-72	11
1144	Computational aspects of the numerical modelling of softening, damage and permanent set in soft biological tissues. 2014 , 130, 57-72	26
1143	Distribution of orientation of smooth muscle bundles does not change along human great and small varicose veins. 2014 , 196, 67-74	3
1142	On the characterisation of elastic properties of long fibre composites using computational homogenisation. 2014 , 83, 149-157	8
1141	Modelling the Evolution of Cerebral Aneurysms: Biomechanics, Mechanobiology and Multiscale Modelling. 2014 , 10, 396-409	11
1140	Compressive mechanical properties of atherosclerotic plaques--indentation test to characterise the local anisotropic behaviour. 2014 , 47, 784-92	43
1139	A gradient-enhanced large-deformation continuum damage model for fibre-reinforced materials. 2014 , 268, 801-842	76
1138	Extremal states of energy of a double-layered thick-walled tube - application to residually stressed arteries. 2014 , 29, 635-54	15
1137	Biomechanical roles of medial pooling of glycosaminoglycans in thoracic aortic dissection. 2014 , 13, 13-25	67
1136	Computational framework to model and design surgical meshes for hernia repair. 2014 , 17, 1071-85	10
1135	A computational model to describe the collagen orientation in statically cultured engineered tissues. 2014 , 17, 251-62	10

1134	Modeling the onset of shear boundary layers in fibrous composite reinforcements by second-gradient theory. 2014 , 65, 587-612	96
1133	What-You-Prescribe-Is-What-You-Get orthotropic hyperelasticity. 2014 , 53, 1279-1298	56
1132	Computational modeling of hypertensive growth in the human carotid artery. 2014 , 53, 1183-1196	34
1131	Experimental Methods for Determining Residual Stresses and Strains in Various Biological Structures. 2014 , 54, 695-708	11
1130	A homogenization approach for nonwoven materials based on fiber undulations and reorientation. 2014 , 65, 12-34	51
1129	Finite element modeling of soft tissues: material models, tissue interaction and challenges. 2014 , 29, 363-72	94
1128	A microstructurally motivated model of arterial wall mechanics with mechanobiological implications. 2014 , 42, 488-502	117
1127	Impact of fluid-structure interaction on direct tumor-targeting in a representative hepatic artery system. 2014 , 42, 461-74	16
1126	Mechano-biology in the thoracic aortic aneurysm: a review and case study. 2014 , 13, 917-28	29
1125	Differential mechanical response and microstructural organization between non-human primate femoral and carotid arteries. 2014 , 13, 1041-51	14
1124	Axial prestretch and circumferential distensibility in biomechanics of abdominal aorta. 2014 , 13, 783-99	48
1123	An energy-deformation decomposition for morphoelasticity. 2014 , 67, 15-39	6
1122	A structural approach including the behavior of collagen cross-links to model patient-specific human carotid arteries. 2014 , 42, 1158-69	17
1121	Finite elastic deformations of transversely isotropic circular cylindrical tubes. 2014 , 51, 1188-1196	20
1120	Poroviscoelastic finite element model including continuous fiber distribution for the simulation of nanoindentation tests on articular cartilage. 2014 , 32, 17-30	18
1119	A generalized prestressing algorithm for finite element simulations of preloaded geometries with application to the aorta. 2014 , 30, 857-72	30
1118	How Constitutive Model Complexity can Affect the Capability to Fit Experimental Data: a Focus on Human Carotid Arteries and Extension/Inflation Data. 2014 , 21, 273-292	12
1117	Bifurcation analysis of a model for atherosclerotic plaque evolution. 2014 , 278-279, 31-43	2

1116	Is the Donnan effect sufficient to explain swelling in brain tissue slices?. 2014 , 11, 20140123	31
1115	Identification and characterisation of regional variations in the material properties of ureter according to microstructure. 2014 , 17, 1653-70	11
1114	Mechanical action of the blood onto atheromatous plaques: influence of the stenosis shape and morphology. 2014 , 17, 527-38	9
1113	Quantification of regional differences in aortic stiffness in the aging human. 2014 , 29, 618-34	83
1112	Computational approaches for analyzing the mechanics of atherosclerotic plaques: a review. 2014 , 47, 859-69	85
1111	Biomechanical properties of native and tissue engineered heart valve constructs. 2014 , 47, 1949-63	173
1110	Constitutive formulations for the mechanical investigation of colonic tissues. 2014 , 102, 1243-54	32
1109	Determination of the material parameters of four-fibre family model based on uniaxial extension data of arterial walls. 2014 , 17, 695-703	9
1108	A model reduction approach for the variational estimation of vascular compliance by solving an inverse fluid-structure interaction problem. 2014 , 30, 055006	18
1107	Calibrating corneal material model parameters using only inflation data: an ill-posed problem. 2014 , 30, 1460-75	10
1106	The effect of stent graft oversizing on radial forces considering nitinol wire behavior and vessel characteristics. 2014 , 36, 1480-6	18
1105	Patient-specific simulation of a stentless aortic valve implant: the impact of fibres on leaflet performance. 2014 , 17, 277-85	21
1104	Experimental evidence of the compressibility of arteries. 2014 , 39, 339-54	24
1103	Structural and mechanical adaptations of right ventricle free wall myocardium to pressure overload. 2014 , 42, 2451-65	61
1102	Sutures in abdominal surgery: biomechanical study and clinical application. 2014 , 9, 849-859	1
1101	Artery buckling analysis using a four-fiber wall model. 2014 , 47, 2790-6	22
1100	Identification of biomechanical properties in vivo in human uterine cervix. 2014 , 39, 27-37	18
1099	Computational modeling of skin: Using stress profiles as predictor for tissue necrosis in reconstructive surgery. 2014 , 143, 32-39	25

1098	A robust anisotropic hyperelastic formulation for the modelling of soft tissue. 2014 , 39, 48-60	124
1097	A novel scheme for the approximation of residual stresses in arterial walls. 2014 , 84, 881-898	20
1096	Permanent set and stress-softening constitutive equation applied to rubber-like materials and soft tissues. 2014 , 225, 1685-1698	26
1095	A goal function approach to remodeling of arteries uncovers mechanisms for growth instability. 2014 , 13, 1243-59	15
1094	Biaxial mechanical properties of the human thoracic and abdominal aorta, common carotid, subclavian, renal and common iliac arteries. 2014 , 13, 1341-59	58
1093	Consistent biomechanical phenotyping of common carotid arteries from seven genetic, pharmacological, and surgical mouse models. 2014 , 42, 1207-23	35
1092	A constructive approach of invariants of behavior laws with respect to an infinite symmetry group \square Application to a biological anisotropic hyperelastic material with one fiber family. 2014 , 51, 3579-3588	5
1091	Computational modeling of cardiac valve function and intervention. 2014 , 16, 53-76	67
1090	Simulation of planar soft tissues using a structural constitutive model: Finite element implementation and validation. 2014 , 47, 2043-54	95
1089	A novel computational formulation for nearly incompressible and nearly inextensible finite hyperelasticity. 2014 , 281, 220-249	15
1088	Mechanics of the pulmonary valve in the aortic position. 2014 , 29, 557-67	12
1087	Passive biaxial mechanical properties and in vivo axial pre-stretch of the diseased human femoropopliteal and tibial arteries. 2014 , 10, 1301-13	43
1086	Uniaxial tensile testing approaches for characterisation of atherosclerotic plaques. 2014 , 47, 793-804	80
1085	A constitutive description of the anisotropic response of the fascia lata. 2014 , 30, 306-23	20
1084	Biaxial mechanical testing of posterior sclera using high-resolution ultrasound speckle tracking for strain measurements. 2014 , 47, 1151-6	23
1083	Unraveling the effect of boundary conditions and strain monitoring on estimation of the constitutive parameters of elastic membranes by biaxial tests. 2014 , 57, 82-89	9
1082	Investigating the role of smooth muscle cells in large elastic arteries: a finite element analysis. 2014 , 358, 1-10	20
1081	Numerical analysis of wrinkled, anisotropic, nonlinearly elastic membranes. 2014 , 57, 1-5	14

1080	Statistical approach for a continuum description of damage evolution in soft collagenous tissues. 2014 , 278, 41-61	30
1079	Modeling collagen recruitment in hyperelastic bio-material models with statistical distribution of the fiber orientation. 2014 , 78, 48-60	33
1078	Computational modeling of soft tissues and ligaments. 2014 , 141-172	6
1077	Computational modelling suggests good, bad and ugly roles of glycosaminoglycans in arterial wall mechanics and mechanobiology. 2014 , 11, 20140397	48
1076	Can isolated annular dilatation cause significant ischemic mitral regurgitation? Another look at the causative mechanisms. 2014 , 47, 1792-9	6
1075	An affine continuum mechanical model for cross-linked F-actin networks with compliant linker proteins. 2014 , 38, 78-90	27
1074	Reconstruction of nonuniform residual stress for soft hyperelastic tissue via inverse spectral techniques. 2014 , 82, 46-73	5
1073	On the mechanics of growing thin biological membranes. 2014 , 63, 128-140	25
1072	Numerical analysis of arterial contraction regulated by smooth muscle stretch and intracellular calcium ion concentration. 2014 , 9, JBSE0002-JBSE0002	3
1071	Real-time in silico experiments on gene regulatory networks and surgery simulation on handheld devices. 2014 , 1, 1	7
1070	Real time simulation for computational surgery: a review. 2014 , 1, 11	23
1069	Supersonic Shear Wave Imaging to Assess Arterial Nonlinear Behavior and Anisotropy: Proof of Principle via Ex Vivo Testing of the Horse Aorta. 2014 , 6, 272586	17
1068	Identifying Hyper-Viscoelastic Model Parameters from an Inflation-Extension Test and Ultrasound Images. 2015 , 55, 1353-1366	5
1067	Limit point instability in pressurization of anisotropic finitely extensible hyperelastic thin-walled tube. 2015 , 77, 107-114	12
1066	Multiscale hierarchical mechanics in soft tissues. 2015 , 15, 35-38	3
1065	Systems biology and mechanics of growth. 2015 , 7, 401-12	25
1064	Morpho-elasticity of inflammatory fibrosis: the case of capsular contracture. 2015 , 12, 20150343	22
1063	A polynomial hyperelastic model for the mixture of fat and glandular tissue in female breast. 2015 , 31, e02723	3

1062	Mechanics of Vascular Smooth Muscle. 2015 , 6, 111-68	16
1061	An error estimator for real-time simulators based on model order reduction. 2015 , 2,	15
1060	Relationship between Postmenopausal Estrogen Deficiency and Aneurysmal Subarachnoid Hemorrhage. 2015 , 2015, 720141	22
1059	Physiology and Pathophysiology of Arterial Flow. 2015 , 533-568	
1058	Biaxial mechanical properties of swine uterosacral and cardinal ligaments. 2015 , 14, 549-60	21
1057	Biomechanical behavior of human crural fascia in anterior and posterior regions of the lower limb. 2015 , 53, 951-9	12
1056	A mechanistic insight into the mechanical role of the stratum corneum during stretching and compression of the skin. 2015 , 49, 197-219	68
1055	Image-Based Predictive Modeling of Heart Mechanics. 2015 , 17, 351-83	39
1054	Recognizing specific human pulse signal based on clustering analysis. 2015 ,	3
1053	Modelling methods for In Vitro biomechanical properties of the skin: A review. 2015 , 5, 241-250	14
1052	Biomechanical and biochemical properties of the thoracic aorta in warmblood horses, Friesian horses, and Friesians with aortic rupture. 2015 , 11, 285	11
1051	A new strain energy function for modelling ligaments and tendons whose fascicles have a helical arrangement of fibrils. 2015 , 48, 3017-25	25
1050	Computational Modeling of the Female Pelvic Support Structures and Organs to Understand the Mechanism of Pelvic Organ Prolapse: A Review. 2015 , 67,	31
1049	Prior Distributions of Material Parameters for Bayesian Calibration of Growth and Remodeling Computational Model of Abdominal Aortic Wall. 2015 , 137, 101001	24
1048	Constitutive modeling of an electrospun tubular scaffold used for vascular tissue engineering. 2015 , 14, 897-913	7
1047	Female patient-specific finite element modeling of pelvic organ prolapse (POP). 2015 , 48, 238-45	29
1046	Stability of active muscle tissue. 2015 , 95, 193-216	3
1045	Transversal isotropy based on a multiplicative decomposition of the deformation gradient within p-version finite elements. 2015 , 95, 742-761	7

1044	Hyperelastic Energy Densities for Soft Biological Tissues: A Review. <i>Journal of Elasticity</i> , 2015 , 120, 129-169	122
1043	Fully non-linear wave models in fiber-reinforced anisotropic incompressible hyperelastic solids. 2015 , 71, 8-21	14
1042	Quantitative diagnostics of soft tissue through viscoelastic characterization using time-based instrumented palpation. 2015 , 41, 149-60	47
1041	Continuum and discrete models for structures including (quasi-) inextensible elasticae with a view to the design and modeling of composite reinforcements. 2015 , 59, 1-17	61
1040	Constitutive modeling of human saphenous veins at overloading pressures. 2015 , 45, 101-8	11
1039	Experimental study of anisotropic stress/strain relationships of the piglet great vessels and relevance to pediatric congenital heart disease. 2015 , 99, 1399-407	7
1038	A regularised continuum damage model based on the mesoscopic scale for soft tissue. 2015 , 58, 20-33	10
1037	A new strain energy function for the hyperelastic modelling of ligaments and tendons based on fascicle microstructure. 2015 , 48, 290-7	40
1036	Numerical implementation of constitutive model for arterial layers with distributed collagen fibre orientations. 2015 , 18, 816-28	6
1035	Influence of isotropic and anisotropic material models on the mechanical response in arterial walls as a result of supra-physiological loadings. 2015 , 64, 29-37	9
1034	Bio-Chemo-Mechanical Models of Vascular Mechanics. 2015 , 43, 1477-87	11
1033	MECHANICAL STRESS IN ABDOMINAL AORTIC ANEURYSMS USING ARTIFICIAL NEURAL NETWORKS. 2015 , 15, 1550029	4
1032	Biopolymer gel swelling analysed with scaling laws and Flory- Behner theory. 2015 , 48, 94-101	51
1031	Dominant negative Poynting effect in simple shearing of soft tissues. 2015 , 95, 87-98	26
1030	Connecting the material parameters of soft fibre-reinforced solids with the formation of surface wrinkles. 2015 , 95, 217-229	1
1029	Selective enzymatic removal of elastin and collagen from human abdominal aortas: uniaxial mechanical response and constitutive modeling. 2015 , 17, 125-36	42
1028	Fluid-structure interaction simulations of cerebral arteries modeled by isotropic and anisotropic constitutive laws. 2015 , 55, 479-498	13
1027	Modelling framework for mass-growth II: The general case. 2015 , 65, 35-42	5

1026	Modeling of human artery tissue with probabilistic approach. 2015 , 59, 152-159	3
1025	Experimental and constitutive modeling approaches for a study of biomechanical properties of human coronary arteries. 2015 , 50, 1-12	18
1024	A model and simulation of uterine contractions. 2015 , 20, 540-564	7
1023	Fast computation of soft tissue deformations in real-time simulation with Hyper-Elastic Mass Links. 2015 , 295, 18-38	20
1022	Methodology for Mechanical Characterization of Soft Biological Tissues: Arteries. 2015 , 110, 74-81	14
1021	A theoretical model of the endothelial cell morphology due to different waveforms. 2015 , 379, 16-23	8
1020	Biomechanical properties of the Marfan's aortic root and ascending aorta before and after personalised external aortic root support surgery. 2015 , 37, 759-66	7
1019	Elasticity/Hyperelasticity. 2015 , 209-307	9
1018	On the Numerical Simulation of Damage for the Visco-hyperelastic Anisotropic Behavior of the Biomaterials in Cyclic Loading: Relationship of the Mullins Effect and Fibers Reinforcement. 2015 , 101, 126-134	2
1017	Investigation of the optimal collagen fibre orientation in human iliac arteries. 2015 , 52, 108-119	27
1016	Local versus global mechanical effects of intramural swelling in carotid arteries. 2015 , 137, 041008	10
1015	Coupled Simulation of Heart Valves: Applications to Clinical Practice. 2015 , 43, 1626-39	5
1014	Comparative analysis of damage functions for soft tissues: Properties at damage initialization. 2015 , 20, 480-492	8
1013	A constitutive modeling interpretation of the relationship among carotid artery stiffness, blood pressure, and age in hypertensive subjects. 2015 , 308, H568-82	22
1012	Quantification of the passive and active biaxial mechanical behaviour and microstructural organization of rat thoracic ducts. 2015 , 12, 20150280	23
1011	Ray W Ogden: An Appreciation. 2015 , 20, 621-624	4
1010	Structure, Mechanics, and Histology of Intraluminal Thrombi in Abdominal Aortic Aneurysms. 2015 , 43, 1488-501	20
1009	Computational vademecums for the real-time simulation of haptic collision between nonlinear solids. 2015 , 283, 210-223	21

1008	Age-related vascular stiffening: causes and consequences. 2015 , 6, 112	166
1007	Finite element formulation and analysis for an arterial wall with residual and active stresses. 2015 , 18, 1143-1159	2
1006	Simulation of swallowing dysfunction and mechanical ventilation after a Montgomery T-tube insertion. 2015 , 18, 1596-605	5
1005	Non-contact, ultrasound-based indentation method for measuring elastic properties of biological tissues using harmonic motion imaging (HMI). 2015 , 60, 2853-68	15
1004	Effects of Carbon Black and the Presence of Static Mechanical Strain on the Swelling of Elastomers in Solvent. 2015 , 8, 884-898	6
1003	Mechanical biocompatibility of highly deformable biomedical materials. 2015 , 48, 100-124	64
1002	Poroelastic modeling of the intervertebral disc: A path toward integrated studies of tissue biophysics and organ degeneration. 2015 , 40, 324-332	15
1001	A mathematical model of the carp heart ventricle during the cardiac cycle. 2015 , 373, 12-25	5
1000	Anisotropic hyperelastic modeling for face-centered cubic and diamond cubic structures. 2015 , 291, 216-239	7
999	Transient solid-fluid interactions in rat brain tissue under combined translational shear and fixed compression. 2015 , 48, 12-27	4
998	Inverse problems in the mechanical characterization of elastic arteries. 2015 , 40, 317-323	5
997	Automatic implementation of finite strain anisotropic hyperelastic models using hyper-dual numbers. 2015 , 55, 229-248	12
996	Use it or lose it: multiscale skeletal muscle adaptation to mechanical stimuli. 2015 , 14, 195-215	80
995	Modelling of tear propagation and arrest in fibre-reinforced soft tissue subject to internal pressure. 2015 , 95, 249-265	12
994	Stability of carotid artery under steady-state and pulsatile blood flow: a fluid-structure interaction study. 2015 , 137, 061007	10
993	Dynamic behavior of suture-anastomosed arteries and implications to vascular surgery operations. 2015 , 14, 1	66
992	Modelling non-symmetric collagen fibre dispersion in arterial walls. 2015 , 12,	135
991	Small amplitude waves in a pre-stressed compressible elastic layer with one fixed and one free face. 2015 , 66, 2741-2757	2

990	Modeling the arterial wall mechanics using a novel high-order viscoelastic fractional element. 2015 , 39, 4767-4780	23
989	A novel non-invasive ultrasonic method to assess total axial stress of the common carotid artery wall in healthy and atherosclerotic men. 2015 , 48, 1860-7	11
988	A study of balloon type, system constraint and artery constitutive model used in finite element simulation of stent deployment. 2015 , 1,	28
987	Material properties of individual menisci and their attachments obtained through inverse FE-analysis. 2015 , 48, 1343-9	13
986	Mechanical characterization of the rat and mice skin tissues using histostructural and uniaxial data. 2015 , 6, 153-60	21
985	Mechanical Programming of Soft Actuators by Varying Fiber Angle. 2015 , 2, 26-32	262
984	On the Use of Biaxial Properties in Modeling Annulus as a Holzapfel-Gasser-Ogden Material. 2015 , 3, 69	16
983	On the tear resistance of skin. 2015 , 6, 6649	206
982	Constitutive modelling of arteries considering fibre recruitment and three-dimensional fibre distribution. 2015 , 12,	38
981	Mechanical factors direct mouse aortic remodelling during early maturation. 2015 , 12, 20141350	17
980	Critical buckling pressure in mouse carotid arteries with altered elastic fibers. 2015 , 46, 69-82	8
979	An animal-specific FSI model of the abdominal aorta in anesthetized mice. 2015 , 43, 1298-309	22
978	A method for incorporating three-dimensional residual stretches/stresses into patient-specific finite element simulations of arteries. 2015 , 47, 147-164	45
977	Material-symmetries congruency in transversely isotropic and orthotropic hyperelastic materials. 2015 , 53, 99-106	21
976	Modelling framework for mass-growth III: Isochoric growth. 2015 , 70, 63-71	2
975	Comparison of transcatheter aortic valve and surgical bioprosthetic valve durability: A fatigue simulation study. 2015 , 48, 3026-34	66
974	The concept of frozen elastic energy as a consequence of changes in microstructure morphology. 2015 , 18 Suppl 1, 1966-7	2
973	Heterogeneous growth-induced prestrain in the heart. 2015 , 48, 2080-9	58

972	Hyperelastic models for hydration of cellular tissue. 2015 , 11, 7579-91	26
971	Micro-Gripper: A new concept for a monolithic single-cell manipulation device. 2015 , 236, 130-139	17
970	A novel CT-FFR method for the coronary artery based on 4D-CT image analysis and structural and fluid analysis. 2015 ,	5
969	Modeling of Experimental Atherosclerotic Plaque Delamination. 2015 , 43, 2838-51	11
968	Layer-specific residual deformations and uniaxial and biaxial mechanical properties of thoracic porcine aorta. 2015 , 50, 55-69	40
967	Remodelling in statistically oriented fibre-reinforced materials and biological tissues. 2015 , 20, 1107-1129	34
966	On the elasticity of blood vessels in one-dimensional problems of hemodynamics. 2015 , 55, 1567-1578	33
965	Crack Propagation and Its Shear Mechanisms in the Bovine Descending Aorta. 2015 , 6, 501-18	20
964	Thermoviscoplastic behaviors of anisotropic shape memory elastomeric composites for cold programmed non-affine shape change. 2015 , 85, 219-244	27
963	UNIAXIAL AND BIAXIAL MECHANICAL PROPERTIES OF THE HUMAN SAPHENOUS VEIN. 2015 , 27, 1550050	1
962	Theory and application of arterial tissue in-host remodelling. 2015 , 2015, 1869-72	
961	Progression of abdominal aortic aneurysm towards rupture: refining clinical risk assessment using a fully coupled fluid-structure interaction method. 2015 , 43, 139-53	34
960	Material model calibration from planar tension tests on porcine linea alba. 2015 , 43, 26-34	8
959	On the modeling of fiber dispersion in fiber-reinforced elastic materials. 2015 , 75, 92-106	30
958	Anisotropic large deformation of geometrically architected unfilled silicone membranes. 2015 , 50, 87-99	5
957	A multi-scale computational assessment of channel gating assumptions within the Meissner corpuscle. 2015 , 48, 73-80	8
956	Simulation of Atherosclerotic Plaque Delamination Using the Cohesive Zone Model. 2015 , 81-88	
955	Effects of age on the physiological and mechanical characteristics of human femoropopliteal arteries. 2015 , 11, 304-13	45

954	The influence of the geometry of the porcine cornea on the biomechanical response of inflation tests. 2015 , 18, 64-77	10
953	Human thoracic and abdominal aortic aneurysmal tissues: Damage experiments, statistical analysis and constitutive modeling. 2015 , 41, 92-107	61
952	Anisotropic hyperelastic behavior of soft biological tissues. 2015 , 18, 1436-44	14
951	Partitioned solution algorithms for fluid-structure interaction problems with hyperelastic models. 2015 , 276, 47-61	14
950	Fluid-structure interaction in abdominal aortic aneurysms: Structural and geometrical considerations. 2015 , 26, 1550038	2
949	An analytical approach to corneal mechanics for determining practical, clinically-meaningful patient-specific tissue mechanical properties in the rehabilitation of vision. 2015 , 43, 274-86	10
948	Structural and mechanical characterisation of bridging veins: A review. 2015 , 41, 222-40	26
947	Mechanical behavior of abdominal aorta aneurysm in rat model treated by cell therapy using mesenchymal stem cells. 2015 , 14, 185-94	10
946	Extension of Murray's law including nonlinear mechanics of a composite artery wall. 2015 , 14, 83-91	3
945	A transversely isotropic visco-hyperelastic constitutive model for soft tissues. 2016 , 21, 747-770	18
944	Collagen. 2016 ,	1
943	Methods in Mechanical Testing of Arterial Tissue: A Review. 2016 , 52, 380-399	27
942	A validated methodology for patient specific computational modeling of self-expandable transcatheter aortic valve implantation. 2016 , 49, 2824-2830	27
941	Hemodynamics. 2016 , 6, 975-1003	70
940	Microstructure and mechanics of human resistance arteries. 2016 , 311, H1560-H1568	13
939	Suppression of electromechanical instability in fiber-reinforced dielectric elastomers. 2016 , 6, 035321	11
938	A Characteristic-Based Constitutive Law for Dispersed Fibers. 2016 , 138,	1
937	Quantifying Variability in Lumbar L4-L5 Soft Tissue Properties for Use in Finite-Element Analysis. 2016 , 1,	2

936	A Paradigm for Materials Design for Surgical Simulators, With Specific Application to the Pleura and Needle Decompression1. 2016 , 10,	2
935	Methods of Blood Flow Modelling. 2016 , 11, 1-25	82
934	The Transverse Isotropy of Spinal Cord White Matter Under Dynamic Load. 2016 , 138,	11
933	Novel Methodology for Characterizing Regional Variations in the Material Properties of Murine Aortas. 2016 , 138,	57
932	Microstructure and Mechanical Property of Glutaraldehyde-Treated Porcine Pulmonary Ligament. 2016 , 138, 061003	6
931	Pulmonary Vascular Mechanics in Pulmonary Hypertension. 2016 , 143-160	
930	Local mechanical properties of human ascending thoracic aneurysms. 2016 , 61, 235-249	29
929	Continuum and discrete models for unbalanced woven fabrics. 2016 , 94-95, 263-284	22
928	A hyperelastic fibre-reinforced continuum model of healing tendons with distributed collagen fibre orientations. 2016 , 15, 1457-1466	12
927	A five-field finite element formulation for nearly inextensible and nearly incompressible finite hyperelasticity. 2016 , 72, 25-47	14
926	Finite element simulation for the mechanical characterization of soft biological materials by atomic force microscopy. 2016 , 62, 222-235	24
925	Constitutive behaviors and mechanical characterizations of fabric reinforced rubber composites. 2016 , 152, 117-123	50
924	Multi-scale modelling of rubber-like materials and soft tissues:. 2016 , 472, 20160060	40
923	Morphometric Properties of the Thoracic Aorta of Warmblood and Friesian Horses with and without Aortic Rupture. 2016 , 154, 225-30	12
922	Coronary Artery Bypass Grafting Following Stent Restenosis. 2016 , 689-701	
921	The secular equation for non-principal Rayleigh waves in deformed incompressible doubly fiber-reinforced nonlinearly elastic solids. 2016 , 84, 23-30	10
920	A nonlinear anisotropic inverse method for computational dissection of inhomogeneous planar tissues. 2016 , 19, 1630-46	4
919	Validation of an arterial constitutive model accounting for collagen content and crosslinking. 2016 , 31, 276-287	16

918	Towards a unified approach in the modeling of fibrosis: A review with research perspectives. 2016 , 17, 61-85	37
917	A novel mixed finite element for finite anisotropic elasticity; the SKA-element Simplified Kinematics for Anisotropy. 2016 , 310, 475-494	27
916	The perivascular environment along the vertebral artery governs segment-specific structural and mechanical properties. 2016 , 45, 286-295	9
915	On referential and spatial formulations of inverse elastostatic analysis. 2016 , 310, 189-207	3
914	A physics based approach to the pulse wave velocity prediction in compliant arterial segments. 2016 , 49, 3460-3466	11
913	MECHANICAL CHARACTERIZATION OF ABDOMINAL AORTIC ANEURYSM WALL IN RAT MODEL TREATED BY MESENCHYMAL STEM CELLS. 2016 , 16, 1650002	
912	Mechanical properties and composition of carotid and femoral atherosclerotic plaques: A comparative study. 2016 , 49, 3697-3704	20
911	Energy-based constitutive modelling of local material properties of canine aortas. 2016 , 3, 160365	6
910	Biomechanical Behavior of Bioprosthetic Heart Valve Heterograft Tissues: Characterization, Simulation, and Performance. 2016 , 7, 309-351	43
909	Efficient evaluation of the material response of tissues reinforced by statistically oriented fibres. 2016 , 67, 1	6
908	Experiments and Constitutive Model for Deep and Superficial Fascia. Digital Image Correlation and Finite Element Validation. 2016 , 52, 436-445	4
907	The relevance of transverse deformation effects in modeling soft biological tissues. 2016 , 99, 57-70	25
906	Computation of the effective nonlinear mechanical response of lattice materials considering geometrical nonlinearities. 2016 , 58, 957-979	31
905	A novel computational remodelling algorithm for the probabilistic evolution of collagen fibre dispersion in biaxially strained vascular tissue. 2017 , 34, 433-467	
904	Analysis of Accuracy of Biaxial Tests Based on their Computational Simulations. 2016 , 52, 424-435	9
903	An anisotropic hyperelastic constitutive model for short glass fiber-reinforced polyamide. 2016 , 106, 262-272	26
902	FINITE STRAIN FORMULATION OF ELASTIC BODY BASED ON MULTIPLE SHEAR MECHANISM CONSIDERING GEOMETRICAL NONLINEARITY. 2016 , 72, I_345-I_356	1
901	Intimal and medial contributions to the hydraulic resistance of the arterial wall at different pressures: a combined computational and experimental study. 2016 , 13,	17

900	Re-examination of the mechanical anisotropy of porcine thoracic aorta by uniaxial tensile tests. 2016 , 15, 167	7
899	Numerical modeling of fluid-structure interaction in arteries with anisotropic polyconvex hyperelastic and anisotropic viscoelastic material models at finite strains. 2016 , 32, e02756	28
898	Development of New Testing Method of Mechanical Properties of Porcine Coronary Arteries. 2016 , 289-297	5
897	A validated software application to measure fiber organization in soft tissue. 2016 , 15, 1467-1478	25
896	Damage Models for Soft Tissues: A Survey. 2016 , 36, 285-307	38
895	Anisotropic constitutive model incorporating multiple damage mechanisms for multiscale simulation of dental enamel. 2016 , 62, 515-533	10
894	Computational method for excluding fibers under compression in modeling soft fibrous solids. 2016 , 57, 178-193	39
893	Anisotropic Elasticity. 2016 , 77-90	
892	An engineering tool to estimate eigenstresses in three-dimensional patient-specific arteries. 2016 , 306, 364-381	10
891	Creating a model of diseased artery damage and failure from healthy porcine aorta. 2016 , 60, 378-393	10
890	A phase-field approach to model fracture of arterial walls: Theory and finite element analysis. 2016 , 312, 542-566	64
889	Computation of the effective mechanical response of biological networks accounting for large configuration changes. 2016 , 58, 28-44	14
888	Relaxed incremental variational approach for the modeling of damage-induced stress hysteresis in arterial walls. 2016 , 58, 149-162	8
887	Numerical modeling of experimental human fibrous cap delamination. 2016 , 59, 322-336	5
886	Artery buckling analysis using a two-layered wall model with collagen dispersion. 2016 , 60, 515-524	12
885	Heart Rate Dependency of Large Artery Stiffness. 2016 , 68, 236-42	53
884	Small Strain Growth and the Human Nail. <i>Journal of Elasticity</i> , 2016 , 124, 57-80	1.5 2
883	Can finite element models of ballooning procedures yield mechanical response of the cardiovascular site to overexpansion?. 2016 , 49, 2778-2784	7

882	Biomechanical behavior of bovine periodontal ligament: Experimental tests and constitutive model. 2016 , 62, 599-606	22
881	Extension, inflation and torsion of a residually stressed circular cylindrical tube. 2016 , 28, 157-174	54
880	On the Theories and Numerics of Continuum Models for Adaptation Processes in Biological Tissues. 2016 , 23, 301-322	7
879	A microstructurally based continuum model of cartilage viscoelasticity and permeability incorporating measured statistical fiber orientations. 2016 , 15, 229-44	37
878	An Anisotropic Multiphysics Model for Intervertebral Disk. 2016 , 83, 0210111-210118	5
877	Handedness-dependent hyperelasticity of biological soft fibers with multilayered helical structures. 2016 , 81, 19-29	20
876	A Micromechanically Based Constitutive Model for the Inelastic and Swelling Behaviors in Double Network Hydrogels. 2016 , 83,	19
875	Effects of the three-dimensional residual stresses on the mechanical properties of arterial walls. 2016 , 393, 118-26	7
874	Microstructure-based biomechanics of coronary arteries in health and disease. 2016 , 49, 2548-59	37
873	Fundamentals of Vascular Bio-fluid and Solid Mechanics. 2016 , 13-45	1
872	How does axial prestretching change the mechanical response of nonlinearly elastic incompressible thin-walled tubes. 2016 , 106, 95-106	7
871	A numerical study of isotropic and anisotropic constitutive models with relevance to healthy and unhealthy cerebral arterial tissues. 2016 , 101, 126-155	15
870	An integrated computational approach for aortic mechanics including geometric, histological and chemico-physical data. 2016 , 49, 2331-40	15
869	Mechanical assessment of arterial dissection in health and disease: Advancements and challenges. 2016 , 49, 2366-73	23
868	Fluid-structure interaction for nonlinear response of shells conveying pulsatile flow. 2016 , 371, 252-276	19
867	Histomechanical Modeling of the Wall of Abdominal Aortic Aneurysm. 2016 , 57-78	4
866	Structure-Based Constitutive Model of Coronary Media. 2016 , 265-283	
865	Geometric multiscale modeling of the cardiovascular system, between theory and practice. 2016 , 302, 193-252	103

864	Microstructural quantification of collagen fiber orientations and its integration in constitutive modeling of the porcine carotid artery. 2016 , 33, 183-93	33
863	Modelling of residually stressed materials with application to AAA. 2016 , 61, 221-234	20
862	Microstructure-Based Constitutive Models for Coronary Artery Adventitia. 2016 , 225-248	4
861	Modeling of Collagenous Tissues Using Distributed Fiber Orientations. 2016 , 15-39	7
860	From Stress-Strain Relations to Growth and Remodeling Theories: A Historical Reflection on Microstructurally Motivated Constitutive Relations. 2016 , 123-133	2
859	Computational modeling of the arterial wall based on layer-specific histological data. 2016 , 15, 1479-1494	4
858	Personalised computational cardiology: Patient-specific modelling in cardiac mechanics and biomaterial injection therapies for myocardial infarction. 2016 , 21, 815-826	22
857	Towards the modelling of ageing and atherosclerosis effects in ApoE(-/-) mice aortic tissue. 2016 , 49, 2390-7	2
856	Length adaptation of smooth muscle contractile filaments in response to sustained activation. 2016 , 397, 13-21	8
855	The cardiac torsion as a sensitive index of heart pathology: A model study. 2015 , 55, 104-119	12
854	Multi-scale modeling of soft fibrous tissues based on proteoglycan mechanics. 2016 , 49, 2349-57	12
853	Finite element modelling of the common carotid artery in the elderly with physiological intimal thickening using layer-specific stress-released geometries and nonlinear elastic properties. 2016 , 19, 1286-96	4
852	On the tension-compression switch of the Gasser-Ogden-Holzapfel model: Analysis and a new pre-integrated proposal. 2016 , 57, 175-89	22
851	Fabrication and characterisation of biomimetic, electrospun gelatin fibre scaffolds for tunica media-equivalent, tissue engineered vascular grafts. 2016 , 61, 473-83	51
850	A Gauss-Kronrod-Trapezoidal integration scheme for modeling biological tissues with continuous fiber distributions. 2016 , 19, 883-93	6
849	Wrinkling, creasing, and folding in fiber-reinforced soft tissues. 2016 , 8, 22-29	13
848	Finite element implementation of a new model of slight compressibility for transversely isotropic materials. 2016 , 19, 745-58	11
847	Automatic Segmentation of Mechanically Inhomogeneous Tissues Based on Deformation Gradient Jump. 2016 , 35, 29-41	5

846	The anisotropic mechanical behaviour of electro-spun biodegradable polymer scaffolds: Experimental characterisation and constitutive formulation. 2016 , 53, 21-39	13
845	Design and finite element analysis of a novel smart clasper for aortic cross-clamping in minimally invasive surgery. 2016 , 25, 15-21	
844	A mechanical argument for the differential performance of coronary artery grafts. 2016 , 54, 93-105	32
843	Computational modelling of atherosclerosis. 2016 , 17, 562-75	30
842	Statistical characterization of the anisotropic strain energy in soft materials with distributed fibers. 2016 , 92, 119-138	33
841	Computational modeling of chemo-bio-mechanical coupling: a systems-biology approach toward wound healing. 2016 , 19, 13-30	28
840	One-dimensional nonlinear elastodynamic models and their local conservation laws with applications to biological membranes. 2016 , 58, 105-121	6
839	Micromechanical model of biphasic biomaterials with internal adhesion: Application to nanocellulose hydrogel composites. 2016 , 29, 149-160	25
838	Finite strain elastoplasticity considering the Eshelby stress for materials undergoing plastic volume change. 2016 , 77, 214-245	36
837	Numerical simulation of fibrous biomaterials with randomly distributed fiber network structure. 2016 , 15, 817-30	11
836	Effect of partial-thickness tear on loading capacities of the supraspinatus tendon: a finite element analysis. 2016 , 19, 875-82	9
835	On the effect of preload and pre-stretch on hemodynamic simulations: an integrative approach. 2016 , 15, 593-627	2
834	A nonlinear-elastic constitutive model for soft connective tissue based on a histologic description: Application to female pelvic soft tissue. 2016 , 58, 65-74	7
833	Poisson's ratio of arterial wall - Inconsistency of constitutive models with experimental data. 2016 , 54, 316-27	25
832	Review of patient-specific simulations of transcatheter aortic valve implantation. 2016 , 8, 2-24	17
831	A poroplastic model of structural reorganisation in porous media of biomechanical interest. 2016 , 28, 579-601	25
830	On the correct interpretation of measured force and calculation of material stress in biaxial tests. 2016 , 53, 187-199	25
829	Adaptation of active tone in the mouse descending thoracic aorta under acute changes in loading. 2016 , 15, 579-92	17

828	A phase-field model for fracture in biological tissues. 2016 , 15, 479-96	50
827	Method for the quantification of rupture probability in soft collagenous tissues. 2017 , 33, e02781	3
826	Identification of the mechanical parameters for the human uterus in vivo using intrauterine pressure measurements. 2017 , 33, e02778	2
825	High resolution imaging of the fibrous microstructure in bovine common carotid artery using optical polarization tractography. 2017 , 10, 231-241	24
824	Finite strain response of crimped fibers under uniaxial traction: An analytical approach applied to collagen. 2017 , 98, 429-453	19
823	Time-evolving collagen-like structural fibers in soft tissues: biaxial loading and spherical inflation. 2017 , 21, 1-29	9
822	Bias extension test on an unbalanced woven composite reinforcement: Experiments and modeling via a second-gradient continuum approach. 2017 , 51, 153-170	21
821	Computational systems mechanobiology of wound healing. 2017 , 314, 46-70	22
820	Contributions of prestrains, hyperelasticity, and muscle fiber activation on mitral valve systolic performance. 2017 , 33, e2806	6
819	Method for the unique identification of hyperelastic material properties using full-field measures. Application to the passive myocardium material response. 2017 , 33, e2866	11
818	The study of equivalent material parameters in a hyperelastic model. 2017 , 89, 142-150	7
817	Modeling of the mechanobiological adaptation in muscular arteries. 2017 , 64, 165-177	2
816	A Combination of Constitutive Damage Model and Artificial Neural Networks to Characterize the Mechanical Properties of the Healthy and Atherosclerotic Human Coronary Arteries. 2017 , 41, E103-E117	17
815	A general framework for the numerical implementation of anisotropic hyperelastic material models including non-local damage. 2017 , 16, 1119-1140	11
814	Effects of Residual Stress, Axial Stretch, and Circumferential Shrinkage on Coronary Plaque Stress and Strain Calculations: A Modeling Study Using IVUS-Based Near-Idealized Geometries. 2017 , 139,	7
813	Histology and Biaxial Mechanical Behavior of Abdominal Aortic Aneurysm Tissue Samples. 2017 , 139,	11
812	The intima with early atherosclerotic lesions is load-bearing component of human thoracic aorta. 2017 , 37, 35-43	4
811	A computational framework for modelling damage-induced softening in fibre-reinforced materials [Application to balloon angioplasty. 2017 , 118-119, 235-256	8

810	Guided waves in pre-stressed hyperelastic plates and tubes: Application to the ultrasound elastography of thin-walled soft materials. 2017 , 102, 67-79	23
809	Mechanics of ultrasound elastography. 2017 , 473, 20160841	42
808	Computation of the homogenized nonlinear elastic response of 2D and 3D auxetic structures based on micropolar continuum models. 2017 , 170, 271-290	43
807	Evaluation of Hemodynamics in a Prestressed and Compliant Tapered Femoral Artery Using an Optimization-Based Inverse Algorithm. 2017 , 139,	1
806	Mechanobiological free energy: a variational approach to tensional homeostasis in tissue equivalents. 2017 , 97, 1011-1019	8
805	A Novel Approach to Assess the In Situ Versus Ex Vivo Mechanical Behaviors of the Coronary Artery. 2017 , 139,	1
804	Three-Dimensional Multiscale, Multistable, and Geometrically Diverse Microstructures with Tunable Vibrational Dynamics Assembled by Compressive Buckling. 2017 , 27, 1605914	39
803	Rupture risk in abdominal aortic aneurysms: A realistic assessment of the explicit GPU approach. 2017 , 56, 1-9	5
802	Identification of residual stresses in multi-layered arterial wall tissues using a variational framework. 2017 , 319, 287-313	3
801	A mixed higher order FEM for fully coupled compressible transversely isotropic finite hyperelasticity. 2017 , 74, 1727-1750	11
800	Mechanobiological modelling of tendons: Review and future opportunities. 2017 , 231, 369-377	11
799	Biomechanical modeling the adaptation of soft biological tissue. 2017 , 1, 71-77	11
798	The cardiovascular system: Mathematical modelling, numerical algorithms and clinical applications *. 2017 , 26, 365-590	97
797	Twist buckling of veins under torsional loading. 2017 , 58, 123-130	12
796	The spherical design algorithm in the numerical simulation of biological tissues with statistical fibre-reinforcement. 2017 , 18, 157-184	7
795	A new approach to modeling early cardiac morphogenesis during c-looping. 2017 , 117, 1-19	6
794	An Inverse Method to Determine Arterial Stiffness with Guided Axial Waves. 2017 , 43, 505-516	15
793	Numerical investigation of the influence of pattern topology on the mechanical behavior of PEGDA hydrogels. 2017 , 49, 247-259	11

792	A new analysis of stresses in arteries based on an Eulerian formulation of growth in tissues. 2017 , 118, 40-55	8
791	Modelling of compressible and orthotropic surgical mesh implants based on optical deformation measurement. 2017 , 74, 400-410	7
790	Coupling Microscale Transport and Tissue Mechanics: Modeling Strategies for Arterial Multiphysics. 2017 , 77-112	2
789	The choice of a constitutive formulation for modeling limb flexion-induced deformations and stresses in the human femoropopliteal arteries of different ages. 2017 , 16, 775-785	7
788	Characterization of arterial wall mechanical properties by a noninvasive method. 2017 , 48, 430-438	1
787	Variational-based energy-momentum schemes of higher-order for elastic fiber-reinforced continua. 2017 , 320, 509-542	8
786	A transverse isotropic viscoelastic constitutive model for aortic valve tissue. 2017 , 4, 160585	14
785	Limb flexion-induced twist and associated intramural stresses in the human femoropopliteal artery. 2017 , 14,	21
784	The counterintuitive out-of-plane strength of some incompressible orthotropic hyperelastic materials. 2017 , 115-116, 170-179	12
783	A Computational Model of the Biochemomechanics of an Evolving Occlusive Thrombus. <i>Journal of Elasticity</i> , 2017 , 129, 125-144	1.5 14
782	Solid Mechanics. 2017 , 263-303	
781	Slight asymmetry in the winding angles of reinforcing collagen can cause large shear stresses in arteries and even induce buckling. 2017 , 52, 3417-3429	7
780	Protective properties of the arterial system against peripherally generated waves. 2017 , 286, 16-21	4
779	The counterintuitive mechanical response in simple tension of arterial models that are separable functions of the I1, I4, I6 invariants. 2017 , 90, 72-81	15
778	Vascular Smooth Muscle Cells and Arterial Stiffening: Relevance in Development, Aging, and Disease. 2017 , 97, 1555-1617	272
777	UNDERSTANDING THE VISCOELASTIC PROPERTIES OF RABBIT CORNEA BASED ON STRESS RELAXATION TESTS AND CYCLIC UNIAXIAL TESTS. 2017 , 17, 1740035	3
776	Anisotropic hierarchic solid finite elements for the simulation of passive-active arterial wall models. 2017 , 74, 3058-3079	3
775	A mechanistic model for drug release from PLGA-based drug eluting stent: A computational study. 2017 , 90, 15-22	10

774	A modified constraint force algorithm for flexible multibody dynamics with loop constraints. 2017 , 90, 1885-1906	9
773	The influence of ligament modelling strategies on the predictive capability of finite element models of the human knee joint. 2017 , 65, 1-11	39
772	The relationship between lymphangion chain length and maximum pressure generation established through in vivo imaging and computational modeling. 2017 , 313, H1249-H1260	12
771	Alterations in biomechanical properties and microstructure of colon wall in early-stage experimental colitis. 2017 , 14, 995-1000	7
770	An anisotropic multiphysics damage model with application to annulus fibrosus. 2017 , 61, 88-93	5
769	Recent advances in studying single bacteria and biofilm mechanics. 2017 , 247, 573-588	30
768	Experimental characterization of the biaxial mechanical properties of porcine gastric tissue. 2017 , 74, 499-506	20
767	On arterial fiber dispersion and auxetic effect. 2017 , 61, 123-130	16
766	Phase field modeling of fracture in anisotropic brittle solids. 2017 , 97, 1-21	139
765	A computational fluid-structure interaction analysis of coronary Y-grafts. 2017 , 47, 117-127	15
764	Biomechanics of human parietal pleura in uniaxial extension. 2017 , 75, 330-335	5
763	Experimental Study of Anisotropic Stress/Strain Relationships of Aortic and Pulmonary Artery Homografts and Synthetic Vascular Grafts. 2017 , 139,	4
762	Computationally Informed Design of a Multi-Axial Actuated Microfluidic Chip Device. 2017 , 7, 5489	6
761	Biaxial loading of arterial tissues with 3D in situ observations of adventitia fibrous microstructure: A method coupling multi-photon confocal microscopy and bulge inflation test. 2017 , 74, 488-498	18
760	Patient-specific stress analyses in the ascending thoracic aorta using a finite-element implementation of the constrained mixture theory. 2017 , 16, 1765-1777	28
759	A Universal Dynamic Inflation Test for Soft Tissue, Tissue Analogues and Grafts. 2017 , 57, 1423-1433	
758	Finite Element Simulation and the Application of Amphoteric pH-sensitive Hydrogel. 2017 , 09, 1750063	9
757	Layered Elastomeric Fibrous Scaffolds: An In-Silico Study of the Achievable Range of Mechanical Behaviors. 2017 , 3, 2907-2921	9

756	A combination of experimental measurement, constitutive damage model, and diffusion tensor imaging to characterize the mechanical properties of the human brain. 2017 , 20, 1350-1363	10
755	Highly elastic binders integrating polyrotaxanes for silicon microparticle anodes in lithium ion batteries. 2017 , 357, 279-283	670
754	Multiscale and Multiaxial Mechanics of Vascular Smooth Muscle. 2017 , 113, 714-727	14
753	A chemo-mechano-biological formulation for the effects of biochemical alterations on arterial mechanics: the role of molecular transport and multiscale tissue remodelling. 2017 , 14,	18
752	Finite Element Modeling of Avascular Tumor Growth Using a Stress-Driven Model. 2017 , 139,	4
751	Efficient probabilistic finite element analysis of a lumbar motion segment. 2017 , 61, 65-74	10
750	A FSI computational framework for vascular physiopathology: A novel flow-tissue multiscale strategy. 2017 , 47, 25-37	21
749	Earliest effects of sudden occlusions on pressure profiles in selected locations of the human systemic arterial system. 2017 , 95, 032414	3
748	Nondestructive mechanical characterization of developing biological tissues using inflation testing. 2017 , 74, 438-447	5
747	Approximate Artery Elasticity Using Linear Springs. 2017 , 37, 899-911	2
746	Measurement of Friction-induced Changes in Pig Aorta Fibre Organization by Non-invasive Imaging as a Model for Detecting the Tissue Response to Endovascular Catheters. 2017 , 12, 24-32	1
745	INFLUENCE OF LEAFLETS MATRIX STIFFNESS AND FIBER ORIENTATION ON THE OPENING DYNAMICS OF A PROSTHETIC TRILEAFLET HEART VALVE. 2017 , 17, 1750096	1
744	Constitutive modeling of jugular vein-derived venous valve leaflet tissues. 2017 , 75, 50-57	7
743	Form Changes of a Toroidal Body with a Crossed Arrangement of Fibers on the Basis of the Two-level Carcass Theory. 2017 , 53, 253-266	2
742	Constitutive description of human femoropopliteal artery aging. 2017 , 16, 681-692	26
741	A 3-field formulation for strongly transversely isotropic compressible finite hyperelasticity. 2017 , 315, 478-500	10
740	Multi-scale Structural Modeling of Soft Tissues Mechanics and Mechanobiology. <i>Journal of Elasticity</i> , 2017 , 129, 7-48	1.5 22
739	Fiber-Network Modeling in Biomechanics: Theoretical and Analytical Approaches. 2017 , 271-307	2

738	Modelling the deep drawing of a 3D woven fabric with a second gradient model. 2017 , 22, 2165-2179	19
737	Determination and Finite Element Validation of the WYPIWYG Strain Energy of Superficial Fascia from Experimental Data. 2017 , 45, 799-810	13
736	A novel constitutive model for passive right ventricular myocardium: evidence for myofiber-collagen fiber mechanical coupling. 2017 , 16, 561-581	41
735	A new formulation of slight compressibility for arterial tissue and its Finite Element implementation. 2017 , 20, 403-414	3
734	Microstructure and Mechanics of Human Aortas in Health and Disease. 2017 , 157-192	
733	Shear Modulus of the Partially Obstructed Rat Small Intestine. 2017 , 45, 1069-1082	5
732	Behaviour of two typical stents towards a new stent evolution. 2017 , 55, 1019-1037	4
731	A homogenization model of the Voigt type for skeletal muscle. 2017 , 414, 50-61	19
730	Hemodynamic Influence on Smooth Muscle Cell Kinetics and Phenotype During Early Vein Graft Adaptation. 2017 , 45, 644-655	7
729	Nonlinear Continuum Mechanics and Modeling the Elasticity of Soft Biological Tissues with a Focus on Artery Walls. 2017 , 83-156	4
728	Arterial and Atherosclerotic Plaque Biomechanics with Application to Stent Angioplasty Modeling. 2017 , 193-231	1
727	Computational Modeling in Liver Surgery. 2017 , 8, 906	16
726	Human Abdomen. 2017 , 267-285	2
725	Blood Flow. 2017 , 1-31	
724	Growth Description for Vessel Wall Adaptation: A Thick-Walled Mixture Model of Abdominal Aortic Aneurysm Evolution. 2017 , 10,	24
723	Skin Mechanics. 2017 , 347-357	3
722	Effect of Wall Flexibility on the Deformation during Flow in a Stenosed Coronary Artery. 2017 , 2, 16	6
721	Constitutive Modeling of the Small Intestine. 2017 , 287-305	1

720	Design and Validation of Equiaxial Mechanical Strain Platform, EQUicycler, for 3D Tissue Engineered Constructs. 2017 , 2017, 3609703	10
719	Modeling of Damage in Soft Biological Tissues. 2017 , 101-123	6
718	3.11 The Mechanics of Native and Engineered Cardiac Soft Tissues. 2017 , 197-218	
717	Hyperelasticity Modeling for Incompressible Passive Biological Tissues. 2017 , 3-30	1
716	Aorta. 2017 , 169-191	6
715	A multiscale active structural model of the arterial wall accounting for smooth muscle dynamics. 2018 , 15,	6
714	Direct and inverse identification of constitutive parameters from the structure of soft tissues. Part 1: micro- and nanostructure of collagen fibers. 2018 , 17, 1011-1036	11
713	Computational Fluid Dynamics Assessment Associated with Transcatheter Heart Valve Prostheses: A Position Paper of the ISO Working Group. 2018 , 9, 289-299	22
712	A biomechanical model for fibril recruitment: Evaluation in tendons and arteries. 2018 , 74, 192-196	6
711	Comparison of different constitutive models to characterize the viscoelastic properties of human abdominal adipose tissue. A pilot study. 2018 , 80, 293-302	14
710	A micro-structure based constitutive model for anisotropic stress-strain behaviors of artery tissues. 2018 , 139-140, 55-64	5
709	Microstructurally-based constitutive modelling of the skin - Linking intrinsic ageing to microstructural parameters. 2018 , 444, 108-123	20
708	Modelling a soft composite accumulator for human mobility assist devices. 2018 , 80, 81-87	1
707	The influence of fiber dispersion on the mechanical response of aortic tissues in health and disease: a computational study. 2018 , 21, 99-112	9
706	A Continuum Model for Fiber-Reinforced Soft Robot Actuators. 2018 , 10,	15
705	A discrete fibre dispersion method for excluding fibres under compression in the modelling of fibrous tissues. 2018 , 15,	34
704	Modeling the effect of collagen fibril alignment on ligament mechanical behavior. 2018 , 17, 543-557	14
703	A mixed finite element formulation for slightly compressible finite elasticity with stiff fibre reinforcement. Two fibre families. Uniaxial tension formulation. 2018 , 75, 2607-2624	1

702	The Turning Point for Morphomechanical Remodeling During Complete Intestinal Obstruction in Rats Occurs After 12-24 h. 2018 , 46, 705-716	1
701	Elastic Fibers and Large Artery Mechanics in Animal Models of Development and Disease. 2018 , 140,	16
700	Image-Driven Constitutive Modeling for FE-Based Simulation of Soft Tissue Biomechanics. 2018 , 55-76	
699	Coupled Finite Element Agent-Based Models for the Simulation of Vascular Growth and Remodeling. 2018 , 283-300	3
698	Two-layered analytical model of arterial wall with residual stress under physiological loading. 2018 , 57, 52-63	2
697	Evaluation of microstructurally motivated constitutive models to describe age-dependent tendon healing. 2018 , 17, 793-814	10
696	Mechanical Properties of Arterial Elastin With Water Loss. 2018 , 140,	14
695	Fracture mechanics of shear crack propagation and dissection in the healthy bovine descending aortic media. 2018 , 68, 53-66	19
694	Bending and wrinkling of composite fiber preforms and prepregs. A review and new developments in the draping simulations. 2018 , 141, 234-249	97
693	Linear spring stiffnesses for two-dimensional finite element modeling of arteries. 2018 , 72, 57-65	1
692	Pulsatile flow measurements and wall stress distribution in a patient specific abdominal aortic aneurysm phantom. 2018 , 98, 2258-2274	7
691	On the preservation of fibre direction during axisymmetric hyperelastic mass-growth of a finite fibre-reinforced tube. 2018 , 109, 173-210	3
690	Improving Mechanical Properties of Molded Silicone Rubber for Soft Robotics Through Fabric Compositing. 2018 , 5, 272-290	38
689	Numerical simulation of fluid-structure interaction problems with hyperelastic models: A monolithic approach. 2018 , 145, 186-208	11
688	Growth and remodeling with application to abdominal aortic aneurysms. 2018 , 109, 113-137	20
687	Time-frequency analyses of fluid-solid interaction under sinusoidal translational shear deformation of the viscoelastic rat cerebrum. 2018 , 22, 1-27	4
686	An exponential constitutive model excluding fibres under compression: Application to extension-inflation of a residually stressed carotid artery. 2018 , 23, 1206-1224	15
685	Uncertainty quantification and sensitivity analysis of an arterial wall mechanics model for evaluation of vascular drug therapies. 2018 , 17, 55-69	6

684	Wave propagation in pre-deformed periodic network materials based on large strains homogenization. 2018 , 184, 860-871	10
683	Over length quantification of the multiaxial mechanical properties of the ascending, descending and abdominal aorta using Digital Image Correlation. 2018 , 77, 434-445	16
682	An Allen-Cahn approach to the remodelling of fibre-reinforced anisotropic materials. 2018 , 109, 139-172	15
681	A General Approach to Derive Stress and Elasticity Tensors for Hyperelastic Isotropic and Anisotropic Biomaterials. 2018 , 15,	9
680	Biomechanical Determinants of Right Ventricular Failure in Pulmonary Hypertension. 2018 , 64, 557-564	8
679	The exponentiated Hencky energy: anisotropic extension and case studies. 2018 , 61, 657-685	4
678	Modeling the Deformation of the Elastin Network in the Aortic Valve. 2018 , 140,	16
677	The role of biomechanics in aortic aneurysm management: requirements, open problems and future prospects. 2018 , 77, 295-307	13
676	Fiber-reinforced computational model of the aortic root incorporating thoracic aorta and coronary structures. 2018 , 17, 263-283	2
675	Modeling fibrous biological tissues with a general invariant that excludes compressed fibers. 2018 , 110, 38-53	21
674	A Brief Review on Computational Modeling of Rupture in Soft Biological Tissues. 2018 , 113-144	3
673	Characterization of mechanical properties of pericardium tissue using planar biaxial tension and flexural deformation. 2018 , 77, 148-156	22
672	Arterial pulse attenuation prediction using the decaying rate of a pressure wave in a viscoelastic material model. 2018 , 17, 589-603	1
671	Biomechanical evaluation of a personalized external aortic root support applied in the Ross procedure. 2018 , 78, 164-174	13
670	Biomechanical property and modelling of venous wall. 2018 , 133, 56-75	13
669	Numerical aspects of anisotropic failure in soft biological tissues favor energy-based criteria: A rate-dependent anisotropic crack phase-field model. 2018 , 331, 23-52	53
668	Predictive capabilities of various constitutive models for arterial tissue. 2018 , 78, 369-380	22
667	Three-dimensional vibrations of a helically wound cable modeled as a Timoshenko rod. 2018 , 229, 677-695	3

666	Validation of the Strain Assessment of a Phantom of Abdominal Aortic Aneurysm: Comparison of Results Obtained From Magnetic Resonance Imaging and Stereovision Measurements. 2018 , 140,	6
665	Dacron graft as replacement to dissected aorta: A three-dimensional fluid-structure-interaction analysis. 2018 , 78, 329-341	12
664	A continuum mechanics constitutive framework for transverse isotropic soft tissues. 2018 , 112, 209-224	30
663	Poisson's Contraction and Fiber Kinematics in Tissue: Insight From Collagen Network Simulations. 2018 , 140,	28
662	Mechanical Characterization and Material Modeling of Diabetic Aortas in a Rabbit Model. 2018 , 46, 429-442	8
661	A viscoelastic anisotropic hyperelastic constitutive model of the human cornea. 2018 , 17, 19-29	22
660	Hemodynamic assessments of the ascending thoracic aortic aneurysm using fluid-structure interaction approach. 2018 , 56, 435-451	9
659	Anisotropic material properties of human left common carotid artery using inverse finite element and analytical methods. 2018 ,	
658	Numerical analyses of the interrelation between extracellular smooth muscle orientation and intracellular filament overlap in the human abdominal aorta. 2018 , 98, 2198-2221	4
657	FluidStructure Interaction Analysis of Bioprosthetic Heart Valves: the Application of a Computationally-Efficient Tissue Constitutive Model. 2018 , 447-469	1
656	Determination of Viscoelastic Properties of human Carotid Atherosclerotic Plaque by Inverse Boundary Value Analysis. 2018 , 381,	2
655	Note on the generality of one plane strain bending universal solution. 2018 , 94, 120-124	2
654	Biomechanics and Modeling of Tissue-Engineered Heart Valves. 2018 , 413-446	
653	Encyclopedia of Continuum Mechanics. 2018 , 1-15	
652	Numerical simulation of nonlinear wave propagation in symmetric cross-ply laminates with hyperelastic material behavior. 2018 ,	
651	Coupling between a fiber-reinforced model and a Hill-based contractile model for passive and active tissue properties of laryngeal muscles: A finite element study. 2018 , 144, EL248	4
650	Non-affine fiber kinematics in arterial mechanics: a continuum micromechanical investigation. 2018 , 98, 2101-2121	15
649	Mechanical Behavior Modeling of Hyperelastic Transversely Isotropic Materials Based on a New Polyconvex Strain Energy Function. 2018 , 10, 1850104	11

648	Hyperelasticity of Soft Biological and Rubber Materials. 151-224	1
647	Nonlinear Static and Dynamic Response of a Blood-Filled and Pressurized Human Aorta. 492-514	
646	Function-refresh algorithms for determining the stored energy density of nonlinear elastic orthotropic materials directly from experimental data. 2018 , 107, 16-33	5
645	Biomechanical Material Characterization of Stanford Type-B Dissected Porcine Aortas. 2018 , 9, 1317	3
644	Magic angles and fibre stretch in arterial tissue: Insights from the linear theory. 2018 , 88, 470-477	5
643	A coupled approach for fluid saturated poroelastic media and immersed solids for modeling cell-tissue interactions. 2018 , 34, e3139	4
642	Influence of the Mullins effect on the stress-strain state of design at the example of calculation of deformation field in tyre. 2018 , 104, 67-74	10
641	Strain-Energy Functions. 2018 , 19-28	
640	Stress Measures. 2018 , 29-48	
639	Mechanical properties of reinforced composite materials under uniaxial and planar tension loading regimes measured using a non-contact optical method. 2018 , 202, 1145-1154	6
638	Integrating MRI-based geometry, composition and fiber architecture in a finite element model of the human intervertebral disc. 2018 , 85, 37-42	18
637	Comparative Analysis of Porcine and Human Thoracic Aortic Stiffness. 2018 , 55, 560-566	20
636	A modular inverse elastostatics approach to resolve the pressure-induced stress state for in vivo imaging based cardiovascular modeling. 2018 , 85, 124-133	9
635	Mechanical response of human subclavian and iliac arteries to extension, inflation and torsion. 2018 , 75, 235-252	11
634	A random field model for anisotropic strain energy functions and its application for uncertainty quantification in vascular mechanics. 2018 , 333, 94-113	30
633	Model Parameters from Test Data. 2018 , 119-127	
632	Hyperelastic models for the swelling of soft material plugs in confined spaces. 2018 , 106, 297-309	6
631	On incorporating osmotic prestretch/prestress in image-driven finite element simulations of cartilage. 2018 , 86, 409-422	8

630	On the use of machine learning techniques for the mechanical characterization of soft biological tissues. 2018 , 34, e3121	12
629	Computational fluid-structure interaction analysis of blood flow on patient-specific reconstructed aortic anatomy and aneurysm treatment with Dacron graft. 2018 , 81, 693-711	12
628	Modelling of Soft Connective Tissues to Investigate Female Pelvic Floor Dysfunctions. 2018 , 2018, 9518076	11
627	Structural modelling of the cardiovascular system. 2018 , 17, 1217-1242	12
626	A prediction of in vivo mechanical stresses in blood vessels using thermal expansion method and its application to hypertension and vascular stenosis. 2018 , 34, 1156-1166	4
625	Biomechanical relevance of the microstructure in artery walls with a focus on passive and active components. 2018 , 315, H540-H549	23
624	Nonlinear model of human descending thoracic aortic segments with residual stresses. 2018 , 17, 1839-1855	9
623	Mechanical Characterization of the Vessel Wall by Data Assimilation of Intravascular Ultrasound Studies. 2018 , 9, 292	4
622	Numerical Parametric Study of Paravalvular Leak Following a Transcatheter Aortic Valve Deployment Into a Patient-Specific Aortic Root. 2018 , 140,	28
621	Sensitivity of Arterial Hyperelastic Models to Uncertainties in Stress-Free Measurements. 2018 , 140,	4
620	A comprehensive fluid-structure interaction model of the left coronary artery. 2018 ,	11
619	Implementation and validation of constitutive relations for human dermis mechanical response. 2018 , 56, 2083-2093	6
618	A biodegradable synthetic graft for small arteries matches the performance of autologous vein in rat carotid arteries. 2018 , 181, 67-80	27
617	Micropatterned cell sheets as structural building blocks for biomimetic vascular patches. 2018 , 181, 126-139	21
616	Compressibility and Anisotropy of the Ventricular Myocardium: Experimental Analysis and Microstructural Modeling. 2018 , 140,	29
615	Comparison of aneurysmal and non-pathologic human ascending aortic tissue in shear. 2018 , 58, 49-56	5
614	Multi-scale modelling of arterial tissue: Linking networks of fibres to continua. 2018 , 341, 740-787	6
613	On the constitutive modelling of recruitment and damage of collagen fibres in soft biological tissues. 2018 , 72, 483-496	25

612	Towards non-invasive in vivo characterization of the pathophysiological state and mechanical wall strength of the individual human AAA wall based on 4D ultrasound measurements. 2018 , 98, 2275-2294	6
611	The Effect of Pentagalloyl Glucose on the Wall Mechanics and Inflammatory Activity of Rat Abdominal Aortic Aneurysms. 2018 , 140,	8
610	Cross-sectional pinching in human femoropopliteal arteries due to limb flexion, and stent design optimization for maximum cross-sectional opening and minimum intramural stresses. 2018 , 15,	5
609	On the lifetime prediction of rolling lobe air springs. 2018 , 94, 313-326	5
608	Mechanical characterization of arteries affected by fetal growth restriction in guinea pigs (<i>Cavia porcellus</i>). 2018 , 88, 92-101	3
607	An investigation into the role of different constituents in damage accumulation in arterial tissue and constitutive model development. 2018 , 17, 1757-1769	16
606	A combined growth and remodeling framework for the approximation of residual stresses in arterial walls. 2018 , 98, 2072-2100	2
605	Predicting Rotation in Fenestrated Endovascular Aneurysm Repair Using Finite Element Analysis. 2018 , 140,	10
604	Tensile biomechanical properties and constitutive parameters of human corneal stroma extracted by SMILE procedure. 2018 , 85, 102-108	9
603	Transmural variation in elastin fiber orientation distribution in the arterial wall. 2018 , 77, 745-753	19
602	On the quasi-incompressible finite element analysis of anisotropic hyperelastic materials. 2019 , 63, 443-453	21
601	Characterization of multilayered carbon-fiber reinforced thermoplastic composites for assembly process. 2019 , 32, 673-689	1
600	Multi-Scale Modelling in Biology. 2019 , 900-905	
599	Correlation between MMP and TIMP levels and elastic moduli of ascending thoracic aortic aneurysms. 2019 , 20, 324-327	4
598	The method of investigation of deformations of solids from fibre-reinforced compressible materials. 2019 , 1158, 022044	
597	Constituent-specific material behavior of soft biological tissue: experimental quantification and numerical identification for lung parenchyma. 2019 , 18, 1383-1400	4
596	Tissue Engineering: A Coupled Agent-Based Finite Element Approach. 2019 , 25, 641-654	4
595	Biomechanics of aortic wall failure with a focus on dissection and aneurysm: A review. 2019 , 99, 1-17	37

594	Comparative finite element modelling of aneurysm formation and physiologic inflation in the descending aorta. 2019 , 22, 1197-1208	4
593	In vivo and in vitro evaluation of a biodegradable magnesium vascular stent designed by shape optimization strategy. 2019 , 221, 119414	39
592	Biaxial biomechanical properties of the nonpregnant murine cervix and uterus. 2019 , 94, 39-48	2
591	Modelling the Temperature Dependent Biaxial Response of Poly(ether-ether-ketone) Above and Below the Glass Transition for Thermoforming Applications. 2019 , 11,	2
590	On the Modeling of Patient-Specific Transcatheter Aortic Valve Replacement: A Fluid-Structure Interaction Approach. 2019 , 10, 437-455	31
589	Anisotropic Elasticity. 2019 , 79-93	
588	Simulating the temporal change of the active response of arteries by finite elements with high-order time-integrators. 2019 , 64, 1669-1684	3
587	Numerical study of biomechanical characteristics of plaque rupture at stenosed carotid bifurcation: a stenosis mechanical property-specific guide for blood pressure control in daily activities. 2019 , 35, 1279-1289 ⁴	
586	High-Resolution Strain Measurement for Biomechanical Parameters Assessment in Native and Decellularized Porcine Vessels. 2019 , 2019, 1-14	
585	Morphoelastic fiber remodeling in pressurized thick-walled cylinders with application to soft tissue collagenous tubes. 2019 , 77, 103800	12
584	Data-driven correction of models for deformable solids. 2019 ,	
583	Three-Dimensional Contractile Mechanics of Artery Accounting for Curl of Axial Strip Sectioned from Vessel Wall. 2019 , 10, 604-617	
582	Mechanical and Microstructural Behavior of Vascular Tissue. 2019 , 63-78	
581	Macro- and mesoscopic mechanical properties of complex fabric rubber composite under different temperatures. 2019 , 230, 111510	14
580	A finite element approach for gastrointestinal tissue mechanics. 2019 , 35, e3269	3
579	Computational simulations of the helical buckling behavior of blood vessels. 2019 , 35, e3277	7
578	Orientable wrinkles in stretched orthotropic films. 2019 , 33, 100579	11
577	Mimicking "J-Shaped" and Anisotropic Stress-Strain Behavior of Human and Porcine Aorta by Fabric-Reinforced Elastomer Composites. 2019 , 11, 33323-33335	16

576	Anisotropic elasticity for inversion-safety and element rehabilitation. 2019 , 38, 1-15	11
575	Efficient integration of evolution equations for a fiber-like Maxwell body. 2019 , 1268, 012078	1
574	On the unicity of a solution in biomechanics of soft tissues: A numerical approach. 2019 ,	
573	Failure properties and microstructure of healthy and aneurysmatic human thoracic aortas subjected to uniaxial extension with a focus on the media. 2019 , 99, 443-456	16
572	Identification of in vivo nonlinear anisotropic mechanical properties of ascending thoracic aortic aneurysm from patient-specific CT scans. 2019 , 9, 12983	10
571	On the effective stress law and its application to finite deformation problems in a poroelastic solid. 2019 , 161-162, 105074	5
570	An anisotropic hyperelastic model with an application to soft tissues. 2019 , 78, 103845	6
569	Finite element simulation of three dimensional residual stress in the aortic wall using an anisotropic tissue growth model. 2019 , 92, 188-196	11
568	Learning Corrections for Hyperelastic Models From Data. 2019 , 6,	29
567	Constitutive Models of Coronary Vasculature. 2019 , 173-308	
566	Influence of coupled hemodynamics-arterial wall interaction on compliance in a realistic pulmonary artery with variable intravascular wall properties. 2019 , 57, 56-71	
565	Computational modeling of progressive damage and rupture in fibrous biological tissues: application to aortic dissection. 2019 , 18, 1607-1628	22
564	Localized bulging in an inflated bilayer tube of arbitrary thickness: Effects of the stiffness ratio and constitutive model. 2019 , 176-177, 173-184	6
563	Failure damage mechanical properties of thoracic and abdominal porcine aorta layers and related constitutive modeling: phenomenological and microstructural approach. 2019 , 18, 1709-1730	7
562	Constitutive Modelling of Skin Ageing. 2019 , 135-192	
561	Moderate thickness of lipid core in shoulder region of atherosclerotic plaque determines vulnerable plaque A parametric study. 2019 , 69, 140-146	0
560	Constitutive Modelling of Skin Mechanics. 2019 , 19-76	3
559	Constitutive Modelling of Wound Healing. 2019 , 101-133	

558	Computational modeling reveals the relationship between intrinsic failure properties and uniaxial biomechanical behavior of arterial tissue. 2019 , 18, 1791-1807	5
557	A Multi-Modality Image-Based FSI Modeling Approach for Prediction of Coronary Plaque Progression Using IVUS and OCT Data with Follow-Up. 2019 ,	4
556	Patient-specific predictions of aneurysm growth and remodeling in the ascending thoracic aorta using the homogenized constrained mixture model. 2019 , 18, 1895-1913	23
555	A minimal continuum representation of a transverse isotropic viscoelastic pulp fibre based on micromechanical measurements. 2019 , 135, 149-161	8
554	Mechanical Properties and Microstructure of the Coronary Vasculature. 2019 , 105-171	
553	Constitutive model of human artery adventitia enhanced with a failure description. 2019 , 1, 1	4
552	Molecular-level collagen damage explains softening and failure of arterial tissues: A quantitative interpretation of CHP data with a novel elasto-damage model. 2019 , 97, 254-271	10
551	A Subdomain Method for Mapping the Heterogeneous Mechanical Properties of the Human Posterior Sclera. 2019 , 7, 129	1
550	A finite element implementation of a growth and remodeling model for soft biological tissues: Verification and application to abdominal aortic aneurysms. 2019 , 352, 586-605	17
549	Mechanical stresses associated with flattening of human femoropopliteal artery specimens during planar biaxial testing and their effects on the calculated physiologic stress-stretch state. 2019 , 18, 1591-1605	9
548	On the role of material properties in ascending thoracic aortic aneurysms. 2019 , 109, 70-78	11
547	Instability of Incompatible Bilayered Soft Tissues and the Role of Interface Conditions. 2019 ,	3
546	Constrained mixture modeling affects material parameter identification from planar biaxial tests. 2019 , 95, 124-135	12
545	On fibre dispersion modelling of soft biological tissues: a review. 2019 , 475, 20180736	34
544	Rivlin's legacy in continuum mechanics and applied mathematics. 2019 , 377, 20190090	4
543	Bidirectional Ultrasound Elastographic Imaging Framework for Non-invasive Assessment of the Non-linear Behavior of a Physiologically Pressurized Artery. 2019 , 45, 1184-1196	3
542	Modeling of anisotropic hyperelastic heterogeneous knitted fabric reinforced composites. 2019 , 127, 47-61	9
541	An in vivo parameter identification method for arteries: numerical validation for the human abdominal aorta. 2019 , 22, 426-441	4

540	A comparative study of methods used to generate the arterial fiber structure in a clinically relevant numerical analysis. 2019 , 35, e3194	1
539	A Formulation for Fluid Structure-Interactions in FEBio Using Mixture Theory. 2019 ,	9
538	Computational Multiscale Solvers for Continuum Approaches. 2019 , 12,	4
537	Micromechanically-motivated analysis of fibrous tissue. 2019 , 96, 69-78	6
536	Bridging finite element and machine learning modeling: stress prediction of arterial walls in atherosclerosis. 2019 ,	22
535	Differential biomechanical properties of mouse distal colon and rectum innervated by the splanchnic and pelvic afferents. 2019 , 316, G473-G481	16
534	Multiscale modeling of fiber recruitment and damage with a discrete fiber dispersion method. 2019 , 126, 226-244	20
533	Constitutive law of healthy gallbladder walls in passive state with damage effect. 2019 , 9, 189-201	2
532	A Nonlinear Elimination Preconditioned Inexact Newton Method for Heterogeneous Hyperelasticity. 2019 , 41, S390-S408	3
531	Donkey pericardium as a select sourcing to manufacture percutaneous heart valves: Decellularization has not yet demonstrated any clear cut advantage to glutaraldehyde treatment. 2019 , 4, 100029	
530	Patient-Specific Bile Flow Simulation to Evaluate Cholecystectomy Outcome. 2019 , 581, 012022	
529	Mathematical modelling of atherosclerosis. 2019 , 14, 603	9
528	The influence of the nylon balloon stiffness on the efficiency of the intra-aortic balloon occlusion. 2019 , 35, e3173	3
527	A Computational Study of Mechanical Performance of Bioresorbable Polymeric Stents with Design Variations. 2019 , 10, 46-60	10
526	Predissection-derived geometric and distensibility indices reveal increased peak longitudinal stress and stiffness in patients sustaining acute type A aortic dissection: Implications for predicting dissection. 2019 , 158, 355-363	17
525	Multiscale modeling of skeletal muscle tissues based on analytical and numerical homogenization. 2019 , 92, 97-117	14
524	Modeling and Identification of the Mechanical Properties of Achilles Tendon With Application in Health Monitoring. 2019 , 2,	1
523	On the computation of in vivo transmural mean stress of patient-specific aortic wall. 2019 , 18, 387-398	13

522	Coupling among deformation, fluid flow, structural reorganisation and fibre reorientation in fibre-reinforced, transversely isotropic biological tissues. 2019 , 111, 1-13	14
521	A mixed finite element formulation for compressible finite hyperelasticity with two fibre family reinforcement. 2019 , 345, 233-262	3
520	Vascular Tissue Biomechanics: Constitutive Modeling of the Arterial Wall. 2019 , 265-274	
519	An incremental deformation model of arterial dissection. 2019 , 78, 1277-1298	
518	Compressibility of arterial wall - Direct measurement and predictions of compressible constitutive models. 2019 , 90, 538-546	4
517	Sew-free anisotropic textile composites for rapid design and manufacturing of soft wearable robots. 2019 , 27, 52-58	26
516	Bifurcation-based embodied logic and autonomous actuation. 2019 , 10, 128	68
515	Estimation of Biomechanical Properties of Normal and Atherosclerotic Common Carotid Arteries. 2019 , 10, 112-123	3
514	Deformation Behavior of Fiber-Reinforced Hydrogel Structures. 2019 , 19, 1950032	14
513	Progressive changes of elastic moduli of arterial wall and atherosclerotic plaque components during plaque development in human coronary arteries. 2019 , 57, 731-740	16
512	Hybrid constitutive modeling: data-driven learning of corrections to plasticity models. 2019 , 12, 717-725	32
511	Anisotropic finite hyper-elastoplasticity of geomaterials with DruckerBrager/Cap type constitutive model formulation. 2019 , 123, 224-250	14
510	Linking hyperelastic theoretical models and experimental data of vaginal tissue through histological data. 2019 , 82, 271-279	5
509	Constitutive interpretation of arterial stiffness in clinical studies: a methodological review. 2019 , 316, H693-H709	12
508	Effects of elastase digestion on the murine vaginal wall biaxial mechanical response. 2018 ,	11
507	Non-axisymmetric dilatation of a thick-walled aortic aneurysmal tissue. 2019 , 109, 172-181	3
506	A structure-based constitutive model of arterial tissue considering individual natural configurations of elastin and collagen. 2019 , 90, 61-72	10
505	Anisotropic finite strain viscoelasticity: Constitutive modeling and finite element implementation. 2019 , 124, 172-188	20

504	A material modeling approach for the effective response of planar soft tissues for efficient computational simulations. 2019 , 89, 168-198	12
503	Cerebral blood vessel damage in traumatic brain injury. 2019 , 64, 98-113	21
502	White Matter Anisotropy for Impact Simulation and Response Sampling in Traumatic Brain Injury. 2019 , 36, 250-263	40
501	Swelling and axial propagation of bulging with application to aneurysm propagation in arteries. 2020 , 25, 1459-1471	9
500	Patient specific characterization of artery and plaque material properties in peripheral artery disease. 2020 , 101, 103453	14
499	Nonlinear coupled thermo-hyperelasticity analysis of thermal and mechanical wave propagation in a finite domain. 2020 , 537, 122755	9
498	A comparative study of hyperelastic constitutive models for colonic tissue fitted to multiaxial experimental testing. 2020 , 102, 103507	9
497	Prediction of the Effective Mechanical Properties of Regular and Random Fibrous Materials Based on the Mechanics of Generalized Continua. 2020 , 63-122	1
496	Comparison of tensile properties of xenopericardium from three animal species and finite element analysis for bioprosthetic heart valve tissue. 2020 , 44, 278-287	8
495	Biomechanics and Mechanobiology of Extracellular Matrix Remodeling. 2020 , 1-20	
494	Modeling the Structural and Mechanical Properties of the Normal and Aneurysmatic Aortic Wall. 2020 , 55-82	0
493	Effects of longitudinal pre-stretch on the mechanics of human aorta before and after thoracic endovascular aortic repair (TEVAR) in trauma patients. 2020 , 19, 401-413	3
492	Comparative study of variations in mechanical stress and strain of human blood vessels: mechanical reference for vascular cell mechano-biology. 2020 , 19, 519-531	2
491	Characterizing the non-linear mechanical behavior of native and biomimetic engineered tissues in 1D with physically meaningful parameters. 2020 , 102, 103509	1
490	Multiscale composite model of fiber-reinforced tissues with direct representation of sub-tissue properties. 2020 , 19, 745-759	7
489	Quantification of the regional bioarchitecture in the human aorta. 2020 , 236, 142-155	4
488	A phase-field model for fracture of unidirectional fiber-reinforced polymer matrix composites. 2020 , 65, 1149-1166	17
487	Mechanical and structural changes in human thoracic aortas with age. 2020 , 103, 172-188	22

486	Reproducibility assessment of ultrasound-based aortic stiffness quantification and verification using Bi-axial tensile testing. 2020 , 103, 103571	4
485	Lymphatic remodelling in response to lymphatic injury in the hind limbs of sheep. 2020 , 4, 649-661	5
484	Transapical mitral valve repair with neochordae implantation: FSI analysis of neochordae number and complexity of leaflet prolapse. 2020 , 36, e3297	15
483	Comparison of the viscoelastic properties of human abdominal and breast adipose tissue and its incidence on breast reconstruction surgery. A pilot study. 2020 , 71, 37-44	1
482	Analysis of the accuracy on computing nominal stress in a biaxial test for arteries. 2020 , 56, e12331	2
481	On the uniform stress/uniform stretch states of prestressed arteries. 2020 , 486, 110100	1
480	An energy approach to Modified Cam-Clay plasticity and damage modeling of cohesive soils. 2020 , 15, 165-177	7
479	Bio-inspired anisotropic polymeric heart valves exhibiting valve-like mechanical and hemodynamic behavior. 2020 , 63, 629-643	5
478	Predicting the mechanical response of the vaginal wall in ball burst tests based on histology. 2020 , 108, 1925-1933	2
477	A review on the biomechanics of coronary arteries. 2020 , 147, 103201	20
476	The materials science of skin: Analysis, characterization, and modeling. 2020 , 110, 100634	16
475	Effect of axial prestretch and adipose tissue on the inflation-extension behavior of the human abdominal aorta. 2020 , 23, 81-91	3
474	Characterization of chemoelastic effects in arteries using digital volume correlation and optical coherence tomography. 2020 , 102, 127-137	5
473	An adaptive global/local approach for phase-field modeling of anisotropic brittle fracture. 2020 , 361, 112744	41
472	On the tension-compression switch hypothesis in arterial mechanics. 2020 , 103, 103558	2
471	Cardiovascular Disease Prevention: The Earlier the Better? A Review of Plant Sterol Metabolism and Implications of Childhood Supplementation. 2019 , 21,	8
470	Mechanism and Model of a Soft Robot for Head Stabilization in Cancer Radiation Therapy. 2020 , 2020, 4609-4615	1
469	A micromechanical model of tendon and ligament with crimped fibers. 2020 , 112, 104086	4

468	A polyethylene glycol functionalized hyaluronic acid coating for cardiovascular catheter lubrication. 2020 , 196, 109080	5
467	Functional Grading of a Transversely Isotropic Hyperelastic Model with Applications in Modeling Tricuspid and Mitral Valve Transition Regions. 2020 , 21,	2
466	A computational multiscale modeling framework for investigating the mechanical properties of meat. 2020 , 26, 100161	3
465	A hyaluronic acid based lubricious coating for cardiovascular catheters. 2020 , 151, 106495	4
464	Geometric deep learning for computational mechanics Part I: anisotropic hyperelasticity. 2020 , 371, 113299	26
463	Large deformation of hyperelastic thick-walled vessels under combined extension-torsion-pressure: analytical solution and FEM. 2020 , 1-18	4
462	Reinforced Gels and Elastomers for Biomedical and Soft Robotics Applications. 2020 , 2, 1073-1091	40
461	Effect of collagen fibril distributions on the crack profile in articular cartilage. 2020 , 195, 105648	3
460	Inversion point and internal volume of pressurized nonlinearly elastic tube. 2020 , 125, 103530	2
459	Is there any objective and independent characterization and modeling of soft biological tissues?. 2020 , 110, 103915	2
458	Using intravascular ultrasound image-based fluid-structure interaction models and machine learning methods to predict human coronary plaque vulnerability change. 2020 , 23, 1267-1276	2
457	A compressible anisotropic hyperelastic model with and strain invariants. 2020 , 23, 1277-1286	2
456	A fluid-structure interaction analysis of anisotropic Dacron fabric used for aortic replacement. 2020 , 97, 103108	1
455	A finite strain model predicts oblique wrinkles in stretched anisotropic films. 2020 , 155, 103354	6
454	Computer simulations of transapical mitral valve repair with neochordae implantation: Clinical implications. 2020 , 3, 27-44	3
453	A selective smoothed finite element method with visco-hyperelastic constitutive model for analysis of biomechanical responses of brain tissues. 2020 , 121, 5123-5149	7
452	A refined dynamic finite-strain shell theory for incompressible hyperelastic materials: equations and two-dimensional shell virtual work principle. 2020 , 476, 20200031	6
451	Fiber splay precludes the direct identification of ligament material properties: Implications for ACL graft selection. 2020 , 113, 110104	3

450	The Macro- and Micro-Mechanics of the Colon and Rectum II: Theoretical and Computational Methods. 2020 , 7,	2
449	Computational Study of Growth and Remodeling in Ascending Thoracic Aortic Aneurysms Considering Variations of Smooth Muscle Cell Basal Tone. 2020 , 8, 587376	3
448	The influence of fibre alignment on the fracture toughness of anisotropic soft tissue. 2020 , 239, 107289	3
447	A three-dimensional vocal fold posturing model based on muscle mechanics and magnetic resonance imaging of a canine larynx. 2020 , 147, 2597	8
446	IDENTIFICATION OF UNIAXIAL DEFORMATION BEHAVIOR AND ITS INITIAL TANGENT MODULUS FOR ATHEROMATOUS INTIMA IN THE HUMAN CAROTID ARTERY AND THORACIC AORTA USING THREE-PARAMETER ISOTROPIC HYPERELASTIC MODELS. 2020 , 20, 2050014	1
445	Microstructural evolution and failure in short fiber soft composites: Experiments and modeling. 2020 , 141, 103973	5
444	An ultrasound-based approach for the characterization of fluid-structure interaction of large arterial vessels. 2020 , 61, 1	
443	An anisotropic constitutive model for fiber-reinforced materials including gradient-extended damage and plasticity at finite strains. 2020 , 108, 102642	6
442	Wrinkling instabilities for biologically relevant fiber-reinforced composite materials with a case study of Neo-Hookean/Ogden-Gasser-Holzappel bilayer. 2020 , 19, 2375-2395	4
441	Design and Computational Modeling of Fabric Soft Pneumatic Actuators for Wearable Assistive Devices. 2020 , 10, 9638	19
440	Modeling intracranial aneurysm stability and growth: an integrative mechanobiological framework for clinical cases. 2020 , 19, 2413-2431	2
439	In vivo based biomechanics of right and left coronary arteries. 2020 , 154, 103281	6
438	Some unexpected predictions from strongly anisotropic hyperelastic constitutive models of soft tissue. 2020 , 2, 1	3
437	A quasi-incompressible and quasi-inextensible finite element analysis of fibrous soft biological tissues. 2020 , 19, 2357-2373	1
436	Finite element models can reproduce the effect of nucleotomy on the multi-axial compliance of human intervertebral discs. 2020 , 23, 934-944	1
435	Biochemomechanics of the thoracic aorta in health and disease. 2020 , 2, 032002	2
434	Finite strain parametric HFGMC micromechanics of soft tissues. 2020 , 19, 2443-2453	1
433	Nearly-constrained transversely isotropic linear elasticity: energetically consistent anisotropic deformation modes for mixed finite element formulations. 2020 , 202, 166-183	4

- 432 A nonlinear thermomechanical formulation for anisotropic volume and surface continua. **2020**, 25, 2076-2117 1
- 431 The Impact of Self-Expandable Transcatheter Aortic Valve Replacement on Concomitant Functional Mitral Regurgitation: A Comprehensive Engineering Analysis. **2020**, 4, 179-191 3
- 430 A low-distortion mesh moving method based on fiber-reinforced hyperelasticity and optimized zero-stress state. **2020**, 65, 1567-1591 15
- 429 3D Constitutive Model of the Rat Large Intestine: Estimation of the Material Parameters of the Single Layers. **2020**, 608-623
- 428 Calibration of hyperelastic constitutive models: the role of boundary conditions, search algorithms, and experimental variability. **2020**, 19, 1935-1952 1
- 427 Modeling the initial-volume dependent approximate compressibility of porcine liver tissues using a novel volumetric strain energy model. **2020**, 109, 109901 1
- 426 The role of stress concentration in calcified bicuspid aortic valve. **2020**, 17, 20190893 13
- 425 A structural-based computational model of tendon-bone insertion tissues. **2020**, 327, 108411 1
- 424 Residual Stress Estimates from Multi-cut Opening Angles of the Left Ventricle. **2020**, 11, 381-393 1
- 423 Experimental and mathematical characterization of coronary polyamide-12 balloon catheter membranes. **2020**, 15, e0234340 1
- 422 Computationally modelling the mechanical behaviour of turtle shell sutures-A natural interlocking structure. **2020**, 110, 103973 3
- 421 A length scale insensitive phase field model for brittle fracture of hyperelastic solids. **2020**, 236, 107196 10
- 420 Heterogeneous mechanical hyperelastic behavior in the porcine annulus fibrosus explained by fiber orientation: An experimental and numerical approach. **2020**, 104, 103672 6
- 419 A complementary energy approach accommodates scale differences in soft tissues. **2020**, 138, 103895 0
- 418 Cellular Geometry Sensing at Different Length Scales and its Implications for Scaffold Design. **2020**, 13, 26
- 417 Characterization of hyperelastic and damage behavior of tendons. **2020**, 23, 213-223 4
- 416 A novel technique for the assessment of mechanical properties of vascular tissue. **2020**, 19, 1585-1594 1
- 415 Mapping pre-dissection aortic wall abnormalities: a multiparametric assessment. **2020**, 57, 1061-1067 5

414	Artificial intelligence to predict atheroma plaque vulnerability. 2020 , 279-312	
413	A model for hyperelastic materials reinforced with fibers resistance to extension and flexure. 2020 , 193-194, 418-433	2
412	The implications of non-anatomical positioning of a meniscus prosthesis on predicted human knee joint biomechanics. 2020 , 58, 1341-1355	2
411	Tricuspid Chordae Tendineae Mechanics: Insertion Site, Leaflet, and Size-Specific Analysis and Constitutive Modelling. 2021 , 61, 19-29	6
410	Potential damage in pulmonary arterial hypertension: An experimental study of pressure-induced damage of pulmonary artery. 2021 , 109, 579-589	5
409	High rate failure properties of porcine aortic tissue under uniaxial tension. 2021 , 26, 109-119	
408	Mechanical, structural, and physiologic differences in human elastic and muscular arteries of different ages: Comparison of the descending thoracic aorta to the superficial femoral artery. 2021 , 119, 268-283	13
407	A discrete approach for modeling degraded elastic fibers in aortic dissection. 2021 , 373, 113511	8
406	Effect of Glycation on Interlamellar Bonding of Arterial Elastin. 2021 , 61, 81-94	5
405	Mechanical and structural contributions of elastin and collagen fibers to interlamellar bonding in the arterial wall. 2021 , 20, 93-106	6
404	Modeling biomechanical interaction between soft tissue and soft robotic instruments: importance of constitutive anisotropic hyperelastic formulations. 2021 , 40, 224-235	8
403	Review of the Techniques Used for Investigating the Role Elastin and Collagen Play in Arterial Wall Mechanics. 2021 , 14, 256-269	4
402	Geometrically nonlinear modelling of pre-stressed viscoelastic fibre-reinforced composites with application to arteries. 2021 , 20, 323-337	2
401	Cross section shape optimization design of fabric rubber seal. 2021 , 256, 113047	8
400	Unraveling the multilayer mechanical response of aorta using layer-specific residual stresses and experimental properties. 2021 , 113, 104070	4
399	Development of a multiscale model of the human lumbar spine for investigation of tissue loads in people with and without a transtibial amputation during sit-to-stand. 2021 , 20, 339-358	3
398	Neural network constitutive model for crystal structures. 2021 , 67, 185-206	5
397	3D finite element models from serial section histology of skeletal muscle tissue - The role of micro-architecture on mechanical behaviour. 2021 , 113, 104109	6

396	A model for 3D deformation and reconstruction of contractile microtissues. 2021 , 17, 10198-10209	1
395	Manifold learning based data-driven modeling for soft biological tissues. 2021 , 117, 110124	6
394	Coronary remodeling and biomechanics: Are we going with the flow in 2020?. 2021 , 320, H584-H592	4
393	Mechanical characterization and modeling of knitted textile implants with permanent set. 2021 , 114, 104210	1
392	Mechanical Properties of the Cranial Meninges: A Systematic Review. 2021 , 38, 1748-1761	2
391	Computational multiscale modelling of soft tissues mechanics: Application to tendons and ligaments. 2021 , 121-153	1
390	Comparison of morphometric, structural, mechanical, and physiologic characteristics of human superficial femoral and popliteal arteries. 2021 , 121, 431-443	4
389	Sensitivity analysis of non-local damage in soft biological tissues. 2021 , 37, e3427	1
388	A whole blood thrombus mimic: Constitutive behavior under simple shear. 2021 , 115, 104216	12
387	Finite bending of hyperelastic beams with transverse isotropy generated by longitudinal porosity. 2021 , 85, 104131	7
386	A generalised neo-Hookean strain energy function for application to the finite deformation of elastomers. 2021 , 128, 103626	19
385	Simple model of atherosclerosis in cylindrical arteries: impact of anisotropic growth on Glagov remodeling. 2021 , 38, 59-82	0
384	Personalized Computational Models of Tissue-Rearrangement in the Scalp Predict the Mechanical Stress Signature of Rotation Flaps. 2021 , 58, 438-445	2
383	Model reduction for the forming process of fibrous composites structures via second gradient enriched continuum models. 2021 , 28, 1061-1072	0
382	Comparison and experimental validation of predictive models for soft, fiber-reinforced actuators. 2021 , 40, 119-135	8
381	Swelling-Induced Interface Crease Instabilities at Hydrogel Bilayers. <i>Journal of Elasticity</i> , 2021 , 145, 31-47.5	1
380	Animal Model Dependent Response to Pentagalloyl Glucose in Murine Abdominal Aortic Injury. 2021 , 10,	4
379	A microstructure-based model for time-dependent mechanics of multi-layered soft tissues and its application to intervertebral disc annulus. 2021 , 56, 585-606	5

378	Regional Mechanical Characterization of Porcine Pulmonary Arteries. 2021 , 61, 285-303		0
377	Modeling Patient-Specific Periaortic Interactions with Static and Dynamic Structures Using a Moving Heterogeneous Elastic Foundation Boundary Condition. 2021 , 315-327		2
376	Incompressible Transversely Isotropic Hyperelastic Materials and Their Linearized Counterparts. <i>Journal of Elasticity</i> , 2021 , 143, 187-194	1.5	6
375	Numerical Determination of the Circumferential Residual Stress of Porcine Aorta by Pulling-Back Method. 2021 , 34, 346-355		0
374	Quantitative susceptibility mapping of carotid arterial tissue ex vivo: assessing sensitivity to vessel microstructural composition.		0
373	The influence of sample geometry and size on porcine aortic material properties from uniaxial tensile tests using custom-designed tissue cutters, clamps and molds. 2021 , 16, e0244390		1
372	Variation of Passive Biomechanical Properties of the Small Intestine along Its Length: Microstructure-Based Characterization. 2021 , 8,		2
371	A pilot study on biaxial mechanical, collagen microstructural, and morphological characterizations of a resected human intracranial aneurysm tissue. 2021 , 11, 3525		3
370	To form and function: on the role of basement membrane mechanics in tissue development, homeostasis and disease. 2021 , 11, 200360		13
369	Constitutive modeling using structural information on collagen fiber direction and dispersion in human superficial femoral artery specimens of different ages. 2021 , 121, 461-474		8
368	Characterization of the transient mechanical properties of human cornea tissue using the tensile test simulation. 2021 , 26, 102122		2
367	The effect of residual stress on the stability of a circular cylindrical tube. 2021 , 127, 1		3
366	A model for fibre-matrix interaction in non-linearly elastic incompressible orthotropic materials. 2021 , 127, 1		
365	Mechanical homeostasis in tissue equivalents: a review. 2021 , 20, 833-850		8
364	A transversely hyperelastic constitutive model of flexible film composite. 152808372110017		
363	On Structure-Function Relationships in the Female Human Urethra: A Finite Element Model Approach. 2021 , 49, 1848-1860		0
362	Mechanical behaviors of non-orthogonal fabric rubber seal. 2021 , 259, 113453		4
361	A framework for incorporating 3D hyperelastic vascular wall models in 1D blood flow simulations. 2021 , 20, 1231-1249		1

360	Generalised viscoelastic fibre at small strain. 2021 , 127, 1		
359	Reduced biomechanical models for precision-cut lung-slice stretching experiments. 2021 , 82, 35		1
358	Non-anatomical placement adversely affects the functional performance of the meniscal implant: a finite element study. 2021 , 20, 1167-1185		1
357	On fibre dispersion in anisotropic soft biological tissues using fourth-order structural tensors. 2021 , 236-237, 111052		
356	Multi-phase, large-strain constitutive models of cartilage for finite element analyses in 3-D. 1		0
355	Longitudinal histomechanical heterogeneity of the internal thoracic artery. 2021 , 116, 104314		0
354	Comparative Analysis of Nonlinear Viscoelastic Models Across Common Biomechanical Experiments. <i>Journal of Elasticity</i> , 2021 , 145, 117-152	1.5	7
353	Implications of the structure-property relationship on the optomechanical characterization of the cornea: A review. 2021 , 232, 166529		0
352	Flow-mediated dilation analysis coupled with nitric oxide transport to enhance the assessment of endothelial function. 2021 , 131, 1-14		2
351	Paired Pressure-Volume Loop Analysis and Biaxial Mechanical Testing Characterize Differences in Left Ventricular Tissue Stiffness of Volume Overload and Angiotensin-Induced Pressure Overload Hearts. 2021 , 143,		2
350	In vivo parameter identification in arteries considering multiple levels of smooth muscle activity. 2021 , 20, 1547-1559		3
349	Influence of Annular Dynamics and Material Behavior in Finite Element Analysis of Barlow's Mitral Valve Disease. <i>Journal of Elasticity</i> , 2021 , 145, 163-190	1.5	1
348	Effect of axonal fiber architecture on mechanical heterogeneity of the white matter-a statistical micromechanical model. 2021 , 1-13		1
347	Global Sensitivity Analysis of a Homogenized Constrained Mixture Model of Arterial Growth and Remodeling. <i>Journal of Elasticity</i> , 2021 , 145, 191-221	1.5	3
346	Impact of Degradation and Material Crystallinity on the Mechanical Performance of a Bioresorbable Polymeric Stent. <i>Journal of Elasticity</i> , 2021 , 145, 243-264	1.5	
345	Finite Element Implementation of Biphasic-Fluid Structure Interactions in febio. 2021 , 143,		1
344	A finite strain non-parametric hyperelastic extension of the classical phenomenological theory for orthotropic compressible composites. 2021 , 212, 108591		1
343	Identification of mechanical properties of arteries with certification of global optimality. 1		

342	Image-Based Polygonal Lattices for Mechanical Modeling of Biological Materials: 2D Demonstrations. 2021 ,		
341	The orthotropic viscoelastic characterisation of sub-zero 3D-printed poly(vinyl alcohol) cryogel. 2021 , 6, 467-471		1
340	Mechano-chemo-biological Computational Models for Arteries in Health, Disease and Healing: From Tissue Remodelling to Drug-eluting Devices. 2021 , 27, 1904-1917		2
339	Patient-specific fluid-structure interaction model of bile flow: comparison between 1-way and 2-way algorithms. 2021 , 24, 1693-1717		0
338	Spontaneous extension wave for in vivo assessment of arterial wall anisotropy. 2021 , 320, H2429-H2437		
337	Comparison of Kinematics and Contact Mechanics in Normal Knee and Total Knee Replacements: A Computational Investigation. 2021 , 49, 2491-2502		1
336	General Finite-Element Framework of the Virtual Fields Method in Nonlinear Elasticity. <i>Journal of Elasticity</i> , 2021 , 145, 265-294	1.5	0
335	Accelerating cardiac and vessel mechanics simulations: An energy-transform variational formulation for soft-tissue hyperelasticity. 2021 , 379, 113764		3
334	Failure Properties of Healthy and Diabetic Rabbit Thoracic Aortas and Their Potential Correlation with Mass Fractions of Collagen. 2021 , 1		1
333	A Hybrid Microstructural-Continuum Multiscale Approach for Modeling Hyperelastic Fibrous Soft Tissue. <i>Journal of Elasticity</i> , 2021 , 145, 295-319	1.5	0
332	A novel hyperelastic model for biological tissues with planar distributed fibers and a second kind of Poisson effect. 2021 , 151, 104377		5
331	Reprint of:The materials science of skin: Analysis, characterization, and modeling. 2021 , 120, 100816		0
330	Is it Possible to Derive the Dresdner Correction Formula Using a Finite Element Program?. 2021 ,		1
329	Inverse modeling framework for characterizing patient-specific microstructural changes in the pulmonary arteries. 2021 , 119, 104448		3
328	Quantitative susceptibility mapping of carotid arterial tissue ex vivo: Assessing sensitivity to vessel microstructural composition. 2021 , 86, 2512-2527		0
327	Evaluation methods for mechanical biocompatibility of hernia repair meshes: respective characteristics, application scope and future perspectives. 2021 , 13, 1826-1840		2
326	Plasticity and Enzymatic Degradation Coupled With Volumetric Growth in Pulmonary Hypertension Progression. 2021 , 143,		2
325	Topologically engineered 3D printed architectures with superior mechanical strength. 2021 , 48, 72-72		5

324	Microstructural and mechanical characterization of the layers of human descending thoracic aortas. 2021 , 134, 401-421	11
323	Experimental investigations of the human oesophagus: anisotropic properties of the muscular layer in large deformation.	
322	Mathematical Modeling and Numerical Simulation of Atherosclerosis Based on a Novel Surgeon's View. 2021 , 28, 1-20	1
321	Viscoelastic characterization of human descending thoracic aortas under cyclic load. 2021 , 130, 291-307	7
320	The Performance of a Spherical-tip Catheter for Stent Post-dilation: Finite Element Analysis and Experiments. 2021 , 12, 734565	1
319	A literature review on large intestinal hyperelastic constitutive modeling. 2021 , 88, 105445	1
318	A Novel Constitutive Parameters Identification Procedure for Hyperelastic Skeletal Muscles Using Two-Way Neural Networks. 2150060	1
317	A novel phenomenological viewpoint for transversely isotropic hyperelastic materials; a new strain energy density function. 2021 , 225, 111064	1
316	Mechanics of hyperelastic composites reinforced with nonlinear elastic fibrous materials in finite plane elastostatics. 2021 , 165, 103491	1
315	Multiscale numerical analyses of arterial tissue with embedded elements in the finite strain regime. 2021 , 381, 113844	3
314	A continuum model and simulations for large deformation of anisotropic fiber-matrix composites for cardiac tissue engineering. 2021 , 121, 104627	3
313	Toward Elucidating the Physiological Impacts of Residual Stresses in the Colorectum. 2022 , 144,	1
312	A finite-strain micromechanical model for the hyperelasticity of tendons and ligaments with crimped fibers. 2021 , 160, 103955	1
311	Pioneering personalised design of femoropopliteal nitinol stents. 2021 , 130, 112462	0
310	Computational fluid dynamics simulations for 3D muscle fiber architecture in finite element analysis: Comparisons between computational fluid dynamics and diffusion tensor imaging. 2021 , e3521	0
309	Bifurcation analysis of elastic residually-stressed circular cylindrical tubes. 2021 , 226-227, 111062	4
308	A comparison of passive and active wall mechanics between elastic and muscular arteries of juvenile and adult rats. 2021 , 126, 110642	0
307	A Parametric Study on Factors Influencing the Onset and Propagation of Aortic Dissection Using the Extended Finite Element Method. 2021 , 68, 2918-2929	0

306	Determination of a Strain Energy Density Function for the Tricuspid Valve Leaflets Using Constant Invariant-Based Mechanical Characterizations. 2021 , 143,		
305	The residually stressed unloaded state of arteries: Membrane and thin cylinder approximations. 2021 , 122, 104521		1
304	Entirely Lagrangian meshfree computational methods for hydroelastic fluid-structure interactions in ocean engineering. Reliability, adaptivity and generality. 2021 , 115, 102822		12
303	Universal deformations in anisotropic nonlinear elastic solids. 2021 , 156, 104598		3
302	An anisotropic constitutive model for 3D printed hydrogel-fiber composites. 2021 , 156, 104611		1
301	Steady diffusion of an ideal fluid through a two-layer thick walled pre-stressed and fiber-reinforced hollow cylinder within the context of mixture theory. 2021 , 169, 103575		0
300	A virtual element method for transversely isotropic hyperelasticity. 2021 , 386, 114108		3
299	A model for irreversible deformation phenomena driven by hydrostatic stress, deviatoric stress and an externally applied field. 2021 , 169, 103573		2
298	Quantitative Determination of Local Density of Iron Oxide Nanoparticles Used for Drug Targeting Employing Inverse Magnetomotive Ultrasound. 2021 , 68, 2482-2495		1
297	Insights into the Microstructural Origin of Brain Viscoelasticity. <i>Journal of Elasticity</i> , 2021 , 145, 99-116	1.5	7
296	Mesosopic approaches for composite reinforcement mechanical behavior. 2021 , 499-536		
295	Constitutive framework of a new hyperelastic model for isotropic rubber-like materials for finite element implementation. 2021 , 18,		1
294	Virtual Fields Method, The. 301-330		16
293	Computational predictions of damage propagation preceding dissection of ascending thoracic aortic aneurysms. 2018 , 34, e2944		15
292	Towards a Computational Methodology for Optimizing Angioplasty Treatments with Stenting. 2006 , 225-240		1
291	Parameter Identification in Arteries Using Constraints. 2006 , 295-305		7
290	Modeling and Simulation of Remodeling in Soft Biological Tissues. 2006 , 77-89		3
289	Finite Element Models for Mechanical Simulation of Coronary Arteries. 2003 , 295-305		4

288	Biological Soft Tissues. 2008 , 169-186	7
287	Collagen in Arterial Walls: Biomechanical Aspects. 2008 , 285-324	31
286	Soft Tissues Characteristics and Strategies for Their Replacement and Regeneration. 2009 , 1-40	5
285	Computational Modeling of Aortic Heart Valve Mechanics Across Multiple Scales. 2010 , 255-275	1
284	Bio-prosthetic Heart Valve Stress Analysis: Impacts of Leaflet Properties and Stent Tip Deflection. 2011 , 73-78	2
283	Identification of Tongue Muscle Fibre Group Contraction from MR Images. 2013 , 185-196	1
282	Intraoperative Damage Monitoring of Endoclamp Balloon Expansion Using Real-Time Finite Element Modeling. 2013 , 39-47	1
281	Need for a Continuum Biochemomechanical Theory of Soft Tissue and Cellular Growth and Remodeling. 2009 , 1-82	3
280	Multi-scale Modelling of the Heart. 2009 , 83-177	3
279	Arterial Tissue in Health and Disease: Experimental Data, Collagen-Based Modeling and Simulation, Including Aortic Dissection. 2009 , 259-344	11
278	Can Numerical Modelling Help Surgeons in Abdominal Hernia Surgery?. 2014 , 167-185	1
277	A Gradient-Enhanced Continuum Damage Model for Residually Stressed Fibre-Reinforced Materials at Finite Strains. 2015 , 19-40	4
276	The Biomechanical Rupture Risk Assessment of Abdominal Aortic Aneurysms Method and Clinical Relevance. 2018 , 233-253	1
275	Elastic Growth Models. 2008 , 1-44	24
274	Advanced Multi-scale Modelling of the Respiratory System. 2011 , 1-32	4
273	FETI Methods for the Simulation of Biological Tissues. 2013 , 91, 503-510	1
272	Nonlinear Elasticity, Anisotropy, Material Stability and Residual Stresses in Soft Tissue. 2003 , 65-108	65
271	Structural and Numerical Models for the (Visco)elastic Response of Arterial Walls with Residual Stresses. 2003 , 109-184	20


270	Remodeling of Arteries in Response to Changes in their Mechanical Environment. 2003 , 221-271	9
269	Computational Biomechanics of the Human Cornea. 2010 , 435-466	5
268	Computational Models of Vascular Mechanics. 2010 , 99-170	3
267	Computational Modeling of Vascular Hemodynamics. 2010 , 171-206	6
266	A numerical study of arterial media dissection processes. 2010 , 21-33	1
265	Patient Specific Computational Modeling in Cardiovascular Mechanics. 2012 , 61-79	2
264	Bridging Scales in Respiratory Mechanics. 2013 , 395-407	2
263	A Mathematical Approach for Studying Ca ²⁺ -Regulated Smooth Muscle Contraction. 2013 , 45-62	1
262	A Coupled Chemomechanical Model for Smooth Muscle Contraction. 2013 , 63-75	3
261	Modelling Cardiac Tissue Growth and Remodelling. <i>Journal of Elasticity</i> , 2017 , 129, 283-305	1.5 12
260	Experiment, modeling and simulation of bypassing holes in composites. 2020 , 234, 111666	2
259	Finite-element modelling of frictional behaviour between oesophagus and endoscope. 2020 , 6, 75-81	1
258	Dynamics and spectral stability of soliton-like structures in fluid-filled membrane tubes. 2020 , 75, 843-882	3
257	Functional Tissue-Engineered Valves from Cell-Remodeled Fibrin with Commissural Alignment of Cell-Produced Collagen. 2008 , 14, 83-95	5
256	Mathematical and computational modelling of skin biophysics: a review. 2017 , 473, 20170257	40
255	A Whole Blood Thrombus Mimic: Constitutive Behavior Under Simple Shear.	2
254	Estimation of in vivo constitutive parameters of the aortic wall: a machine learning approach.	1
253	Combining IVUS and Optical Coherence Tomography for More Accurate Coronary Cap Thickness Quantification and Stress/Strain Calculations: A Patient-Specific Three-Dimensional Fluid-Structure Interaction Modeling Approach. 2018 , 140,	20

252	Veins are more compressible than arteries: A new method of testing. 2019 ,	1
251	A Recruitment Model of Tendon Viscoelasticity That Incorporates Fibril Creep and Explains Strain-Dependent Relaxation. 2020 , 142,	10
250	Stress-Swelling Finite Element Modeling of Cervical Response With Homeostatic Collagen Fiber Distributions. 2020 , 142,	7
249	Specialized Strain Energy Functions for Modeling the Contribution of the Collagen Network (Waniso) to the Deformation of Soft Tissues. 2020 , 87,	2
248	Performance of a Nitinol Honeycomb Stent for the Management of Atherosclerotic Aortic Plaque: Crimping, Sealing, and Fluid-Structure Interaction Analysis. 2021 , 88,	1
247	Characterization of the mechanical behavior and pathophysiological state of abdominal aortic aneurysms based on 4D ultrasound strain imaging. 2017 ,	2
246	Fiber-Matrix Models of the Dermis. 2014 , 133-159	2
245	Anisotropic hyperelastic models in Abaqus. 2009 , 365-369	1
244	Large deformation analysis of inflated air-spring shell made of rubber-textile cord composite. 2006 , 24, 31-50	5
243	IVUS validation of patient coronary artery lumen area obtained from CT images. 2014 , 9, e86949	13
242	Fluid-Structure Interaction Simulation of Prosthetic Aortic Valves: Comparison between Immersed Boundary and Arbitrary Lagrangian-Eulerian Techniques for the Mesh Representation. 2016 , 11, e0154517	44
241	MRI-based patient-specific human carotid atherosclerotic vessel material property variations in patients, vessel location and long-term follow up. 2017 , 12, e0180829	6
240	Mechanical and geometrical determinants of wall stress in abdominal aortic aneurysms: A computational study. 2018 , 13, e0192032	19
239	Consideration of stiffness of wall layers is decisive for patient-specific analysis of carotid artery with atheroma. 2020 , 15, e0239447	3
238	Non-Linear Mechanical Behavior of Visco-Elastic Biological Structures [Measurements and Models. 2004 , 47, 297-300	2
237	Constitutive Relation for Large Deformations of Fiber-Reinforced Rubberlike Materials with Different Response in Tension and Compression. 2016 , 44, 51-72	0
236	A Data-Driven Learning Method for Constitutive Modeling: Application to Vascular Hyperelastic Soft Tissues. 2020 , 13,	5
235	Finite Element Analysis based on A Parametric Model by Approximating Point Clouds. 2020 , 12, 518	7

234	Contralateral Eye Comparison of SMILE and Flap-Based Corneal Refractive Surgery: Computational Analysis of Biomechanical Impact. 2017 , 33, 444-453	34
233	Modeling and simulation in tissue biomechanics: Modern tools to face an ancient challenge. 2013 , 06, 1-5	3
232	On the theoretical basis of rational continuum mechanics in softmatter. 2016 , 65, 188103	2
231	Multi Element Diverging Beam from a Linear Array Transducer for Transverse Cross Sectional Imaging of Carotid Artery: Simulations and Phantom Vessel Validation. 2011 , 50, 07HF05	6
230	Mechano-regulated cell-cell signaling in the context of cardiovascular tissue engineering. 2021 , 1	0
229	Torsion of rubber-like hollow and solid circular cylinders for incompressible hyperelastic materials with limiting chain extensibility. 2021 , 104443	8
228	A biologically-inspired mesh optimizer based on pseudo-material remodeling. 1	1
227	A novel framework for quantifying the subject-specific three-dimensional residual stress field in the aortic wall. 2022 , 125, 104906	0
226	Fiber Rearrangement and Matrix Compression in Soft Tissues: Multiscale Hypoelasticity and Application to Tendon. 2021 , 9, 725047	0
225	Patient-specific analysis of bicuspid aortic valve hemodynamics using a fully coupled fluid-structure interaction (FSI) model.	1
224	Developing a Lung Model in the Age of COVID-19: A Digital Image Correlation and Inverse Finite Element Analysis Framework. 2021 , 9, 684778	5
223	A Computational Growth Framework for Biological Tissues: Application to Growth of Aortic Root Aneurysm Repaired by the V-shape Surgery.	1
222	Fibrillar Collagen: A Review of the Mechanical Modeling of Strain Mediated Enzymatic Turnover. 2021 ,	2
221	Necking Phenomena of a Fiber-Reinforced Bar modeled by Multisurface Plasticity. 2003 , 211-220	1
220	Mathematical Modeling of Three-Dimensional Delamination Processes of Laminated Composites. 2004 , 85-99	
219	Structure and Mechanics of the Artery. 2007 , 45-81	
218	Surgical planning and patient-specific biomechanical simulation for tracheal endoprotheses interventions. 2009 , 12, 275-82	1
217	Strain energy function for arterial walls based on limiting fiber extensibility. 2009 , 1910-1913	

- 216 Modeling of Rubberlike Materials. **2009**, 147-202
- 215 Hysteretic Behavior of Ligaments and Tendons: Microstructural Analysis of Damage, Softening and Non-Recoverable Strain. **2010**, 31-43
- 214 Formulation and Computational Implementation of Constitutive Models for Cardiovascular Soft Tissue Simulations. **2010**, 157-190
- 213 Viscoelasticity. **2011**, 61-108
- 212 A Study on Effect of Residual Stress on Stress Distribution of Arterial Walls Under High Blood Pressure. **2011**, 35, 1219-1227
- 211 Patient-Specific Biomechanical Framework for Aiding Clinical Decisions in Eye Surgery. **2012**, 161-193
- 210 A quasi-lumped model for the peripheral distortion of the arterial pulse. **2012**, 9, 175-98
- 209 Mechanics of Biosolids and Computational Analysis. **2012**, 19-86
- 208 Detection of Boundaries of Carotid Arterial Wall by Analyzing Ultrasonic RF Signals. **2012**, 51, 07GF07
- 207 Three-Dimension Stress and Strain Distributions Across Five-Layer Human Aortic Wall. **2013**, 116-119 1
- 206 Modeling of Smooth Muscle Activation. **2013**, 77-89
- 205 Role of Elastin in Arterial Mechanics. 267-281
- 204 Comparing the Passive Biomechanics of Tension-Pressure Loading of Porcine Renal Artery and Its First Branch. **2014**, 35-40
- 203 Fundamental Aspects in Modelling the Constitutive Behaviour of Fibered Soft Tissues. **2014**, 3-49
- 202 Modelo biomecánico del globo ocular. **2014**, 359-366
- 201 Physiology and Pathophysiology of Arterial Flow. **2014**, 1-41
- 200 Arterial Flow. **2014**, 1-42
- 199 Biomimetic Composites Reinforced by Branched Nanofibers. **2015**, 7-23 1

- 198 Model-Based Interpretation of Skin Microstructural and Mechanical Measurements. **2015**, 1-20
- 197 Long Range Force Transmission in Fibrous Matrices Enabled by Tension-Driven Alignment of Fibers. **2015**, 1
- 196 Model-Based Interpretation of Skin Microstructural and Mechanical Measurements. **2017**, 1019-1037
- 195 Multi-scale Structural Modeling of Soft Tissues Mechanics and Mechanobiology. **2018**, 7-48 **1**
- 194 A Computational Model of the Biochemomechanics of an Evolving Occlusive Thrombus. **2018**, 125-144
- 193 Modelling Cardiac Tissue Growth and Remodelling. **2018**, 283-305
- 192 Encyclopedia of Continuum Mechanics. **2018**, 1-14
- 191 Anisotropic Continuum Stored Energy Functional Solved by Lie Group and Differential Geometry. **2018**, 08, 631-651 **1**
- 190 Encyclopedia of Continuum Mechanics. **2018**, 1-12
- 189 Can we obtain in vivo transmural mean hoop stress of the aortic wall without knowing patient-specific material properties and residual deformations?.
- 188 A Systematic Survey of the Realm of Biomechanics. **2019**, 1-35
- 187 Intrinsic Optical Imaging of ECM Mechanics. **2020**, 165-202 **1**
- 186 Finite Deformation Elasticity Theory. **2020**, 17-52 **1**
- 185 FITTING OF HYPERELASTIC CONSTITUTIVE MODELS IN DIFFERENT SHEEP HEART REGIONS BASED ON BIAXIAL MECHANICAL PROPERTIES. **0**
- 184 Encyclopedia of Continuum Mechanics. **2020**, 562-576
- 183 Mechanical Testing of Vascular Grafts. **2020**, 1-28
- 182 Computational Investigation of the Stability of Stenotic Carotid Artery under Pulsatile Blood Flow Using a Fluid-Structure Interaction Approach. **2020**, 12, 2050110 **4**
- 181 A selective smoothed finite element method for 3D explicit dynamic analysis of the human annulus fibrosus with modified composite-based constitutive model. **2022**, 134, 49-65 **1**

- 180 Analysis of expansion within a pressure inflated section of a simplified urethral model. **2021**, 54, 85-90
- 179 Continuum Mechanics and Nonlinear Elasticity. **2020**, 51-154
- 178 Inception of Material Instabilities in Arteries. **2020**, 297-304
- 177 Damage and Failure of the Vascular Wall. **2020**, 551-562
- 176 Mechanical Testing of Vascular Grafts. **2020**, 35-61 ○
- 175 Constitutive Modelling of Knitted Abdominal Implants in Numerical Simulations of Repaired Hernia Mechanics. **2020**, 550-559
- 174 Encyclopedia of Continuum Mechanics. **2020**, 1987-2000
- 173  **2020**, 75, 59-100 1
- 172 Multiscale finite element musculoskeletal model for intact knee dynamics. **2021**, 141, 105023 2
- 171 Physically-based structural modeling of a typical regenerative tissue analog bridges material macroscale continuum and cellular microscale discreteness and elucidates the hierarchical characteristics of cell-matrix interaction.. **2021**, 126, 104956 ○
- 170 Optical Coherence Tomography-Derived Changes in Plaque Structural Stress Over the Cardiac Cycle: A New Method for Plaque Biomechanical Assessment. **2021**, 8, 715995 ○
- 169 Reduced biomechanical models for precision-cut lung-slice stretching experiments.
- 168 A Coupled FE Analysis of the Intervertebral Disc Based on a Multiphasic TPM Formulation. **2006**, 405-419
- 167 Kinematics and Mechanics of Large Deformations. **2007**, 507-557 1
- 166 Tendon and Ligament. **2007**, 559-594
- 165 Theoretical Modeling of Enlarging Intracranial Aneurysms. **2007**, 101-123
- 164 Fluid-Structure Interaction Applied to Blood Flow Simulations. **2009**, 253-271
- 163 Multi-Physical Simulation of Left-ventricular Blood Flow Based On Patient-specific MRI Data. **2009**, 1542-1545

162 The Influence of Anterior Cruciate Ligament Matrix Mechanical Properties on Simulated Whole-Knee Biomechanics. **2020**, 142,

161 Modeling of Damage Evolution in a Patient-Specific Stenosed Artery upon Stent Deployment. **2020**, 12, 2050101

160 Blood vessel-on-a-chip examines the biomechanics of microvasculature. **2021**, 3

159 Passive biaxial mechanical behavior of newborn mouse aorta with and without elastin. **2021**, 126, 105021 0

158 Iterative Methods for the Biomechanical Evaluation of Corneal Response. A Case Study in the Measurement Phase. **2021**, 11, 10819 3

157 Efficient computational modelling of smooth muscle orientation and function in the aorta. **2021**, 477,

156 Experimental analysis and biaxial biomechanical behaviour of ex-vivo sheep trachea.

155 Personalised nitinol stent for focal plaques: Design and evaluation. **2021**, 130, 110873 0

154 Contravariant tensor algebra for anisotropic hyperelasticity. **2021**, 2070, 012161

153 Understanding the deformation gradient in Abaqus and key guidelines for anisotropic hyperelastic user material subroutines (UMATs).. **2021**, 126, 104940 0

152 Multiscale modeling of skeletal muscle to explore its passive mechanical properties and experiments verification.. **2022**, 19, 1251-1279

151 A Micro-Mechanical Model for the Fibrous Tissues of Vocal Folds.

150 In-silico Modeling of the Micromechanics of Fibrous Scaffolds and Stiffness Sensing by Cells. 1

149 Risky interpretations across the length scales: continuum vs. discrete models for soft tissue mechanobiology.. **2022**, 1 3

148 A Review on Damage and Rupture Modelling for Soft Tissues.. **2022**, 9, 1

147 A Constitutive Model of Human Dermis Skin Incorporating Different Collagen Fiber Families. **2022**, 89, 0

146 Elastic fibers: The near ideal linear springs of the extracellular matrix. **2022**, 193-227

145 The Implicit Finite Difference Method in the Deformation Mechanics of Homogeneous and Piecewise Homogeneous Bodies. **2022**, 57, 795-812

- 144 An ultrastructural 3D reconstruction method for observing the arrangement of collagen fibrils and proteoglycans in the human aortic wall under mechanical load.. **2022**, 1
- 143 Effects of Material Non-Symmetry on the Mechanical Behavior of Arterial Wall.
- 142 Structural Mechanisms in Soft Fibrous Tissues: A Review. **2022**, 8, 2
- 141 Role of smooth muscle activation in the static and dynamic mechanical characterization of human aortas.. **2022**, 119, 4
- 140 Multiscale mechanobiology: coupling models of adhesion kinetics and nonlinear tissue mechanics.. **2022**, 0
- 139 A computational framework for biomaterials containing three-dimensional random fiber networks based on the affine kinematics.. **2022**, 21, 685 1
- 138 Biomechanical characterization and constitutive modeling of the layer-dissected residual strains and mechanical properties of abdominal porcine aorta.. **2022**, 132, 110909
- 137 Cell twisting during desiccation reveals axial asymmetry in wall organization.. **2022**, 1
- 136 A Strain-Rate Dependent Constitutive Model for Göttingen Minipig Cerebral Arteries.. **2022**, 1
- 135 The Vascular Wall, an Active Entity. **2021**, 353-401
- 134 Conduit Vessels. **2021**, 233-304
- 133 A Discrete Fiber Network Finite Element Model of Arterial Elastin Network Considering Inter-Fiber Crosslinking Property and Density.
- 132 Anisotropic Failure Criteria in Relation to Crack Phase-Field Modeling at Finite Strains. **2022**, 151-159
- 131 Impact of Variation in Interleaflet Triangle Height Between Fused Leaflets in the Functionally Bicuspid Aortic Valve on Hemodynamics and Tissue Biomechanics. **2022**, 5, 0
- 130 Biomechanical characterization of the small intestine to simulate gastrointestinal tract chyme propulsion.. **2022**, e3588
- 129 Soft Tissue Hybrid Model for Real-Time Simulations.. **2022**, 14, 1
- 128 Micromechanical and Ultrastructural Properties of Abdominal Aortic Aneurysms. **2022**, 28, 15-30 0
- 127 The Effects of the Mechanical Properties of Vascular Grafts and an Anisotropic Hyperelastic Aortic Model on Local Hemodynamics during Modified Blalock-Taussig Shunt Operation, Assessed Using FSI Simulation.. **2022**, 15, 0

- 126 Comparative study of arterial wall models for numerical fluid-structure interaction simulation of aortic arch aneurysms. **2022**, 44, 1
- 125 Molecular mechanisms mediating stiffening in the mechanically adaptable connective tissues of sea cucumbers.. **2022**, 2
- 124 A micro-mechanical model for the fibrous tissues of vocal folds.. **2022**, 128, 105118 0
- 123 Effects of material non-symmetry on the mechanical behavior of arterial wall.. **2022**, 129, 105157 1
- 122 An anisotropic hyper-visco-pseudo-elastic model and explicit stress solutions for fabric reinforced rubber composites. **2022**, 242, 111519 0
- 121 Cerebral aneurysm evolution modeling from microstructural computational models to machine learning: A review.. **2022**, 98, 107676 0
- 120 New Boundary Conditions for One-Dimensional Network Models of Hemodynamics. **2021**, 61, 2102-2117 0
- 119 Kelvin decomposition for nonlinear hyperelastic modeling in large deformation. **2021**, 9, 337-365
- 118 Effects of Contact Pressure in Reflectance Photoplethysmography in an In Vitro Tissue-Vessel Phantom.. **2021**, 21, 0
- 117 Pitchfork bifurcations in simple hyperelastic orthotropic arterial models and their constitutive implications. 108128652210849
- 116 Viscoelastic Behavior of Porcine Arterial Tissue: Experimental and Numerical Study. 1
- 115 Effects of Laser Keratomileusis and Small-Incision Lenticule Extraction on Corneal Biomechanical Behavior: A Finite Element Analysis.. **2022**, 10, 855367 0
- 114 Poisson's ratio and compressibility of arterial wall - Improved experimental data reject auxetic behaviour.. **2022**, 131, 105229
- 113 Data_Sheet_1.ZIP. **2018**,
- 112 Medical Image-Based Computational Fluid Dynamics and Fluid-Structure Interaction Analysis in Vascular Diseases.. **2022**, 10, 855791 2
- 111 Differences in Collagen Fiber Diameter and Waviness between Healthy and Aneurysmal Abdominal Aortas.. **2022**, 1-15 0
- 110 Multiscale Simulations Suggest a Protective Role of Neo-Adventitia in Abdominal Aortic Aneurysms.. **2022**, 0
- 109 Experimental fracture mechanics analysis of tearing in oriented polyethylene films using digital image correlation and full-field solid mechanics post-processing. 1

- 108 Predicting Coronary Stenosis Progression Using Plaque Fatigue From IVUS-Based Thin-Slice Models: A Machine Learning Random Forest Approach. **2022**, 13,
- 107 Elastomeric Tubes with Self-Regulated Distension. **2022**, 104369
- 106 Effect of a Gradient Distribution of Cross-Links on the Deformation Behaviors of Corneal Stroma: Theoretical Model and Finite Element Simulation. **2022**, 9, 0
- 105 Unraveling the distinct germination processes of sporopollenin-based pollen grains and spores through morphological analyses upon natural nano-architectonics process. **2022**, 27, 101471 1
- 104 Decellularization of Porcine Carotid Arteries: From the Vessel to the High-Quality Scaffold in Five Hours. **2022**, 10,
- 103 Efficient Finite Element Modeling of Steel Cables in Reinforced Rubber. **2022**, 6, 152 0
- 102 Numerical simulations of the nonsymmetric growth and remodeling of arteries under axial twisting. **2022**, 140, 111165
- 101 Nonlinear free and forced vibrations of a fiber-reinforced dielectric elastomer-based microbeam. **2022**, 144, 104092 1
- 100 Global Parameter Identification in Soft Tissues. **2022**, 369-389
- 99 Simulation of Arterial Walls: Growth, Fiber Reorientation, and Active Response. **2022**, 181-209 1
- 98 Biomechanics of the Main Artery in the Lower Limb. **2022**, 157-179
- 97 Classification of Biomechanical Models: The Wrong Battle Between Phenomenological and Structural Approaches, the Partly Underestimated Strength of Phenomenology and Challenges for Future (Clinical) Applications. **2022**, 335-352
- 96 Configurational Forces in Penetration Processes. **2022**, 429-437
- 95 Rational choice of modelling assumptions for simulation of blood vessel end-to-side anastomosis. 0
- 94 Design and Simulation of the Biomechanics of Multi-Layered Composite Poly(Vinyl Alcohol) Coronary Artery Grafts. 9, 0
- 93 Fluid-Structure Interaction Simulations of Repaired Type A Aortic Dissection: a Comprehensive Comparison With Rigid Wall Models. 13, 0
- 92 Measurement of Layer-Specific Mechanical Properties of Intact Blood Vessels Based on Intravascular Optical Coherence Tomography.
- 91 Design and fabrication of fiber mesh actuators. **2022**, 29, 101562

- 90 A study of hyperelastic continuum models for isotropic athermal fibrous networks. 1
- 89 Some Effects of Fiber Dispersion on the Mechanical Response of Incompressible Soft Solids. *Journal of Elasticity*, 1.5
- 88 Modelling the rate-dependency of the mechanical behaviour of the aortic heart valve: An experimentally guided theoretical framework. **2022**, 105341
- 87 Phosphotungstic acid (PTA) preferentially binds to collagen-rich regions of porcine carotid arteries and human atherosclerotic plaques using 3D micro-computed tomography (CE-CT).
- 86 Tough, aorta-inspired soft composites. **2022**, 119, 3
- 85 Data-driven tissue mechanics with polyconvex neural ordinary differential equations. **2022**, 398, 115248 0
- 84 Computational analysis of the role of mechanosensitive Notch signaling in arterial adaptation to hypertension. **2022**, 133, 105325 0
- 83 Correlation between age, location, orientation, loading velocity and delamination strength in the human aorta. **2022**, 133, 105340 0
- 82 Convexity, polyconvexity and finite element implementation of a four-fiber anisotropic hyperelastic strain energy density. Application to the modeling of femoral, popliteal and tibial arteries. **2022**, 399, 115294
- 81 The Universal Program of Nonlinear Hyperelasticity. 1
- 80 Buckling of Thin-Walled Cylinders from Three Dimensional Nonlinear Elasticity. *Journal of Elasticity*, 1.5
- 79 An agent-based model of vibration-induced intimal hyperplasia. 1
- 78 Shear stress and intravascular pressure effects on vascular dynamics: two-phase blood flow in elastic microvessels accounting for the passive stresses. 0
- 77 Strain Measures and Energies for Crimped Fibres and Novel Analytical Expressions for Fibre Populations: Ingredients for Structural Fibre Network Models. **2022**, 150, 401-448
- 76 An intricate interplay between stent drug dose and release rate dictates arterial restenosis. **2022**, 349, 992-1008 1
- 75 Impact of mathematical requirements on the invariant-based anisotropic constitutive models for non-linear biomaterials. **2022**, 147, 104188
- 74 Group theoretical approach to elasticity under constraints and predeformations. **2022**, 106, 0
- 73 A discrete fiber network finite element model of arterial elastin network considering inter-fiber crosslinking property and density. **2022**, 134, 105396 0

72	Numerical analysis of biothermal-fluids and cardiac thermal pulse of abdominal aortic aneurysm. 2022 , 19, 10213-10251	1
71	Ogden material calibration via magnetic resonance cartography, parameter sensitivity and variational system identification. 2022 , 380,	1
70	Modelling brain tissue elasticity with the Ogden model and an alternative family of constitutive models. 2022 , 380,	1
69	Biology and Hemodynamics of Aneurysm Rupture. 2022 ,	0
68	Constitutive Formulations for Network Materials. 2022 , 252-277	0
67	Quantification of patient-specific coronary material properties and their correlations with plaque morphological characteristics: An in vivo IVUS study. 2022 ,	0
66	Mechanical Behavior of Subcutaneous and Visceral Abdominal Adipose Tissue in Patients with Obesity. 2022 , 10, 1798	0
65	Data-driven computational models of ventricular-arterial hemodynamics in pediatric pulmonary arterial hypertension. 13,	0
64	On the choice of mathematical functions to model damage in anisotropic soft tissues. 2022 ,	0
63	Effect of Nonlinear Hyperelastic Property of Arterial Tissues on the Pulse Wave Velocity based on the Unified-Fiber-Distribution (UFD) Model.	0
62	Image-Based Finite Element Modeling Approach for Characterizing In Vivo Mechanical Properties of Human Arteries. 2022 , 13, 147	0
61	Fluid-Structure Interaction Analysis of Aerodynamic and Elasticity Forces During Vocal Fold Vibration. 2022 ,	0
60	On viscoelastic deformation of growing skin in reconstructive surgery. 2022 , 128,	0
59	Changes in the microstructure of the human aortic medial layer under biaxial loading investigated by multi-photon microscopy. 2022 , 151, 396-413	0
58	A detailed methodology to model the Non Contact Tonometry: a Fluid Structure Interaction study. 10,	0
57	Hemodynamic characteristics in a cerebral aneurysm model using non-Newtonian blood analogues. 2022 , 34, 103101	0
56	Pentagalloyl Glucose (PGG) Prevents and Restores Mechanical Changes Caused by Elastic Fiber Fragmentation in the Mouse Ascending Aorta.	0
55	Modeling and experimental approaches for elucidating multi-scale uterine smooth muscle electro- and mechano-physiology: A review. 13,	0

- 54 Stochastic modeling of inhomogeneities in the aortic wall and uncertainty quantification using a Bayesian encoder-decoder surrogate. **2022**, 401, 115594 ○
- 53 Patient-Specific Finite Element Modeling of Aneurysmal Dilatation After Chronic Type B Aortic Dissection. **2022**, 15-38 ○
- 52 Layer-Specific Damage Modeling of Porcine Large Intestine under Biaxial Tension. **2022**, 9, 528 ○
- 51 Region-dependent mechanical characterization of porcine thoracic aorta with a one-to-many correspondence method to create virtual datasets using uniaxial tensile tests. 10, ○
- 50 Numerical analysis of a brain artery in ANSYS. **2022**, 44, ○
- 49 Computational aspects of viscoelastic growth mechanics of skin in plastic surgery. 1-11 ○
- 48 Importance of posterior tibial slope in joint kinematics with an anterior cruciate ligament-deficient knee. **2022**, 11, 739-750 ○
- 47 Oil Palm Fibers Micromechanics: Anisotropic Behavior. 1-11 ○
- 46 A numerical investigation of the mechanics of intracranial aneurysms walls: Assessing the influence of tissue hyperelastic laws and heterogeneous properties on the stress and stretch fields. **2022**, 136, 105498 ○
- 45 Constitutive relationship of fabric rubber composites and its application. **2023**, 304, 116302 ○
- 44 Hyperelastic structures: A review on the mechanics and biomechanics. **2023**, 148, 104275 ○
- 43 A new family of Constitutive Artificial Neural Networks towards automated model discovery. **2023**, 403, 115731 ○
- 42 On skin growth using hyperelastic membrane model. **2022**, 44, ○
- 41 Automated model discovery for human brain using Constitutive Artificial Neural Networks. ○
- 40 Strain energy density as a Gaussian process and its utilization in stochastic finite element analysis: Application to planar soft tissues. **2023**, 404, 115812 ○
- 39 Importance of experimental evaluation of structural parameters for constitutive modelling of aorta. **2023**, 138, 105615 ○
- 38 Modeling large-volume subcutaneous injection of monoclonal antibodies with anisotropic porohyperelastic models and data-driven tissue layer geometries. **2023**, 138, 105602 ○
- 37 Abdominal Aortic Wall Cross-coupled Stiffness Could Potentially Contribute to Aortic Length Remodeling. **2022**, 28, 113-127 ○

- 36 The Lumbar Facet Capsular Ligament Becomes More Anisotropic and the Fibers Become Stiffer with Intervertebral Disc and Facet Joint Degeneration. **2022**, 1-47 ○
- 35 Automated model discovery for skin: Discovering the best model, data, and experiment. ○
- 34 Constituent-based quasi-linear viscoelasticity: A revised quasi-linear modelling framework to capture non-linear viscoelasticity in arteries. ○
- 33 Multiscale Mechanical Characterization and Computational Modeling of Fibrin Gels. ○
- 32 A novel approach for tetrahedral-element-based finite element simulations of anisotropic hyperelastic intervertebral disc behavior. 10, 1
- 31 Large Isotropic Elastic Deformations: On a Comprehensive Model to Correlate the Theory and Experiments for Incompressible Rubber-Like Materials. ○
- 30 A coupled thermal-electrical-structural model for balloon-based thermoplasty treatment of atherosclerosis. **2023**, 40, ○
- 29 Fitting mechanical properties of the aortic wall and individual layers to experimental tensile tests including residual stresses. **2023**, 138, 105647 ○
- 28 Quantitative analysis of second harmonic generated images of collagen fibers: a review. ○
- 27 A Review of Hyperelastic Constitutive Models for Dielectric Elastomers. **2023**, 1-17 ○
- 26 Finite element implementation of the aortic double-dispersion fibre model and development of a predictive damage model. 030932472211500 ○
- 25 Mechanical investigations of the peltate leaf of *Stephania japonica* (Menispermaceae): Experiments and a continuum mechanical material model. 13, ○
- 24 Phosphotungstic acid (PTA) preferentially binds to collagen- rich regions of porcine carotid arteries and human atherosclerotic plaques observed using contrast enhanced micro-computed tomography (CE- μ CT). 14, ○
- 23 Effect of aging on the biaxial mechanical behavior of human descending thoracic aorta: Experiments and constitutive modeling considering collagen crosslinking. **2023**, 140, 105705 ○
- 22 Characterization and modeling of the anisotropic behavior of the porcine dermis. **2023**, 129, 104098 ○
- 21 Biaxial hyperelastic and anisotropic behaviors of the corneal anterior central stroma along the preferential fibril orientations. Part II: Quantitative computational analysis of mechanical response of stromal components. **2023**, 142, 105802 ○
- 20 Point-to-point optical coherence elastography using a novel phase velocity method. **2023**, 163, 107489 ○
- 19 Automated model discovery for skin: Discovering the best model, data, and experiment. **2023**, 410, 116007 ○

18	Inflation-induced bulge initiation and evolution in graded cylindrical tubes of arbitrary thickness. 2023 , 178, 104561	○
17	Automated model discovery for human brain using Constitutive Artificial Neural Networks. 2023 , 160, 134-151	○
16	Biomechanics of keratoconus: Two numerical studies. 2023 , 18, e0278455	○
15	Mechanical Characterization of Human Fascia Lata: Uniaxial Tensile Tests from Fresh-Frozen Cadaver Samples and Constitutive Modelling. 2023 , 10, 226	1
14	Computational modeling reveals inflammation-driven dilatation of the pulmonary autograft in aortic position.	○
13	A multiscale continuum model for the mechanics of hyperelastic composite reinforced with nanofibers. 2023 , 267, 112168	○
12	Changes in the microstructure of the human aortic adventitia under biaxial loading investigated by multi-photon microscopy. 2023 , 161, 154-169	○
11	Acute Mechanical Consequences of Vessel-Specific Coronary Bypass Combinations.	○
10	Multiscale Multimodal Characterization and Simulation of Structural Alterations in Failed Bioprosthetic Heart Valves.	○
9	High-resolution confocal and light-sheet imaging of collagen 3D network architecture in very large samples. 2023 , 26, 106452	○
8	Mechanical modeling of the maturation process for textile reinforced tissue-engineered heart valves. 2023 , 22,	○
7	Simulations of the snap-through behavior of a fiber reinforced elastomer structure for the design of a simple clamping mechanism. 2023 , 22,	○
6	A novel anisotropic stress-driven model for bioengineered tissues accounting for remodeling and reorientation based on homeostatic surfaces. 2023 , 22,	○
5	Comparative modelling results between a separable and a non-separable form of principal stretchesBased strain energy functions for a variety of isotropic incompressible soft solids: Ogden model compared with a parent model. 2023 , 5,	○
4	Mechanical behavior and collagen structure of degenerative mitral valve leaflets and a finite element model of primary mitral regurgitation. 2023 ,	○
3	A multiscale computational model of arterial growth and remodeling including Notch signaling.	○
2	Fluid flow and heat transfer in carotid sinuses of different sizes and locations in an open surgery: CFD vs FSI.	○
1	Region- and layer-specific investigations of the human menisci using SHG imaging and biaxial testing. 11,	○

